

PEDIATRIC TB RADIOLOGY

FOR CLINICIANS



PEDIATRIC TB RADIOLOGY FOR CLINICIANS

KIM C. SMITH, MD, MPH · SUSAN D. JOHN, MD



PRODUCED BY HEARTLAND NATIONAL TB CENTER. CONSULTATION TO HEALTHCARE PROVIDERS AT
1-800-TEX-LUNG
2303 SE MILITARY DRIVE, SAN ANTONIO, TX 78223
WWW.HEARTLANDNTBC.ORG

THIS PRODUCT PRODUCED WITH FUNDS AWARDED
BY THE CENTERS FOR DISEASE CONTROL & PREVENTION (CDC)

BY
KIM C. SMITH, MD, MPH
SUSAN D. JOHN, MD

PEDIATRIC TB RADIOLOGY

FOR CLINICIANS



About the Authors

Kim Connelly Smith, MD, MPH, is a Professor of Pediatrics at the University of Texas Health Science Center at Houston Medical School.

She is the director of the Children's Tuberculosis Clinics at Children's Memorial Hermann and Lyndon B. Johnson Hospitals in Houston, Texas.

Susan D. John, MD, is the Chair of Diagnostic and Interventional Imaging and Professor of Diagnostic Imaging and Pediatrics at the University of Texas Health Science Center at Houston Medical School.

Reviewers

James B. McAuley, MD, MPH

Ewell Clarke, MD

Alan Schlesinger, MD

Barbara Seaworth, MD

Andrea T. Cruz, MD, MPH

Lisa Y. Armitige, MD, PhD

Jeffrey R. Starke, MD

Thanks to Stephanie McAlpin and Creative Blend Design for artistic design and Dwight C. Andrews for photography.

Table of Contents:

	Introduction	3
	• Learning Objectives	3
	Chapter I: Basics of Normal Chest Radiographs in Children	5
	• Infant chest radiograph	5
	• Child and adolescent chest radiographs	8
	Chapter II: Basic patterns of disease	11
	• Air space opacities	11
	• Central peribronchial opacities	15
	• Interstitial opacities	16
	• Hilar opacities	17
	• Pleural opacities	18
	Chapter III: Pediatric Intrathoracic Tuberculosis	21
	• Primary disease	22
	• Ghon complex	23
	• Hilar lymphadenopathy	26
	• Considerations for CT in Children with TB	29
	• Complications of lymphadenopathy	33
	• Tuberculosis pneumonia	39
	• Miliary tuberculosis	40
	• Pleural effusions	43
	• Air filled cysts	47
	• Congenital tuberculosis	55
	• Healed intrathoracic disease	55
	Chapter IV: Pediatric Extrapulmonary Tuberculosis	57
	• Central Nervous System tuberculosis	57
	• Abdominal tuberculosis	66
	• Musculoskeletal tuberculosis	70
	• Pericardial Tuberculosis	78
	Chapter V: Other diseases that can mimic tuberculosis	79
	Chapter VI: Clinical Case Studies	87
	References	105

PEDIATRIC TB RADIOLOGY

FOR CLINICIANS

Introduction

Tuberculosis is one of the leading infectious diseases in developing countries, with an estimated 40% of people infected. Globalization, mobility and immigration continue to diversify populations throughout the world. TB can present with a myriad of clinical findings in children ranging from asymptomatic to life threatening disease. The diagnosis is often more difficult to recognize in children than in adults. Radiographic findings remain one of the most important diagnostic tools for pediatric TB, yet the abnormalities can be subtle and the findings in children do not follow patterns typical of adult disease.

This book for clinicians shows and describes examples of radiographic abnormalities common in pediatric tuberculosis, emphasizing pulmonary, lymphatic and meningeal disease. The utility of CT scan and MRI in pediatric TB are also discussed. Radiographs and case studies are used as illustrations throughout the book.



Learning Objectives

- Understand normal findings and variation in chest radiographs by age
- Recognize basic pulmonary disease patterns in child chest radiographs
- Become familiar with the spectrum of pediatric TB including primary, miliary, lymph node, extrapulmonary and healed disease
- Understand the value of CT in children with TB
- Become familiar with the expected clinical evolution of radiographs in children with TB during and after treatment
- Recognize typical MRI findings in children with central nervous system TB
- Appreciate other diseases that can mimic TB radiographically



Basics of Normal Chest Radiographs in Children

Basics of Normal Chest Radiographs in Children

Infant Chest Radiograph

The anatomic differences in the chest of infants below the age of 1 year are significant and can confuse the inexperienced observer who is investigating the possible diagnosis of tuberculosis. As with other solid organs in the body, the heart appears relatively large in relationship to the overall size of the chest during infancy. The thymus gland is large during the first years of life in infants and young children. Because the thymus gland is soft tissue in nature, it has the same density on radiographs as the heart that is composed of soft tissue and fluid. The thymus gland sits anterosuperior to the heart and is contiguous with it, causing the two structures to be indistinguishable on radiographs. The combination of a normal large thymus gland and the heart can cause the cardiomeastinal silhouette to appear abnormally large (Fig. 1), so the observer must be aware of this complicating factor when interpreting chest radiographs in infants.

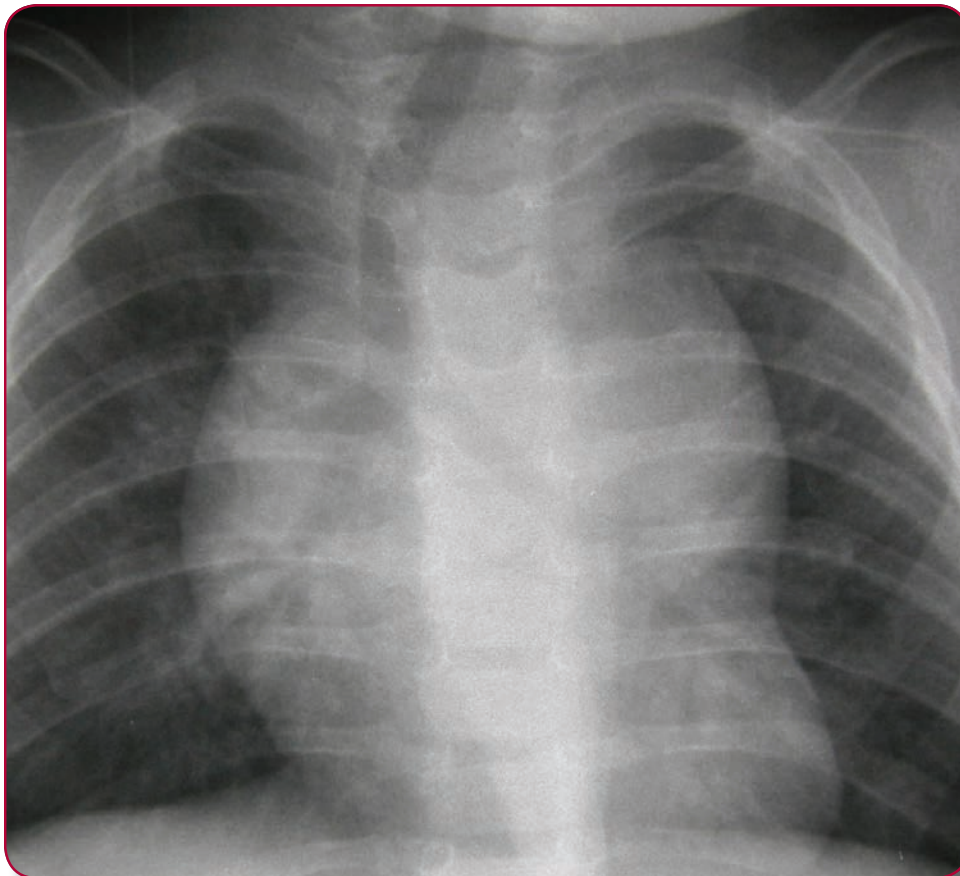


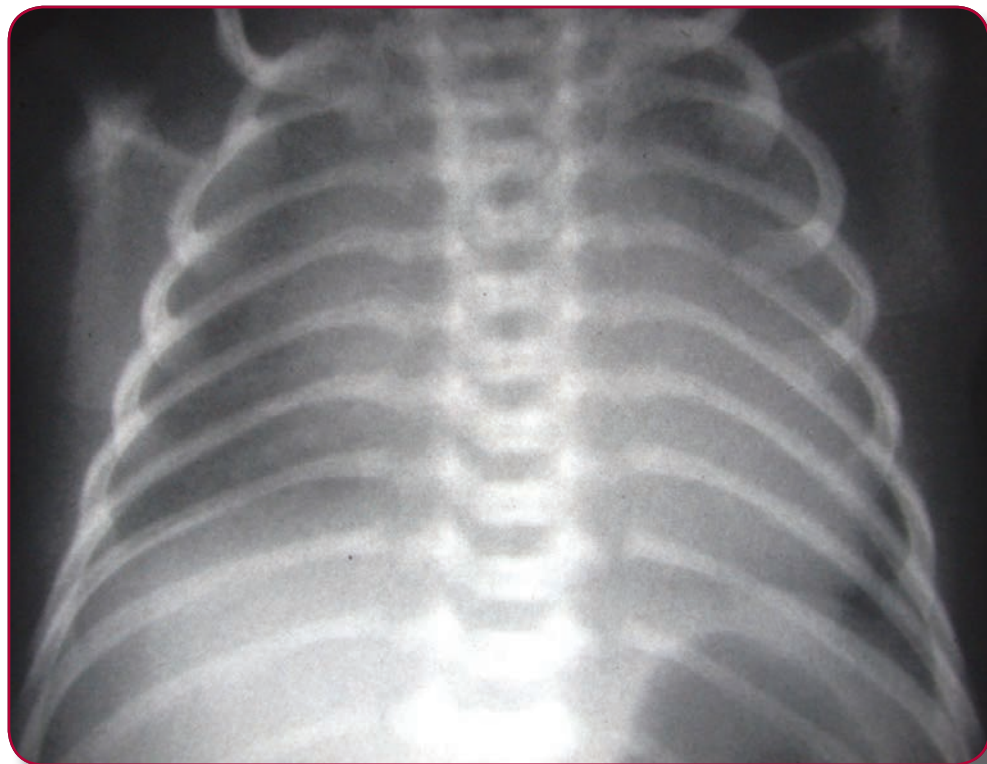
Fig. 1. Normal thymus gland in an infant. Prominent tissue in the anterior mediastinum represents normal thymus gland. Buckling of the trachea to the right is a normal phenomenon when the infant exhales and does not indicate displacement by the thymus gland.

Basics of Normal Chest Radiographs in Children (cont...)

Use of a comparative ratio of cardiac to thoracic diameter on radiographs in children is less reliable than in adults, but the general rule of thumb is that the diameter of the heart in the infant and young child is equal to or less than approximately 55% of the thoracic diameter. The aortic arch is usually relatively small in infancy and is often not clearly visible behind the thymus gland.

Radiographs of good technical quality are essential when evaluating the chest and are sometimes challenging to obtain. The radiograph should be taken in an adequate degree of inspiration, producing lungs that are equally distended with air. When radiographs are obtained in a suboptimal phase of inspiration, the amount of air within the lungs is decreased causing the lungs to appear more opaque than normal. The degree of opacity of the lungs on an expiratory radiograph in a young infant can be quite striking as the pulmonary compliance is very good and end expiratory volumes can be small. The absence of visible air within the trachea and mainstem bronchi can be a clue to the expiratory nature of a radiograph (Fig. 2). Be aware that the trachea elevates during expiration and can have a buckled appearance, usually displaced to the right (see Fig. 1). This deviation from the usual straight position of the trachea over the right side of the spine may suggest mass effect, but don't be fooled by this finding.

Fig 2.
Expiratory radiograph. Note that the lungs appear small in volume and hazy in density. No air is visible in the tracheobronchial tree, indicating that the image was obtained near the end of expiration.



Basics of Normal Chest Radiographs in Children (cont...)

The lung hilum is a difficult area to evaluate in infants. The pulmonary vasculature is relatively small during infancy, and a prominent thymus gland can obscure the central vasculature. Lateral views of the chest are helpful. Linear vascular markings should be visible coursing towards the hila, but no nodular opacities should be seen.

Straight positioning is also important in chest radiography. When the patient is rotated toward one side on a radiograph, important areas of the chest and lungs can be obscured by the heart and mediastinum (Fig. 3). Overall density of the lungs can appear artificially asymmetrical with rotated positioning, mimicking pathology. The thymus can simulate atelectasis or pulmonary infiltrates, especially in a rotated radiograph such as Fig. 3. Asymmetry of the skeletal structures in the chest is good evidence that the positioning of the patient is suboptimal.

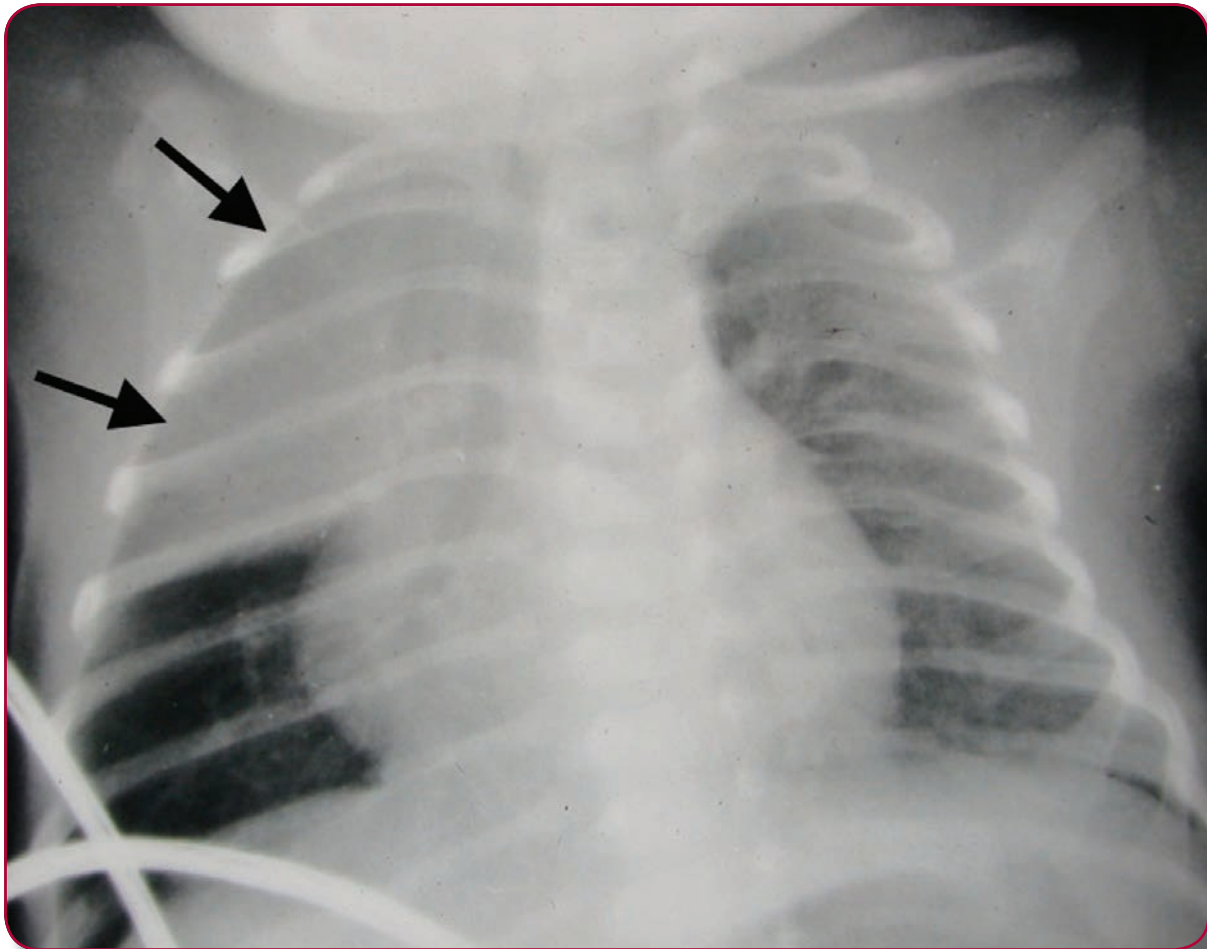


Fig. 3.
Rotated positioning. When the patient is rotated on the radiograph, anterior mediastinal structures such as thymus gland are projected over portions of the lung and obscure visualization (arrows).

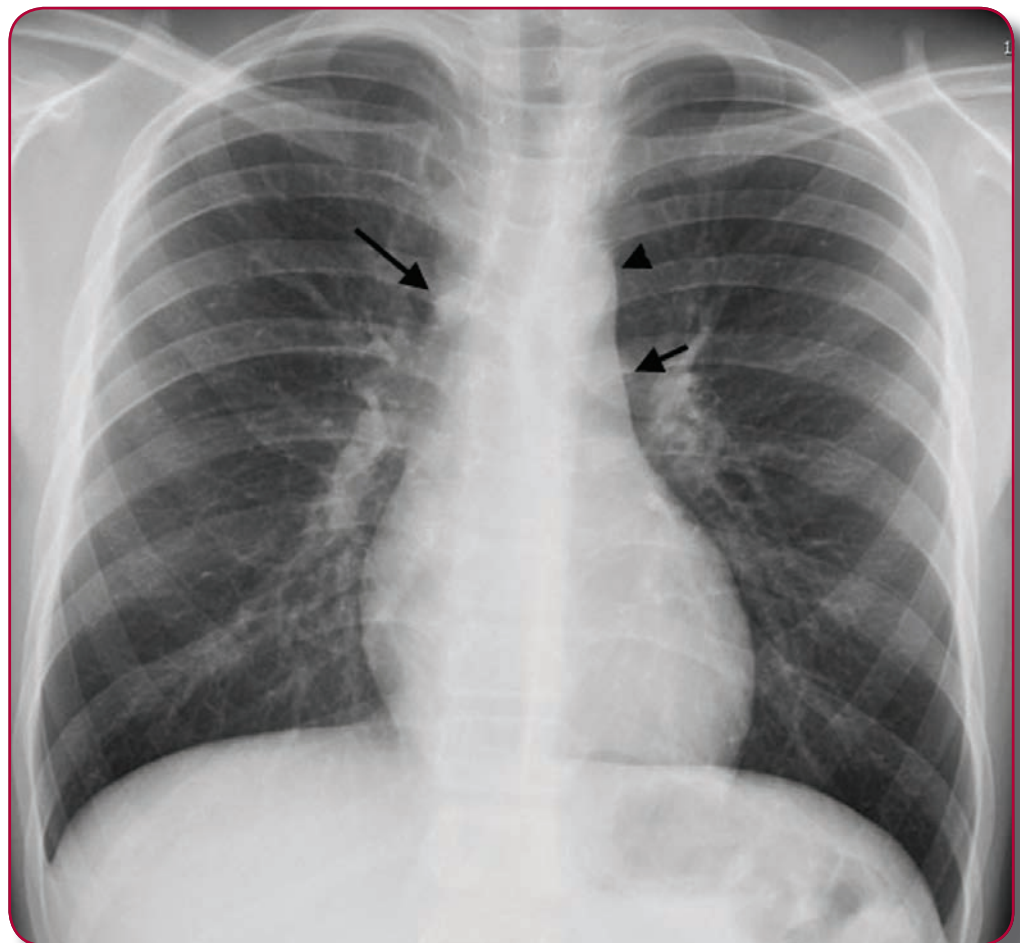
Basics of Normal Chest Radiographs in Children (cont...)

◦Child and adolescent chest radiographs

As a child grows beyond infancy, the thymus gland decreases in size, but some thymic tissue may be visible on radiographs up to 5 or 6 years of age. The rate of thymic regression is variable between individuals. The central pulmonary vasculature becomes more easily visible and more prominent as the child grows. The left lung hilum continues to be more difficult to evaluate than the right lung hilum throughout childhood.

As the thymus gland regresses, the main pulmonary artery and the aorta become visible as discrete bulges in the contour of the left side of the cardiac and mediastinal border (Fig. 4A). The azygous vein appears as a small round opacity to the right of the trachea just above the takeoff of the right mainstem bronchus. Normal pulmonary vessels are usually not seen clearly in the outer 1/3 of lungs because of their small size. Good inspiratory radiographs continue to be a challenge until the child reaches a cooperative age, usually around 4-5 years. Therefore, the lungs may not appear as large in young children as they do in older children and adolescents who can obey the command to "take a deep breath and hold it."

Fig 4A.
Normal chest
(older child).
PA view.
Aorta (arrowhead),
main pulmonary
artery (short
arrow), azygos vein
(long arrow).



Basics of Normal Chest Radiographs in Children (cont...)

The lateral view of the chest is important for complete evaluation of normal structures and pathology. The lungs should be assessed for any focal areas of increased opacity. The lung bases contain a larger volume of air than the upper lungs and, therefore, should be slightly blacker. This can be observed by looking at the spine on lateral view, which should appear blacker in the lower thoracic region than in the upper chest. The pulmonary vessels radiate as thin linear structures from the region of the lung hilum. The right pulmonary artery is normally seen as a round structure anterior to the trachea on lateral view and should not be mistaken for a mass or a lymph node (Fig. 4B). Once the thymus gland has regressed, the retrosternal region of the chest on lateral view should appear black.

The hemidiaphragms have a slightly domed contour on both PA and lateral views when the lungs are normally inflated. The right hemidiaphragm usually sits slightly higher than the left hemidiaphragm because of the underlying liver. The angles formed by the juncture of the ribs and the margins of the hemidiaphragms (costophrenic angles) should be fairly deep and sharply pointed.

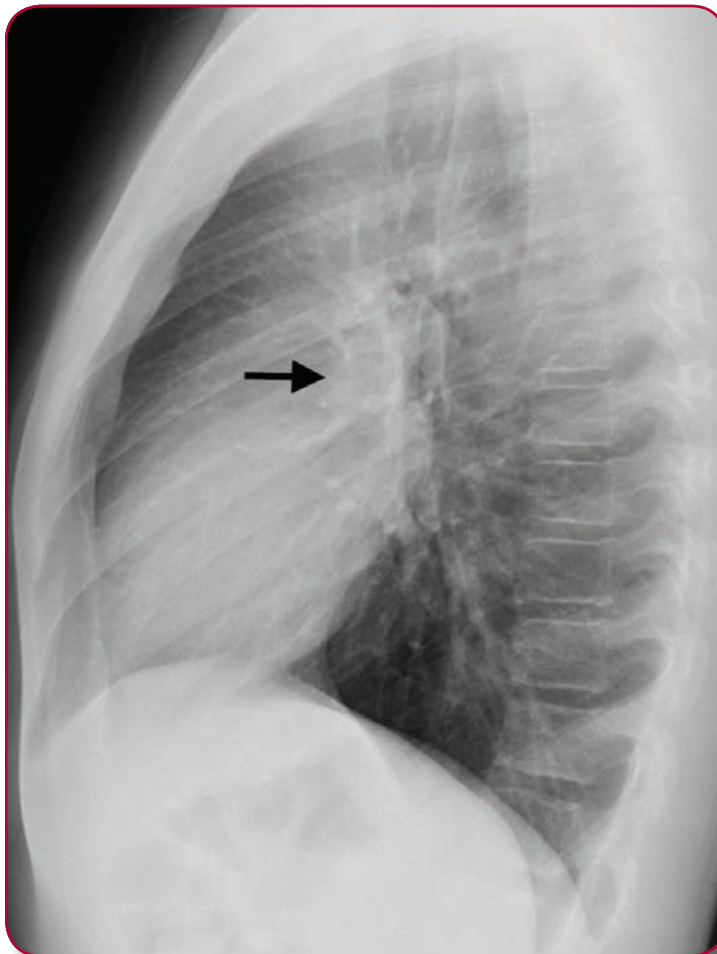


Fig. 4B.
Lateral view.
Right pulmonary
artery (arrow).



Basic Patterns of Disease

Basic Patterns of Disease

Air Space Opacities

Pulmonary conditions that involve primarily the alveolar air space consist mainly of space occupying pathologies, air space collapse (atelectasis), and lung masses or nodules. All of these abnormalities cause some degree of opacification of the lung that is usually homogeneous in density, unless fat or calcifications are also present.

Conditions that fill the lung with fluid, such as bacterial pneumonia or pulmonary edema, displace the air from the alveolus causing it to appear white (or less black) on the radiograph. Often the bronchioles or bronchi in the area remain filled with air and are black (ie, air bronchogram). Pneumonia tends to be located in one or more focal areas within a lung, whereas pulmonary edema is more likely to be distributed evenly in both lungs. The portions of the lung affected by such air space abnormalities usually maintain their volume and can even become larger than the unaffected parts of the lung (Fig. 5).

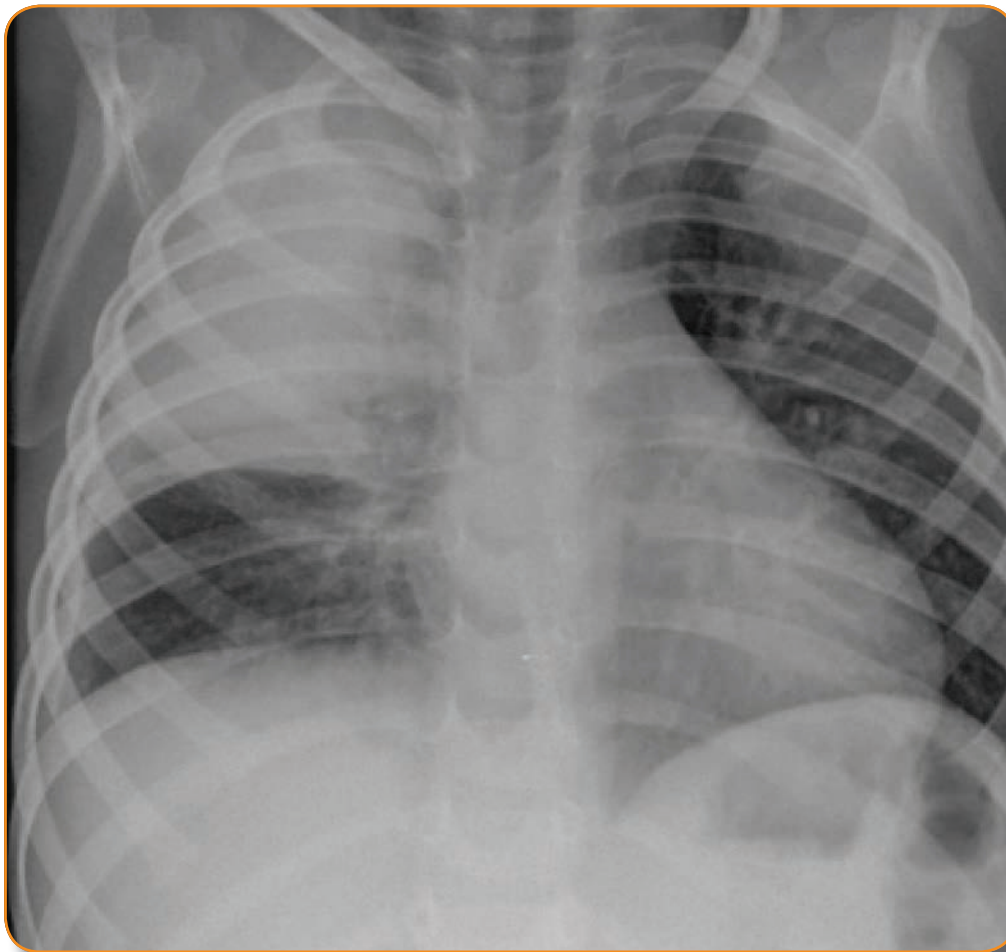


Fig. 5A.
Bacterial pneumonia.
Dense consolidation involves only the right upper lobe of the lung.

Basic Patterns of Disease (cont...)

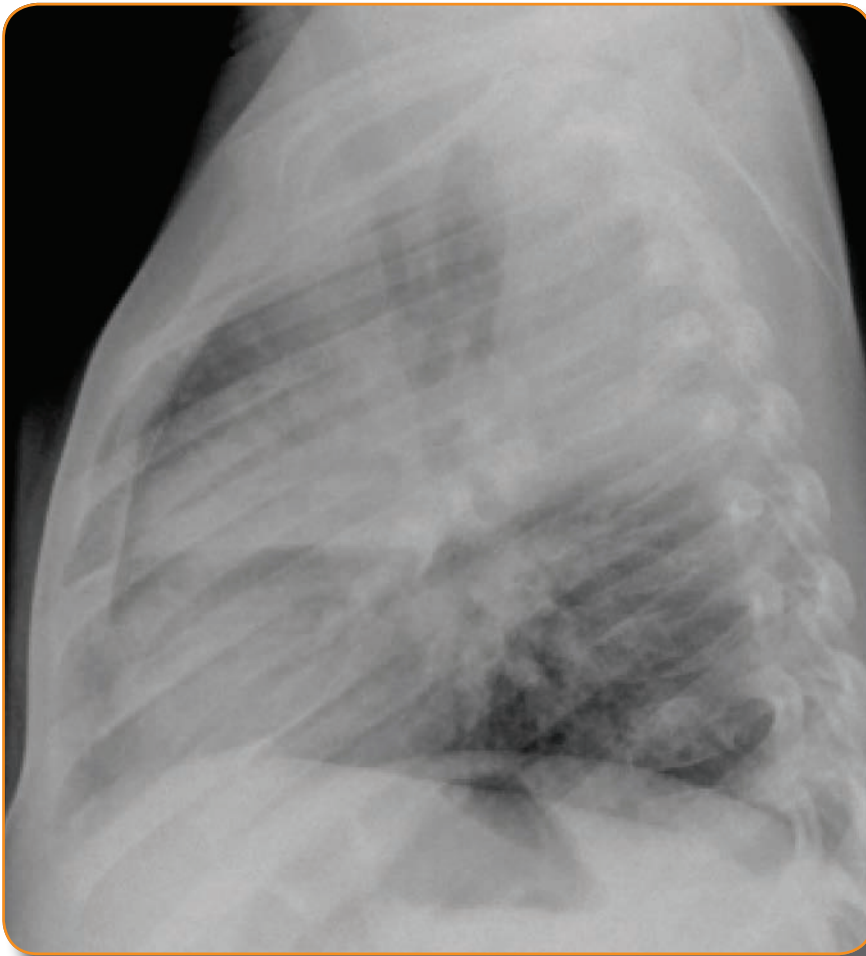


Fig. 5B.
Lateral radiograph,
same patient.
The horizontal
fissure remains in
a normal position,
indicating a space
occupying process
with no volume
loss.

Basic Patterns of Disease (cont...)

Areas of the lung that become collapsed also become white because of the absence of normal air in the alveolar space. However, atelectasis differs from space-occupying conditions in that the volume of a collapsed portion of the lung will be decreased. The loss of volume causes near-by structures (eg., fissures, hemidiaphragm, trachea) to shift toward the side of volume loss (Fig. 6), an important finding to distinguish atelectasis from lung consolidation. When atelectasis is caused by a bronchial obstruction, the affected bronchus will also be opaque, so air bronchograms are less common with atelectasis than with pneumonia in children.

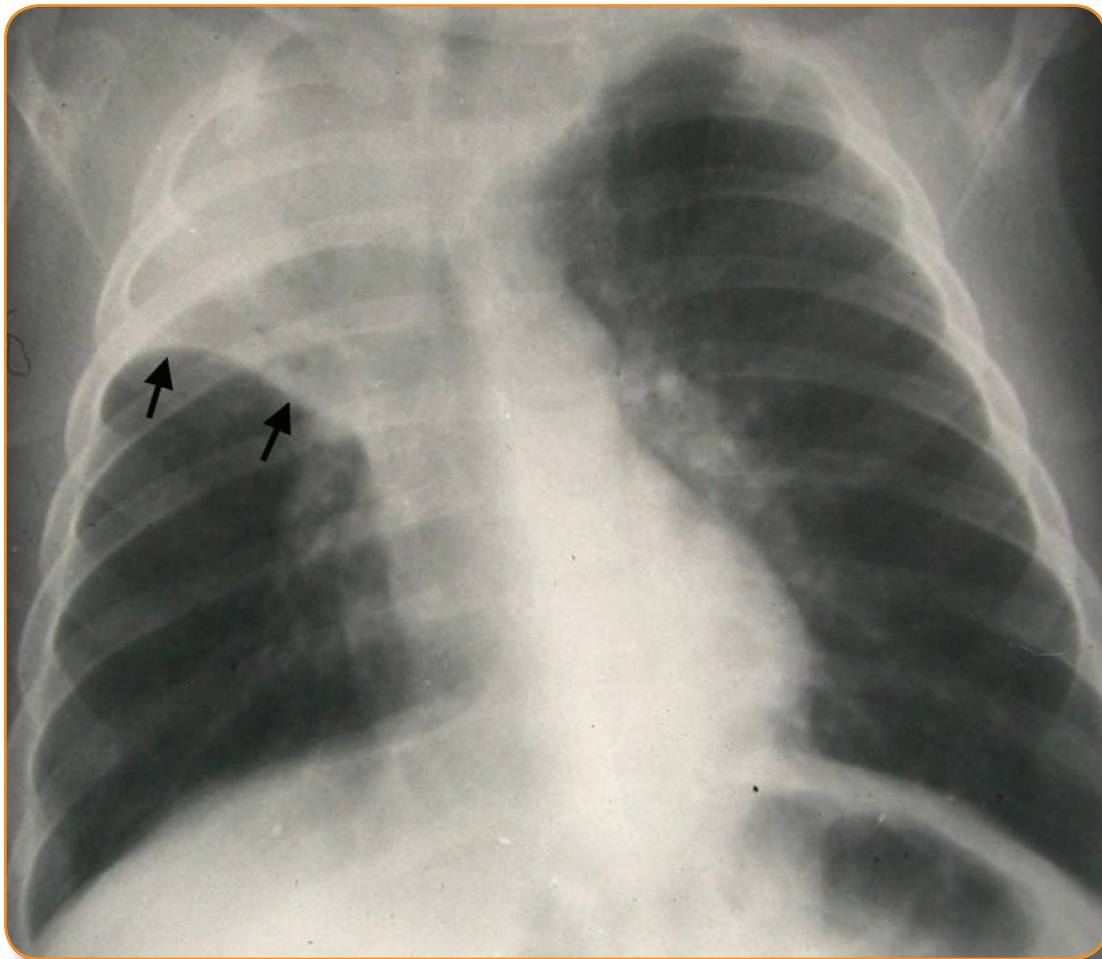


Fig. 6.
Right upper lobe atelectasis. Note that the horizontal fissure on the right is elevated (arrows) indicating volume loss in the right upper lobe.

Basic Patterns of Disease (cont...)

Lung masses or nodules cause the same kind of increased opacity in the alveolar space as pneumonia or atelectasis, except that they have a more well-defined contour in most cases. Large pulmonary masses are quite rare in infancy and childhood, and most apparent pulmonary masses in these age groups represent congenital or developmental abnormalities such as pulmonary sequestration or congenital bronchopulmonary malformations. Smaller nodules or masses are usually caused by infections or occasional congenital or acquired lung cysts. Be aware that a bacterial pneumonia can sometimes have a round, well-defined appearance in children that mimics a pulmonary mass (Fig. 7). Pulmonary neoplasms in childhood are exceedingly rare.

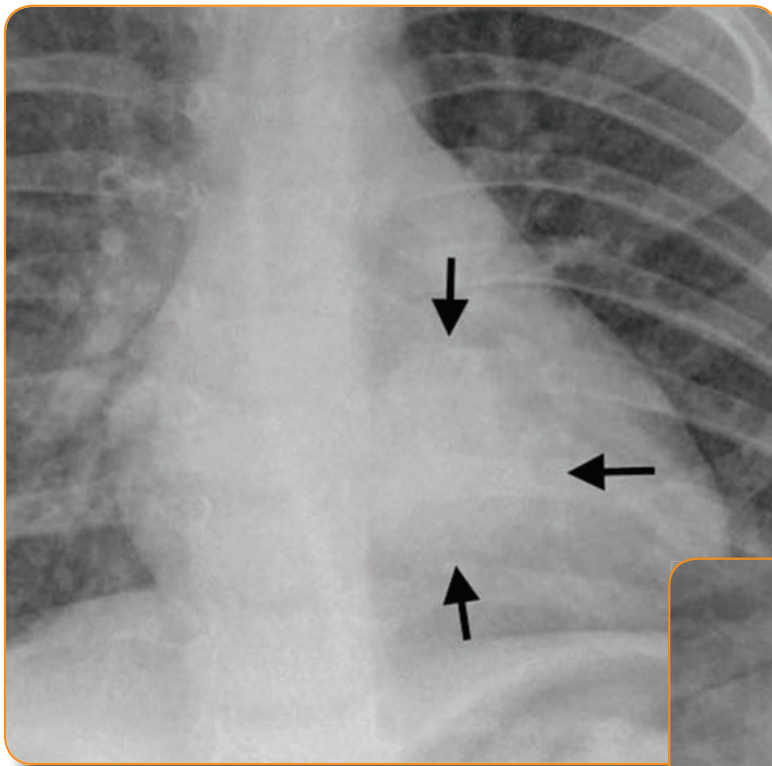


Fig. 7A.
Round pneumonia.
Note the rounded
solid opacity in the
left lower lobe on
PA (arrows).

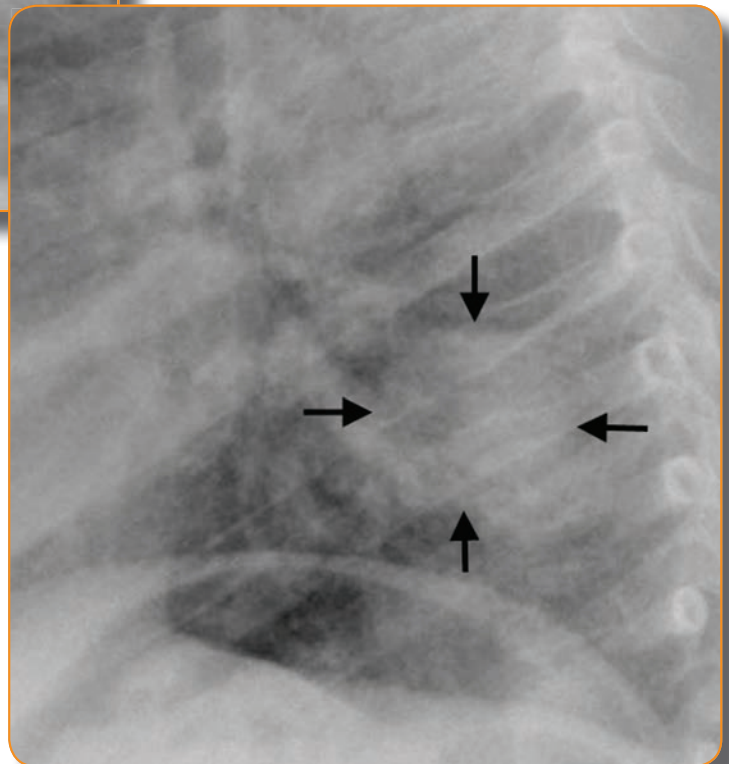


Fig. 7B.
Lateral view.
Bacterial pneumonia
in children
sometimes appears
round and well-
defined resembling
a pulmonary mass.

Central peribronchial opacities

Conditions that primarily affect the trachea and smaller airways can sometimes cause radiographic abnormalities in the lungs. Viral lower respiratory tract infection is a common cause of such a lung pattern. Tracheobronchial infections and inflammatory conditions are associated with mild edema that can leak into the peribronchial and interstitial spaces to cause ill-defined, hazy or streaky increased opacity in the central parahilar regions of the lungs. The abnormal opacities are bilateral and symmetrical (Fig. 8), distinguishing them from the localized, more peripheral opacities that characterize bacterial pneumonia. Similar opacities can be seen chronically in the lungs of children with chronic bronchial diseases such as chronic aspiration or cystic fibrosis.

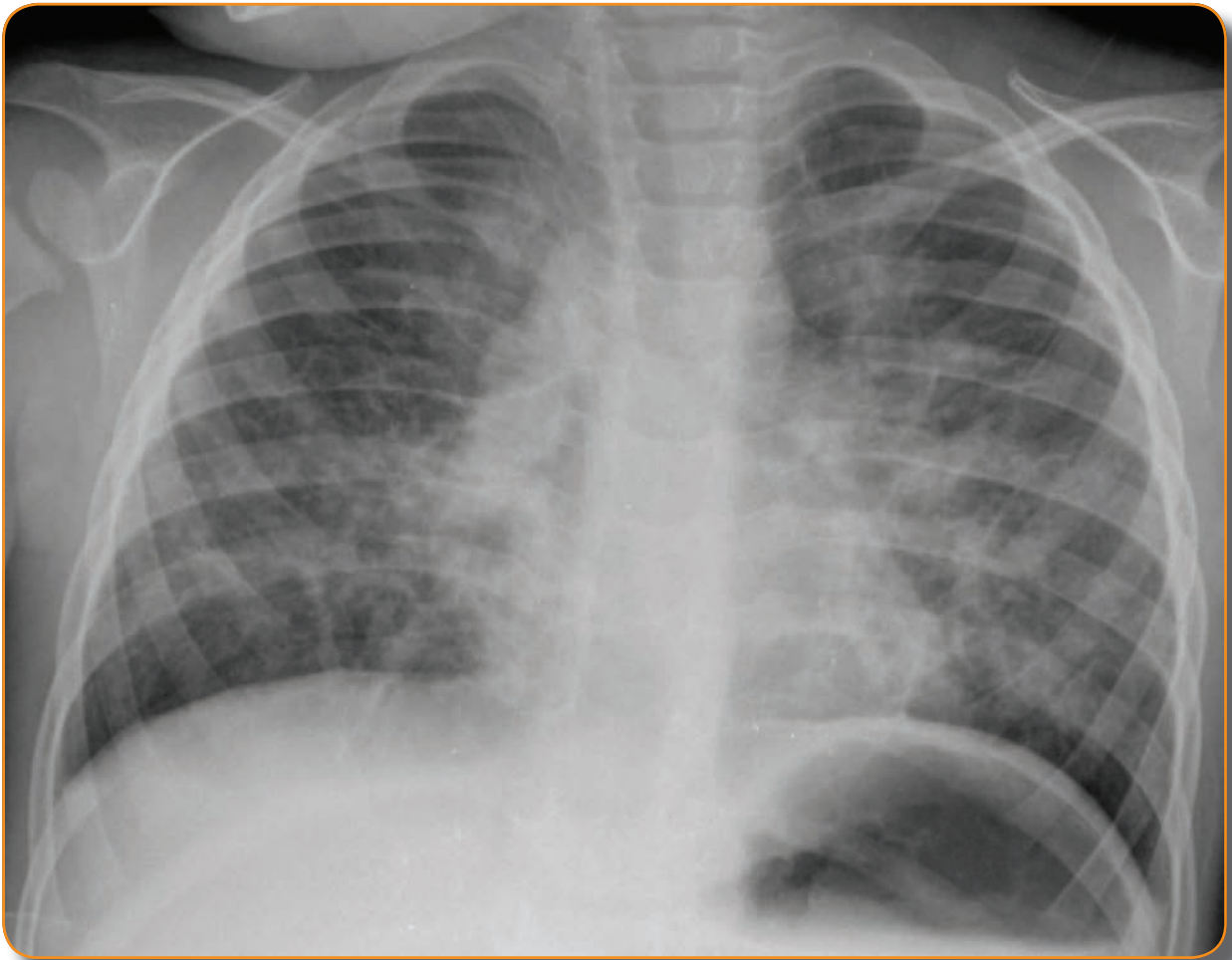


Fig. 8
Viral respiratory tract infection.
Note the central, ill-defined, parahilar peribronchial opacities, typical of viral bronchiolitis infection in children.

Interstitial opacities

Conditions that involve the lung interstitium (ie., pulmonary edema, viral infections, interstitial pneumonitis), create a net-like pattern that reflects thickening of the interstitial lung spaces (Fig. 9). As interstitial processes become more severe, the interstitial markings can begin to restrict the size of the alveolar space, and the decreased air in the space will cause the lung to appear hazy. When interstitial disease is very severe, the air spaces can be so compromised that the pattern on radiographs resembles air space consolidation such as that seen in pneumonia.

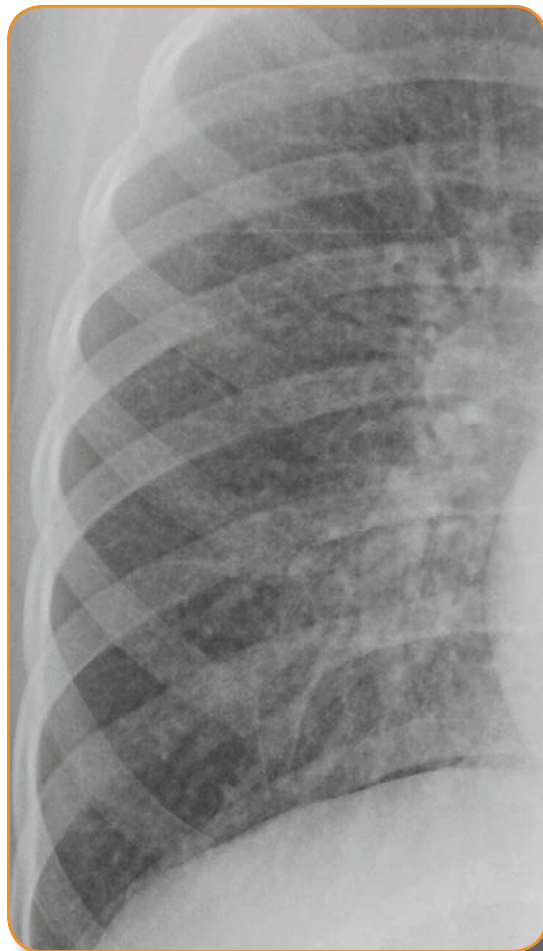


Fig. 9
Interstitial lung
pattern in a child with
lymphocytic interstitial
pneumonitis. The
thickened interstitial
markings create a net-
like pattern in the lungs.

Hilar opacities

Abnormal hilar opacities most commonly represent lymphadenopathy in infants and children. Identifying hilar lymphadenopathy can be difficult in infants because of overlying thymus gland. In some patients, prominent central pulmonary vessels can resemble lymph nodes. The most reliable clue to the correct identification of hilar lymphadenopathy is a convex appearance to the opacities in the hilar region between the radiating vessels on PA view (Fig. 10A) and discrete rounded opacities in the lung hilum on lateral view (Fig. 10B). Hilar lymph nodes are most common and most easily visible in the subcarinal region on lateral view.

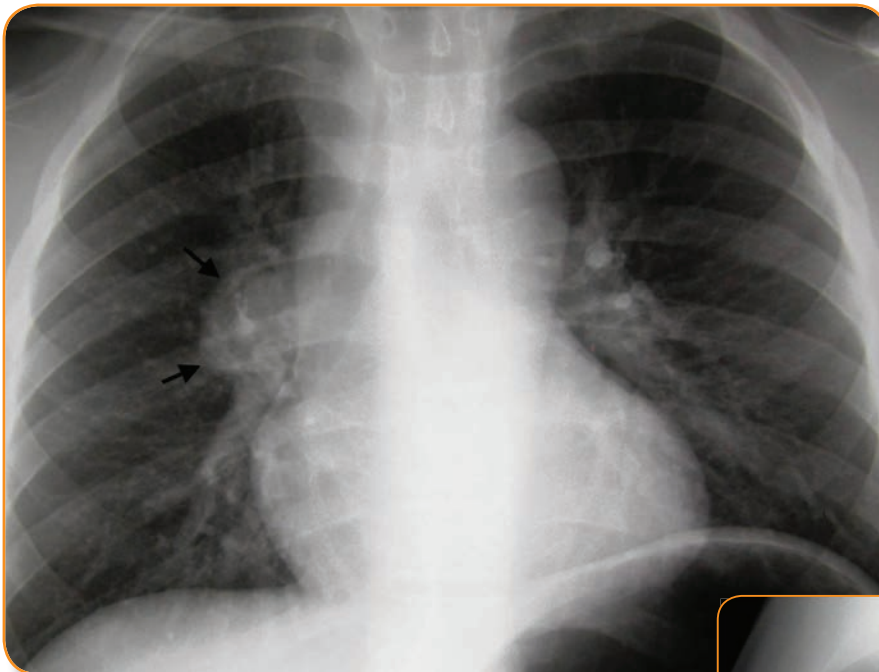
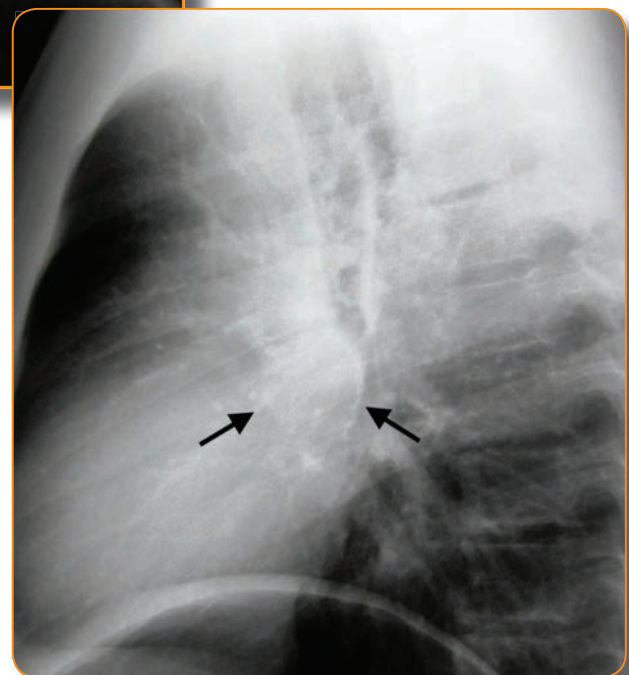


Fig. 10A.
Hilar lymphadenopathy.
The enlarged right hilar lymph nodes create a convex shadow between the hilar vessels (arrows). Note the straight margin of the normal pulmonary vessels on the left.

Fig. 10B.
On lateral view, the round lymph node is visible at the lower margin of the lung hilum (arrows).



Pleural opacities

Abnormal radiographic findings related to the pleural space in infants and children are most often caused by pleural effusions or other types of fluid filling the pleural space. Since fluids all have the same density on radiographs, it is usually not possible to determine the type of pleural fluid from the appearance on the images. Transudates tend to be free-flowing and will be larger in the dependent portions of the pleural space on upright views (Fig. 11A). Small pleural effusions may cause only slight blunting of the costophrenic angle (Fig. 11B). On supine radiographs, free-flowing pleural effusions will layer posteriorly, causing a generalized increase in haziness over the affected hemithorax. Lateral decubitus radiographs can help distinguish free flowing from loculated pleural fluid (Fig. 11C). Fluid that tends to be loculated, such as empyema or hemothorax, will usually cause uneven areas of thickening in the pleural space around the periphery of the lung (Fig. 12). Decubitus views with the affected side of the chest down may help by demonstrating lack of movement of the pleural fluid in loculated collections. Ultrasound is a safe and effective imaging modality to help localize and characterize pleural fluid collections in children.

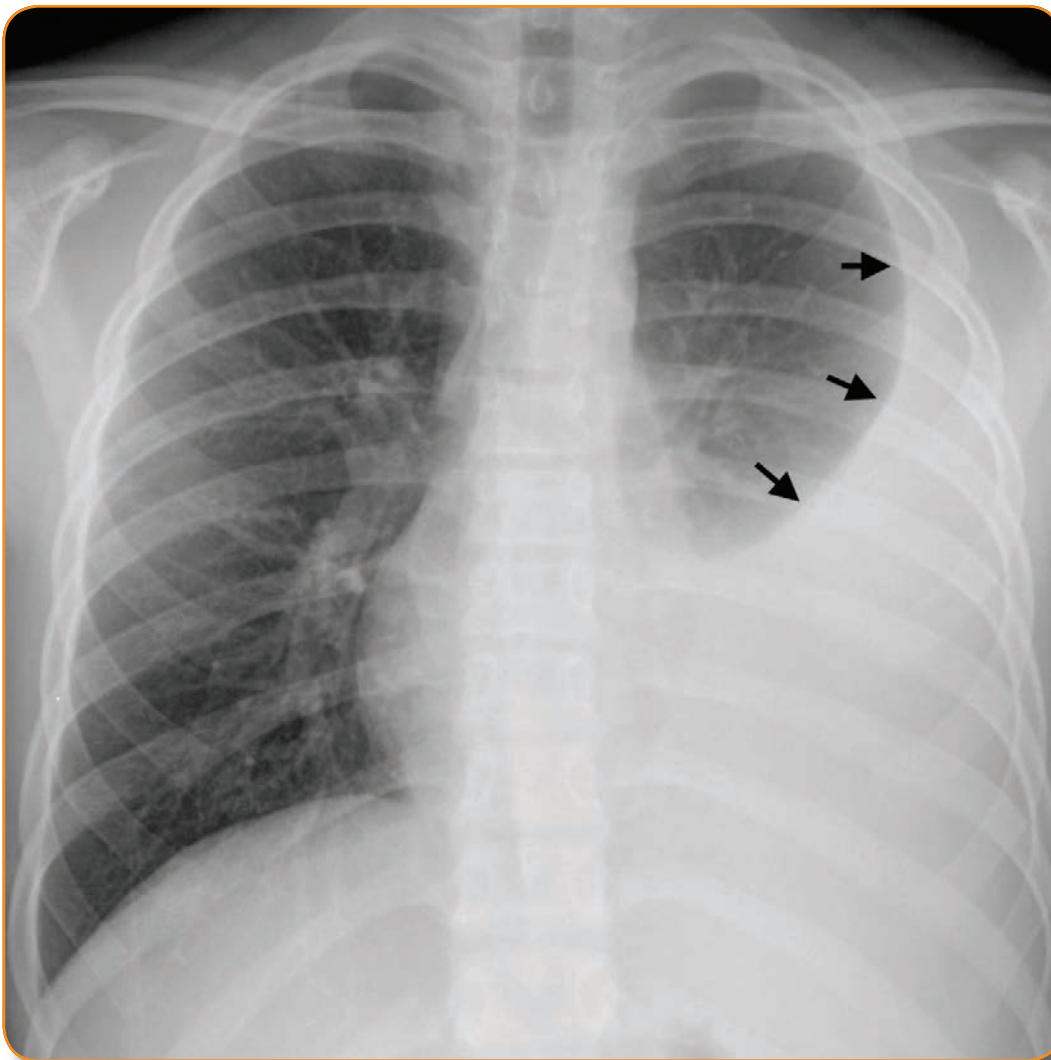


Fig. 11A.
Pleural effusion.
This free-flowing pleural effusion is larger in the base of the hemithorax and decreases in size superiorly (arrows).

Basic Patterns of Disease (cont...)

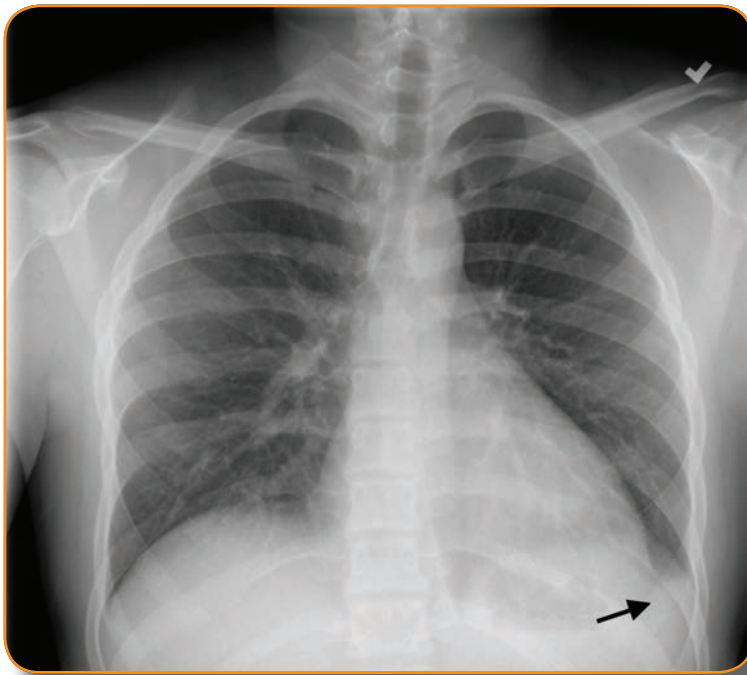
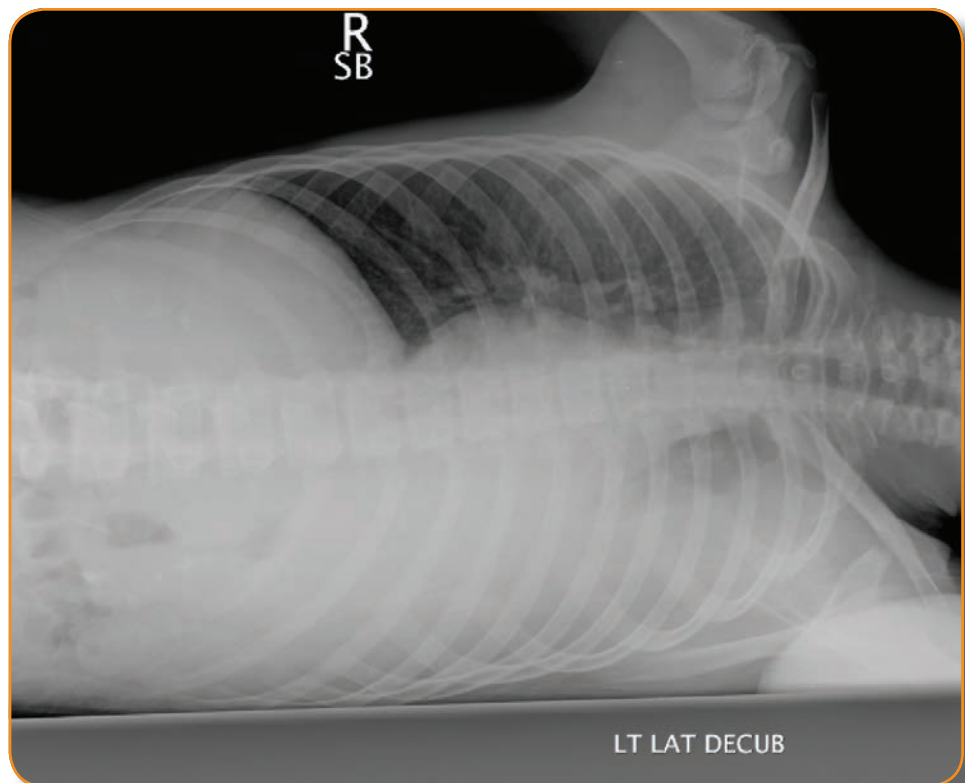


Fig. 11B.
Note blunting of
the costophrenic
angle by a small
effusion (arrow).

Fig. 11C.
A left lateral
decubitus radiograph
in the same patient
as 11A shows the free
flowing nature of the
pleural fluid.



Basic Patterns of Disease (cont...)

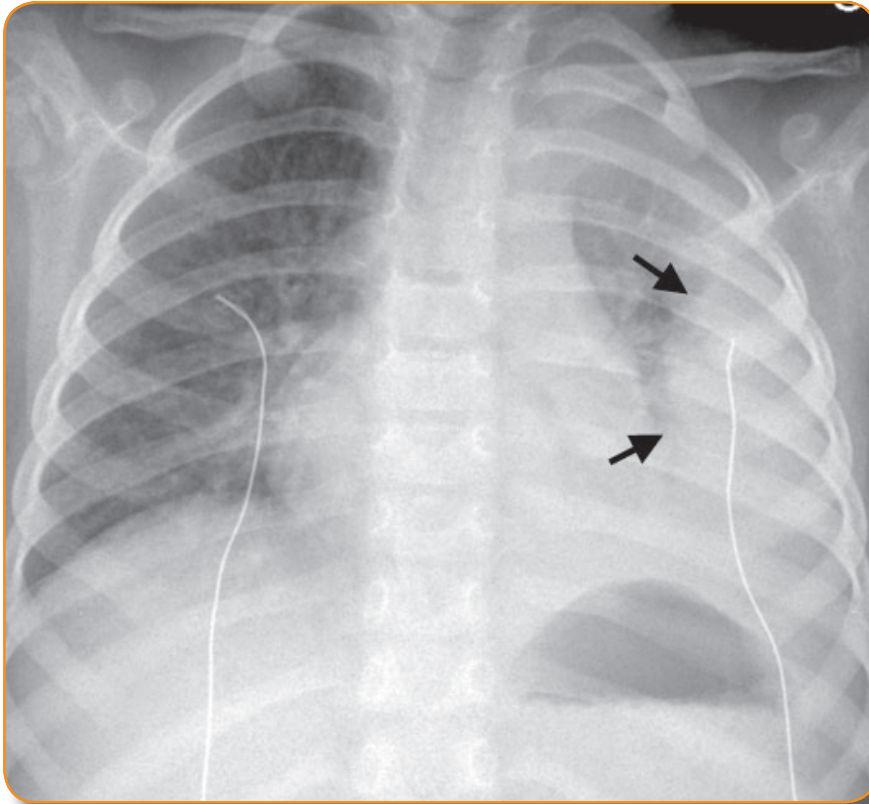


Fig 12A.
Loculated pleural fluid (empyema).
Radiograph shows a convex contour of the fluid collection in the left pleural space (arrows).



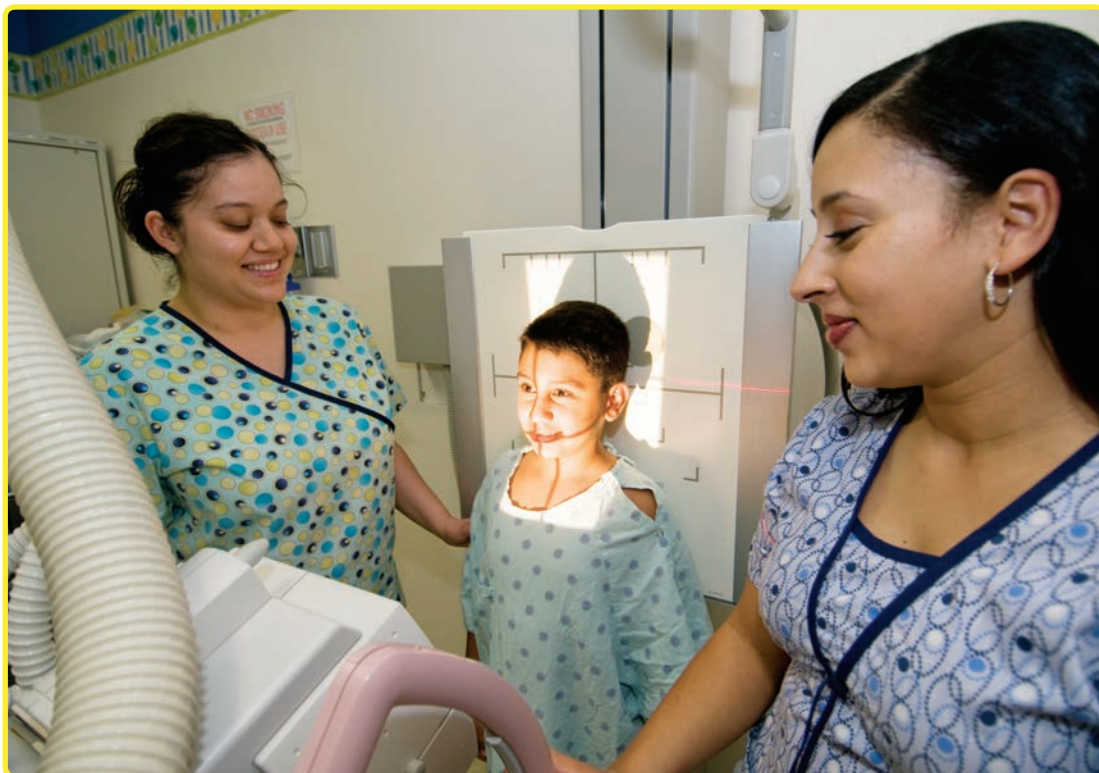
Fig. 12B.
CT of the same patient reveals multiple loculated pleural fluid collections on the left (arrows).

Pediatric Intrathoracic Tuberculosis

Pediatric Intrathoracic Tuberculosis

The diagnosis of intrathoracic TB in children depends largely on the interpretation of the chest radiograph since clinical diagnostic features are often nonspecific, AFB smears and cultures for TB are usually negative and half of children with disease identified in industrialized nations may be asymptomatic.^{1,2} Both posteroanterior (PA) and lateral chest views are important for optimal visualization in pediatric patients since a relatively wide mediastinum may hide enlarged hilar and/or paratracheal lymph nodes. Findings on imaging reflect the natural progression of infection to either latent TB, primary disease or disseminated disease depending on the response of the host and the clinical stage at the time of evaluation.

A normal chest radiograph in a clinically well child with a positive tuberculin skin test or interferon-gamma releasing assay (IGRA) is the standard for the diagnosis of latent TB infection (LTBI). Clinical trials over decades have demonstrated the efficacy of treatment of children diagnosed with LTBI with isoniazid to prevent progression to TB disease.



Pediatric Intrathoracic Tuberculosis (cont...)

Primary disease

In primary TB, the chest radiograph usually shows hilar lymphadenopathy and/or pulmonary air space opacities.³ Primary TB may be seen in any age group but is most common in younger children, before the age of adolescence. A review of TB disease in teens found that only 10% had radiologic findings of primary disease with lymphadenopathy.⁴ Adolescents are more likely to have adult-like TB with cavitary disease. Lymphohematogenous spread following infection is typical and may progress to disseminated disease. In many cases, the primary lung focus will resolve undetected and the infection can remain dormant as LTBI. The risk of disease progression and disease severity depend on host factors including the age of the child when the infection occurs. Infants have the highest risk of disease progression as well as more severe forms of disease. Children 5 years of age and less and teenagers have a higher risk of progression of TB disease when compared to children infected between 6-10 years of age.(Table 1)

Table 1. Risk of progression to TB disease by age in untreated patients with LTBI^{1,3}

Age at Infection	Risk of TB Disease
Birth-12 months	43-50%
1-5 years	20-25%
6-10 years	2%
11-15 years	16%
Healthy Adults	5-10% lifetime risk
HIV Infected Adults	30-50% lifetime risk

The radiographic appearance of primary TB typically includes enlargement of regional lymph nodes, with or without a small localized focus of air space consolidation. In the absence of clinical symptoms, the subtle changes of primary TB may be difficult to detect radiographically. Unlike adult reactivation disease, pediatric primary TB is characteristically pauci-bacillary and non-cavitary. The primary focus is reported in the right chest more commonly, although it may occur anywhere in the lungs. Due to the mediastinal lymphatic drainage, right sided adenopathy normally accompanies right lung primary opacities whereas bilateral lymphadenopathy is often seen with left sided opacities.⁵ Hilar lymphadenopathy is the hallmark of pediatric tuberculosis and is often the only radiographic finding.

Ghon complex

The Ghon focus is the primary site of infection in the lung which usually occurs in the subpleural alveolar space as a small hazy, solid or ill-defined opacity (Fig. 13). This transient inflammatory response is frequently followed by regional lymph node enlargement. The combination of the Ghon focus (primary parenchymal infiltrate) and local lymph node involvement is called the Ghon or primary complex (Fig. 14).^{1,3,5} The pulmonary lesion is often short-lived or may be hidden, with only mild pleural reaction. The size of the Ghon complex may be variable or radiographically subclinical depending on the degree of infection, host response and timing of evaluation. Local progression or intrabronchial spread can occur.

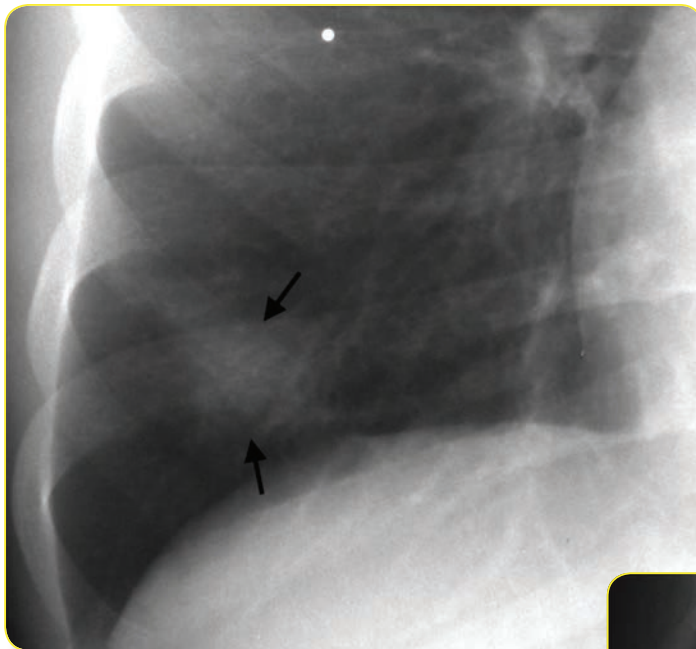
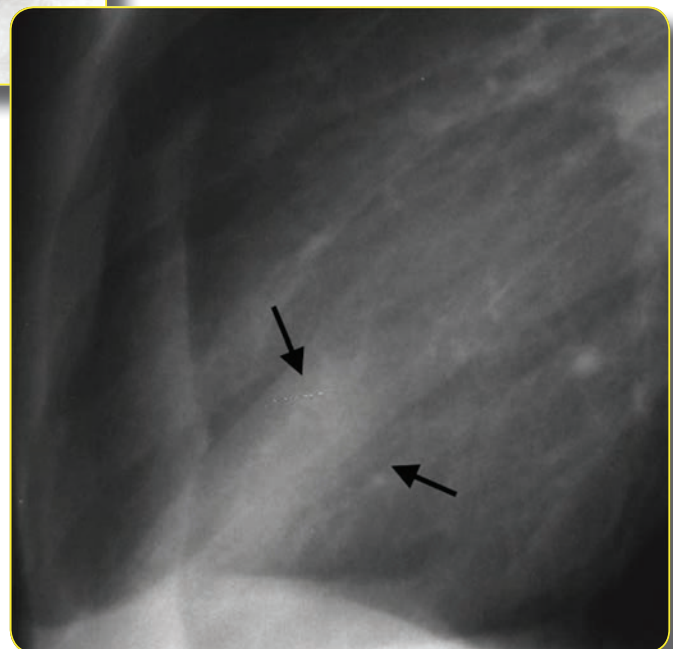


Fig. 13A. Ghon focus. When visible on radiographs, the Ghon focus usually appears as a small hazy opacity (arrows)

Fig. 13B. Lateral view of Ghon focus.



Pediatric Intrathoracic Tuberculosis (cont...)

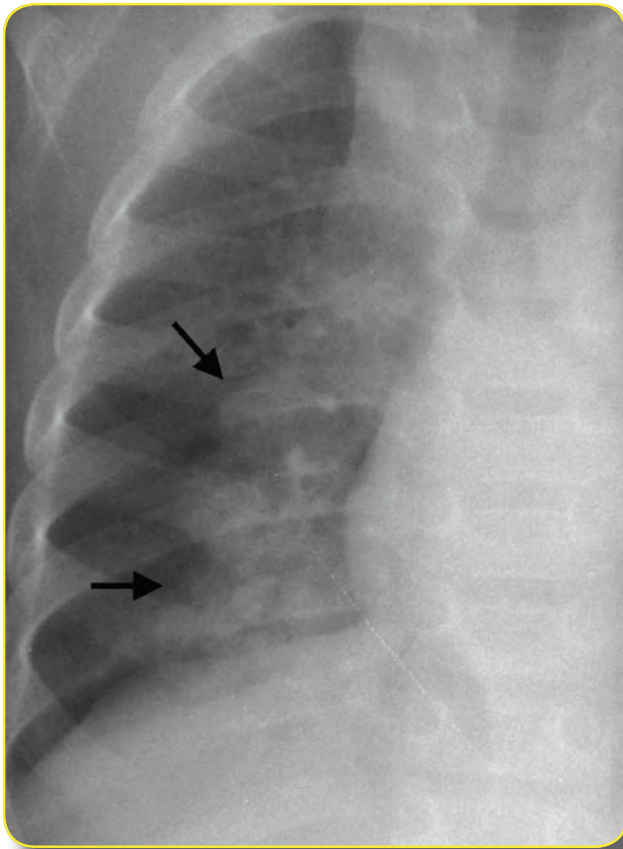
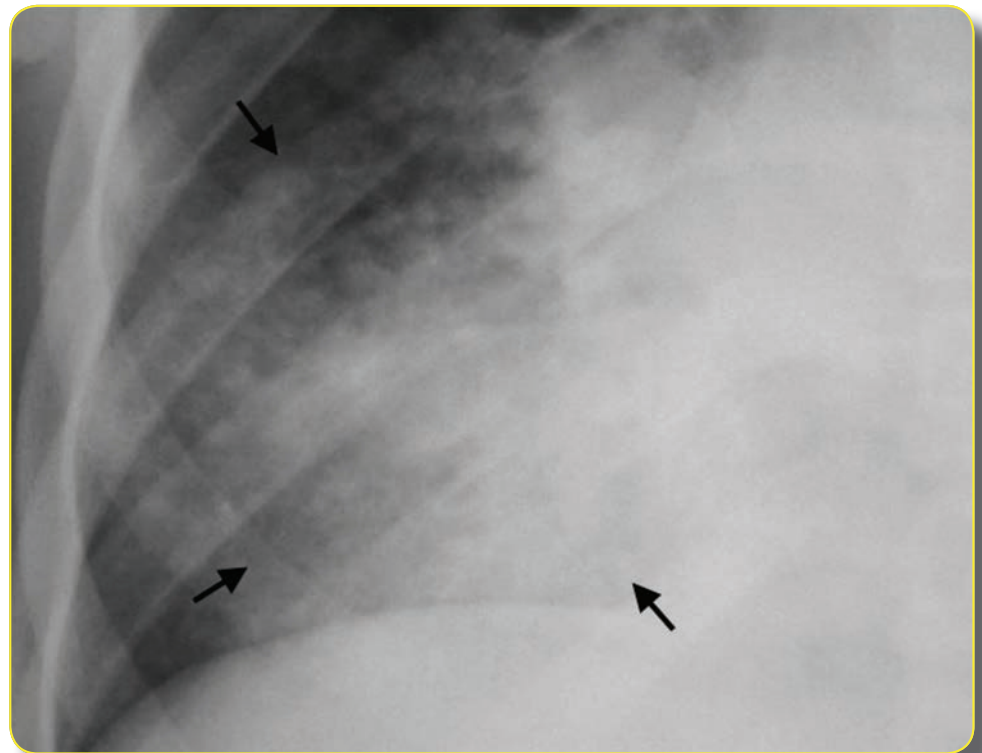


Fig. 13C.
Radiograph in a
different child shows
a larger and denser
area of consolidaton
resulting from primary
TB (arrows).

Fig. 13D.
Denser
consolidation in
primary TB.



Pediatric Intrathoracic Tuberculosis (cont...)

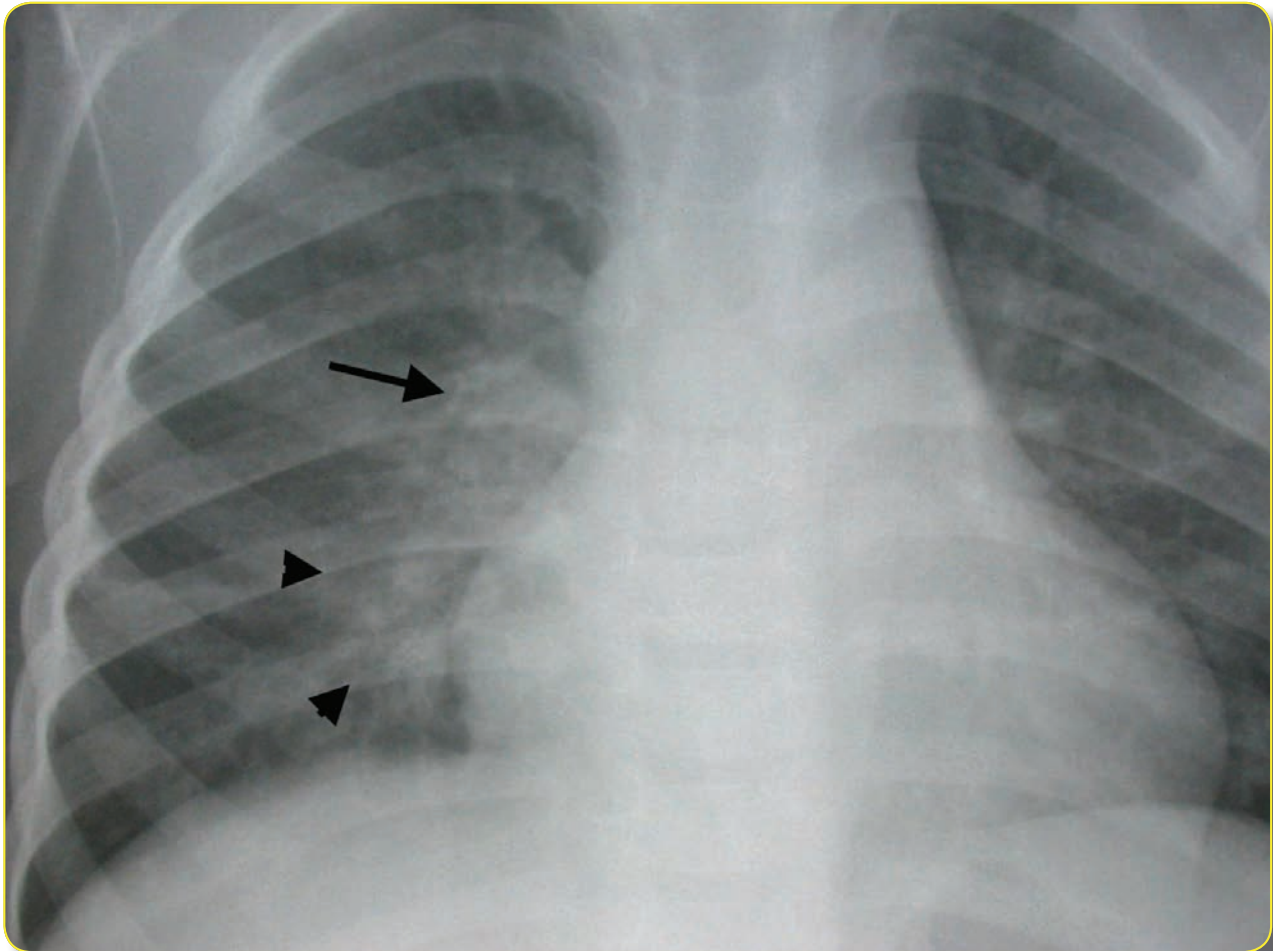


Fig 14.
Ghon complex.
PA radiograph of a child with primary TB shows airspace consolidation in the right lower lung (arrowheads) that partially obscures lymphadenopathy in the right lung hilum (long arrow).

Pediatric Intrathoracic Tuberculosis (cont...)

Hilar Lymphadenopathy

Intrathoracic lymphadenopathy is the most common and characteristic radiographic finding of primary tuberculosis in children. Enlargement of the intrathoracic lymph nodes represents a local inflammatory response following pulmonary infection and may be the only radiographic finding in 50% of pediatric cases. TB lymphadenopathy is typical in children less than 5 years of age. Unilateral involvement is more common than bilateral disease on plain radiographs. Lymphadenopathy should be visible on posteroanterior (PA) and lateral chest radiographs (see Fig. 10). Lateral views are important since enlarged nodes may be hidden on a single PA view due to the relatively wider mediastinal silhouette in children (Fig. 15). Central pulmonary vessels are part of the normal hilar structures that must be recognized and distinguished from lymphadenopathy (Fig. 16).

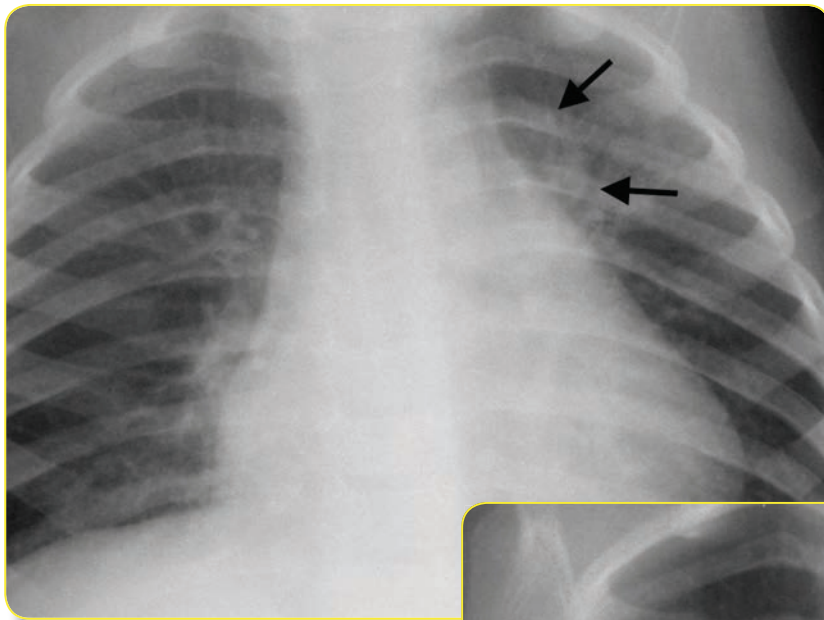
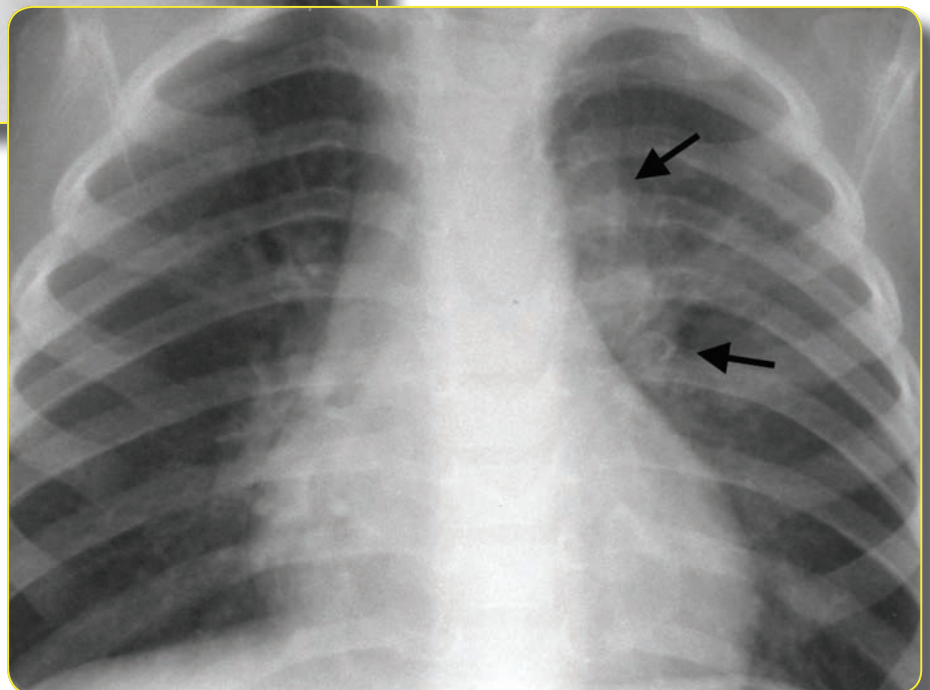


Fig. 15A.
Hidden hilar
lymphadenopathy.
Left hilar enlarged
lymph nodes (arrows)
are partially hidden
by the thymus gland
on this rotated
radiograph.

Fig. 15B.
A better positioned
radiograph of
the same patient
makes the
lymphadenopathy
easier to see
(arrows).

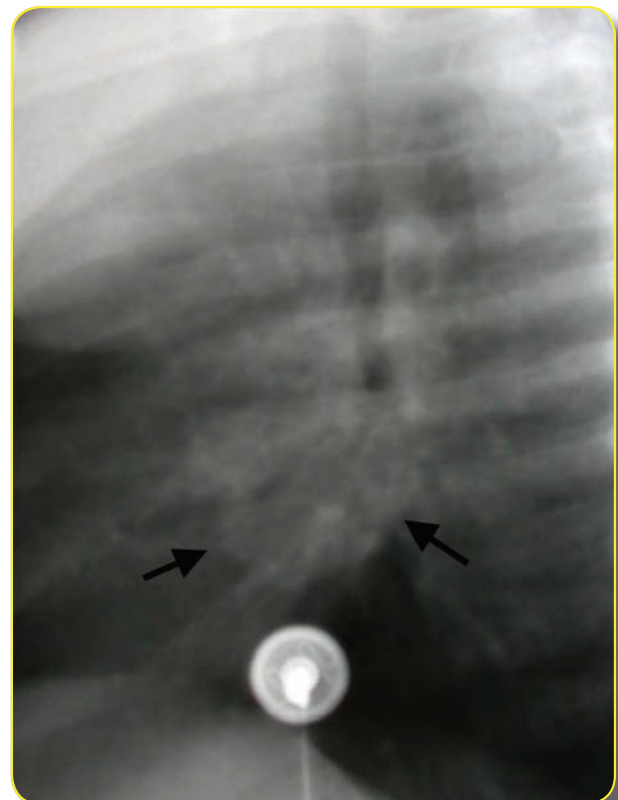


Pediatric Intrathoracic Tuberculosis (cont...)



Fig. 16A.
Hilar lymphadenopathy
versus normal vessels.
Lateral radiograph shows
normal linear vessels
emanating from the lung
hilum.

Fig. 16B.
Lateral radiograph
of a different child
shows nodular opacity
in the lower hilum
(arrows) representing
lymphadenopathy.



Pediatric Intrathoracic Tuberculosis (cont...)

In some cases, lymphadenopathy may be difficult to detect with confidence on plain chest radiographs. The normal thymus gland can be large in infants and can appear indistinguishable from paratracheal or anterior mediastinal lymph nodes, sometimes requiring further imaging with CT (Fig. 17). Ultrasonography has been suggested as another modality for the detection of mediastinal lymphadenopathy, although not commonly used.⁶

TB lymphadenopathy gradually decreases in size after 3 months of treatment, but in some cases there can be a paradoxical, transient increase in lymph node size in the first period of therapy.⁷ In some cases, hilar lymphadenopathy can be visible on radiographs for years. Pre-chemotherapy studies documented the natural history of pediatric tuberculosis describing the resolution of hilar lymph nodes within 6 months in 40%, 1 year in 30% and up to 4 years for the remainder of children followed with no antibiotic treatment.^{1,3,8}

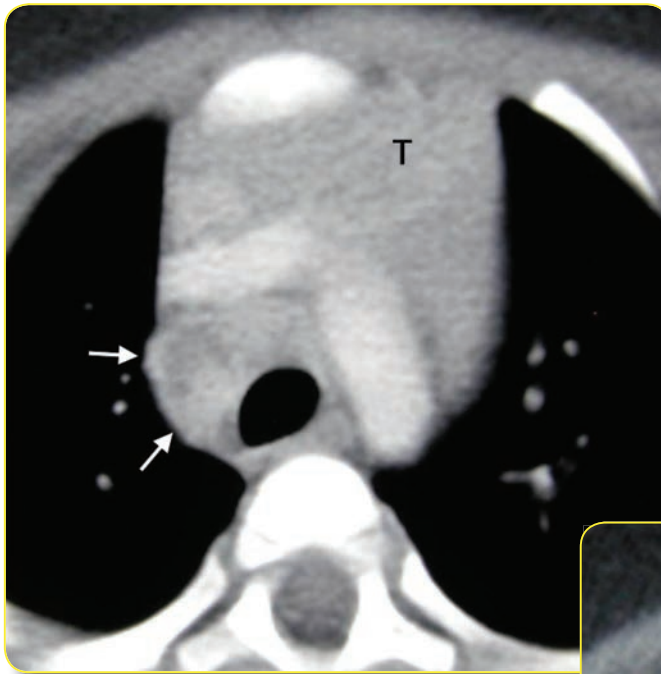
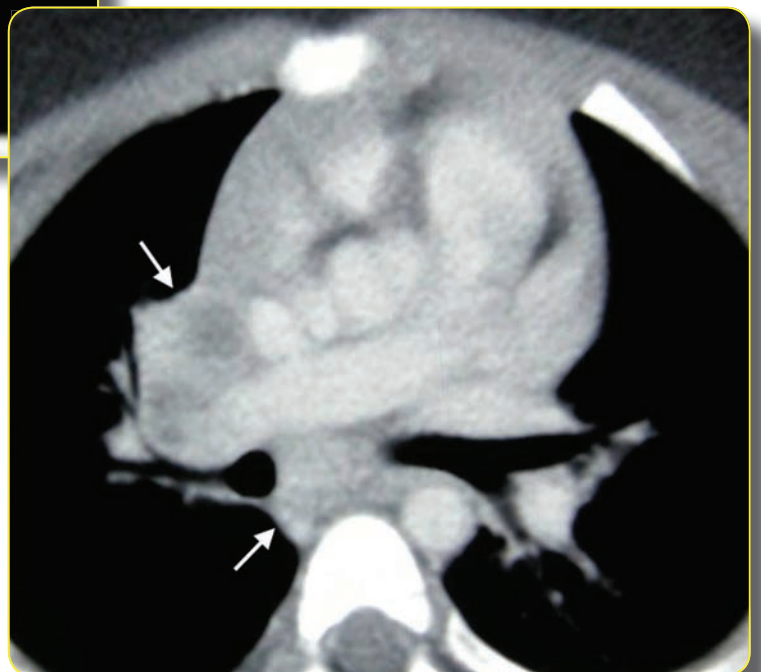


Fig. 17A.
Hilar and mediastinal lymphadenopathy on CT. Contrast enhanced CT images help to distinguish mediastinal lymph node (arrows) from adjacent enhanced vessels. Normal prominent thymus gland (T) enhances homogeneously in this young child.

Fig. 17B.
Another CT image of the same child with primary TB shows enlarged lymph nodes in the right hilar and subcarinal regions (arrows).

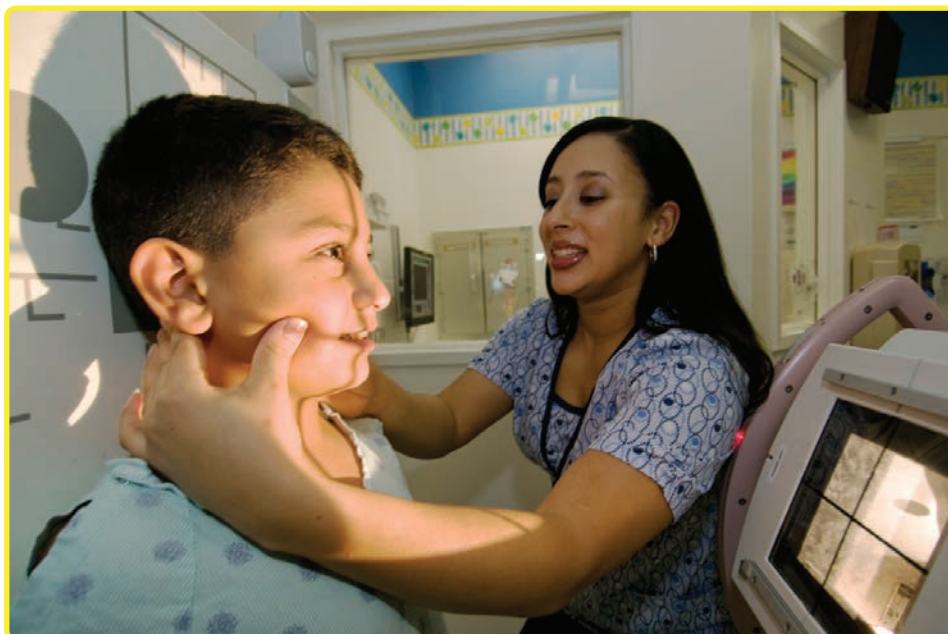


Pediatric Intrathoracic Tuberculosis (cont...)

Considerations for CT in Children

A normal chest radiograph in an otherwise healthy child with a positive tuberculin skin test or interferon-gamma release blood assay is the hallmark of latent TB infection. Chest CT is not indicated for further evaluation of a normal plain chest radiograph in a healthy appearing child being assessed for tuberculosis. Normal chest radiographs are occasionally reported in children with clinically suspected TB and positive gastric aspirate or sputum cultures (3-4%).^{9,10} Small air space opacities may be detected on repeat chest radiograph a few days later or on CT scan. For patients with clinical symptoms of disease but no findings on radiographs, CT becomes an important consideration. Since CT improves detection of lymphadenopathy, it is used in many research publications.^{11,12,13} Even with CT, detection of intrathoracic lymphadenopathy can be difficult with less than perfect agreement demonstrated between radiologists.^{14,15}

The increased cost and higher radiation exposure with CT must be taken into consideration. Infants and children are more vulnerable to the effects of radiation because of more rapidly dividing cells and longer remaining life span.¹⁶ One CT scan of the chest delivers a radiation dose equal to approximately 150 chest radiographs. CT techniques should be adjusted for the smaller size of children to reduce radiation exposure. Chest CT for TB should be performed with intravenous contrast to help distinguish normal structures from lymphadenopathy (Fig. 18). Newer generation multidetector CT scanners provide better resolution than older single detector scanners.



Pediatric Intrathoracic Tuberculosis (cont...)

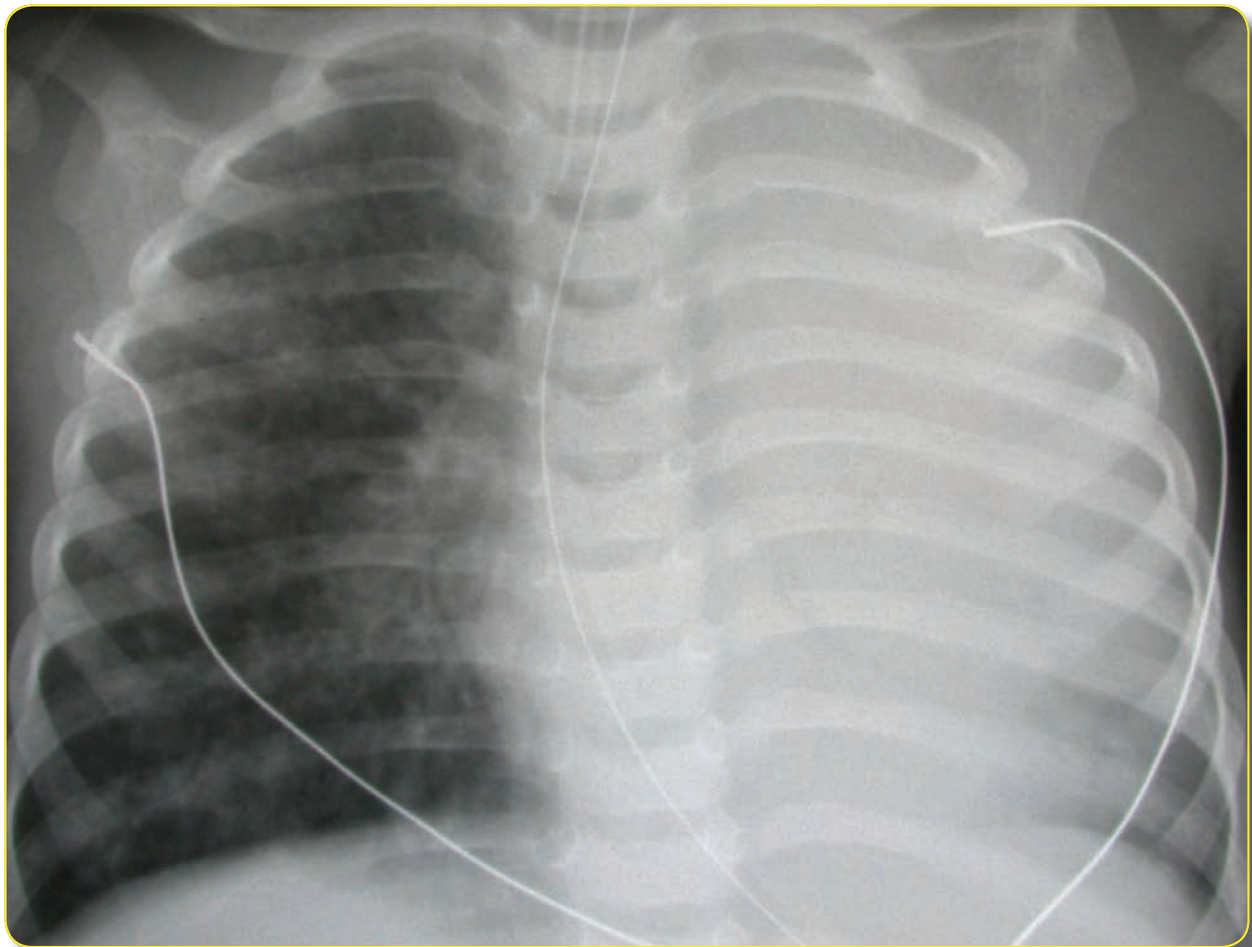


Fig. 18A.
Radiograph of a child with tuberculosis shows dense consolidation in the left upper lobe, masking the presence of lymphadenopathy.

Pediatric Intrathoracic Tuberculosis (cont...)

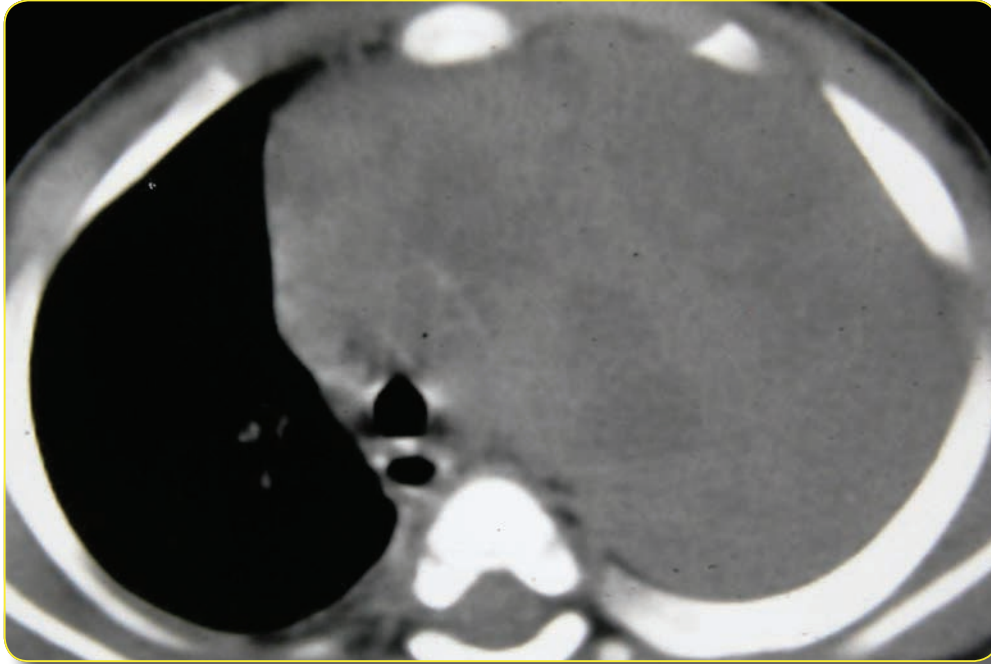


Fig. 18B.
CT performed without intravenous contrast shows only heterogeneous consolidation. The mediastinal structures and vessels are not distinguishable without contrast.

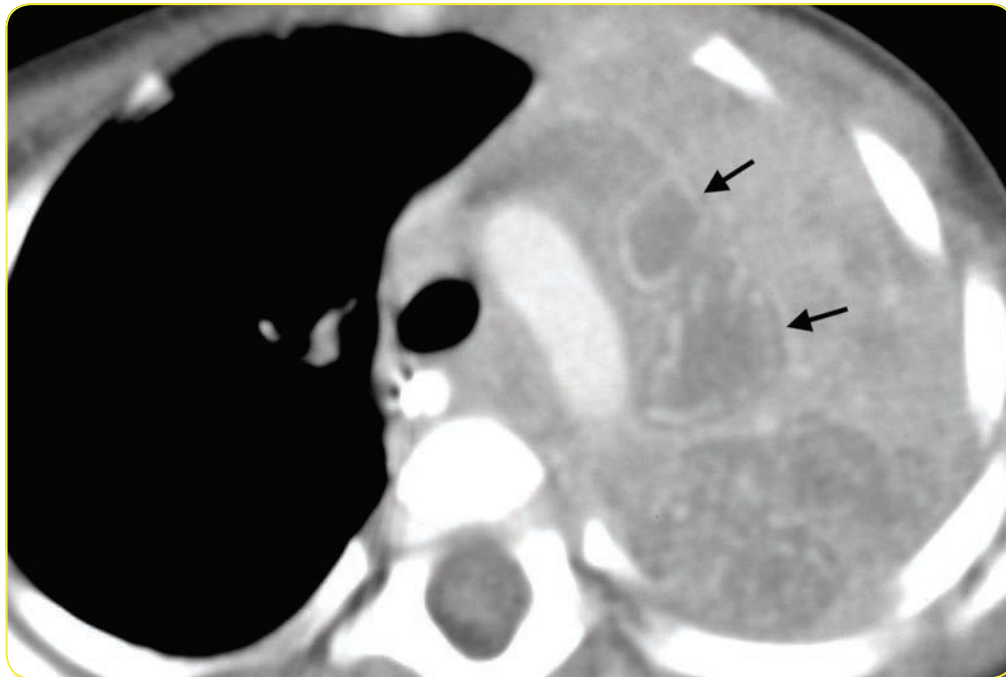


Fig. 18C.
Contrast-enhanced CT of the same child better identifies anterior mediastinal low attenuation lymph nodes with peripheral enhancement (arrows), with a large area of adjacent lung consolidation.

Pediatric Intrathoracic Tuberculosis (cont...)

Tuberculous lymphadenopathy often shows a characteristic pattern on CT consisting of a low-attenuation center surrounded by a thin, sometimes interrupted rim of enhancement (Fig. 19).^{11,12} Bilateral hilar involvement is more commonly seen on CT compared to plain radiographs. Reported sites of lymphadenopathy on CT, include subcarinal (90%), hilar (bilateral 72%), anterior mediastinal, pericarinal, right paratracheal and multiple sites (96%) on chest CT among children with TB.¹¹ Calcification is less common in children with TB than in adults (Fig. 20). Calcification, a later finding, is more easily seen on CT than on radiographs but can be masked by contrast enhancement.

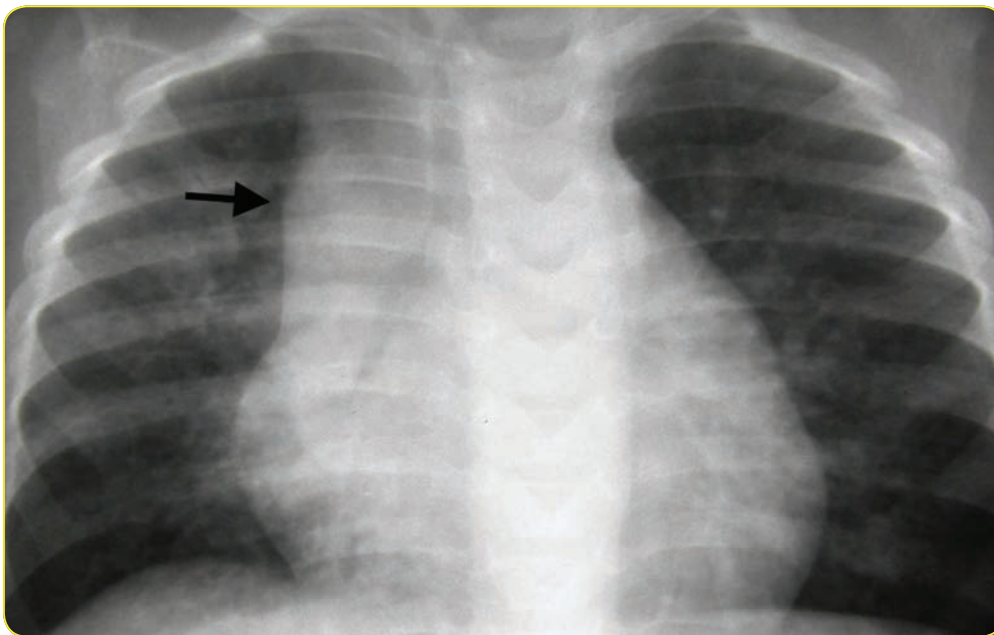
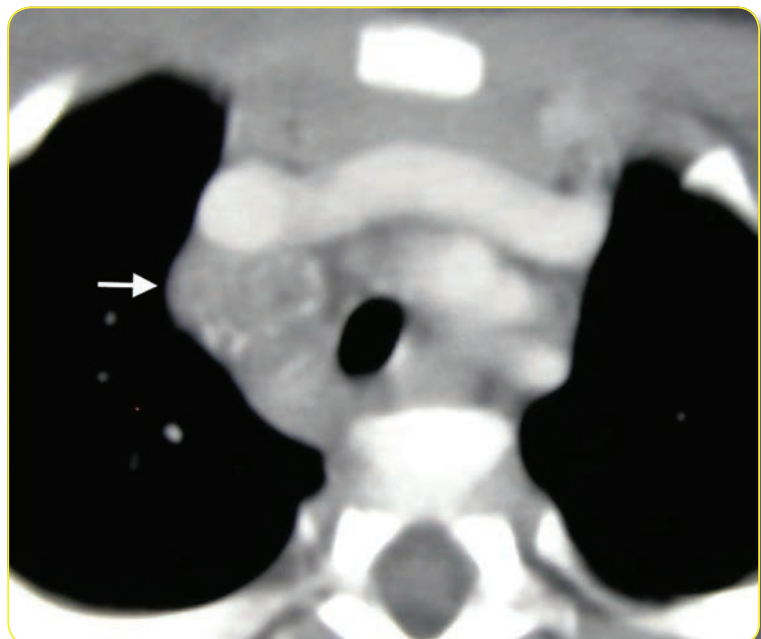


Fig 19A.
Mediastinal lymphadenopathy with overlying thymus gland. Plain radiograph in this infant shows prominent tissue in the right paratracheal region that could represent normal thymus gland (arrow).

Fig. 19B.
Contrast enhanced CT shows retrocaval lymphadenopathy with characteristic thin, slightly interrupted rim of contrast enhancement (arrow).



Pediatric Intrathoracic Tuberculosis (cont...)

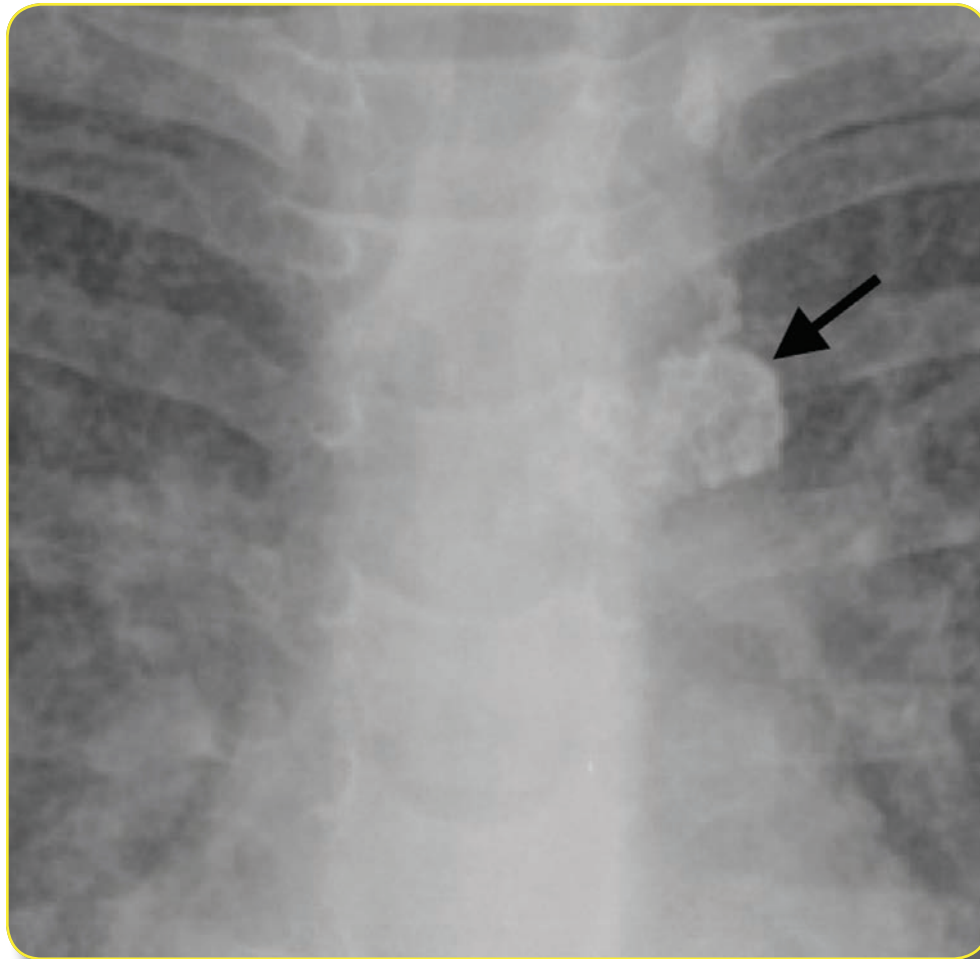


Fig. 20.
Calcified lymphadenopathy.
Note the densely calcified nodule representing a lymph node in the left mediastinum or hilum (arrow).

Complications of lymphadenopathy

Intrathoracic lymphadenopathy may lead to complications as a result of partial or complete airway obstruction or erosion into airways. Partial bronchial obstruction secondary to compression by lymphadenopathy or luminal narrowing by endobronchial granulomas can cause a ball-valve phenomenon that results in progressive over inflation of a portion of the lung (Fig. 21). Atelectasis may be seen with complete extrinsic compression or intrinsic endobronchial involvement causing obstruction (Fig. 22, 23). Rarely, erosion may result in intrabronchial spread with patchy consolidation affecting multiple distal lung segments (Fig. 24).¹⁷ Bronchiectasis may result, especially after extensive TB disease or in cases with severe secondary pulmonary infections such as viral bronchiolitis, pertussis or other infections.

Pediatric Intrathoracic Tuberculosis (cont...)

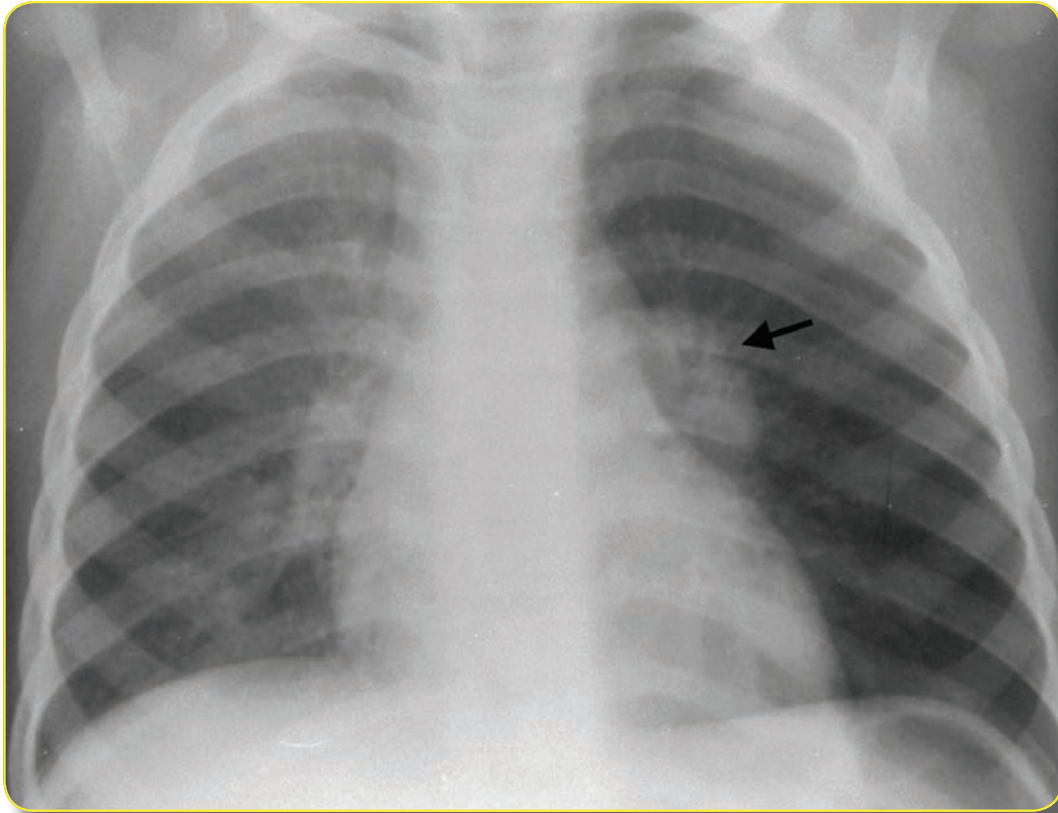
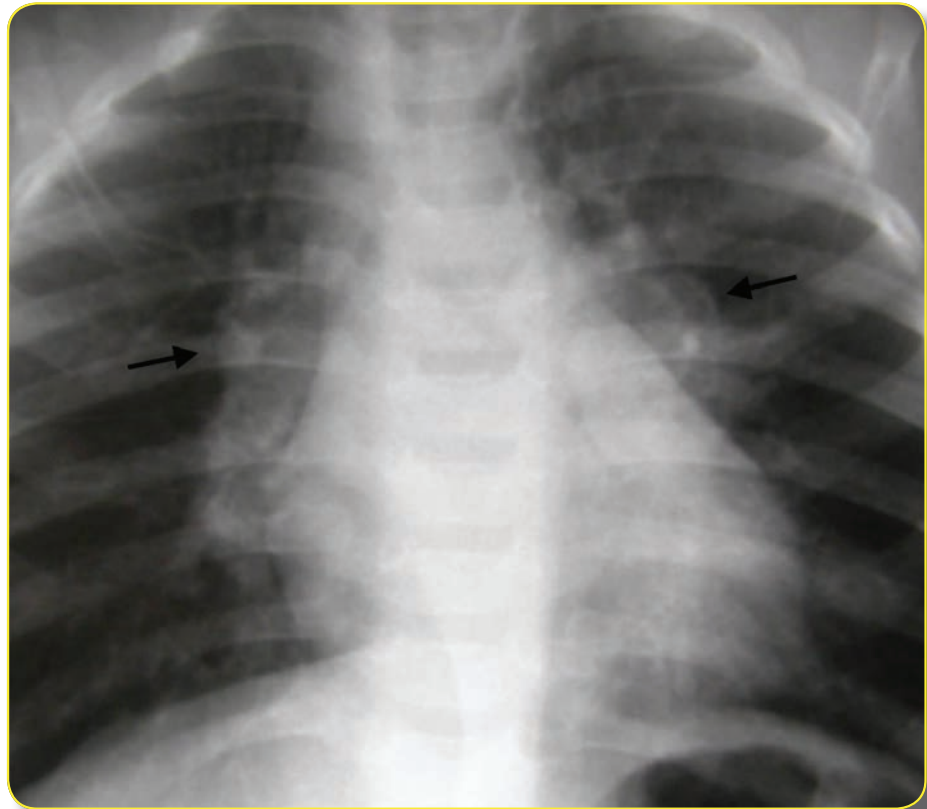


Fig. 21.
Obstructive emphysema caused by hilar lymphadenopathy. Overinflation of the left lung is the result of partial obstruction of the left mainstem bronchus by adjacent hilar lymphadenopathy (arrow).

Fig. 22A.
Progressive atelectasis in a child with primary TB. This initial radiograph shows prominent bilateral hilar lymphadenopathy (arrows).



Pediatric Intrathoracic Tuberculosis (cont...)

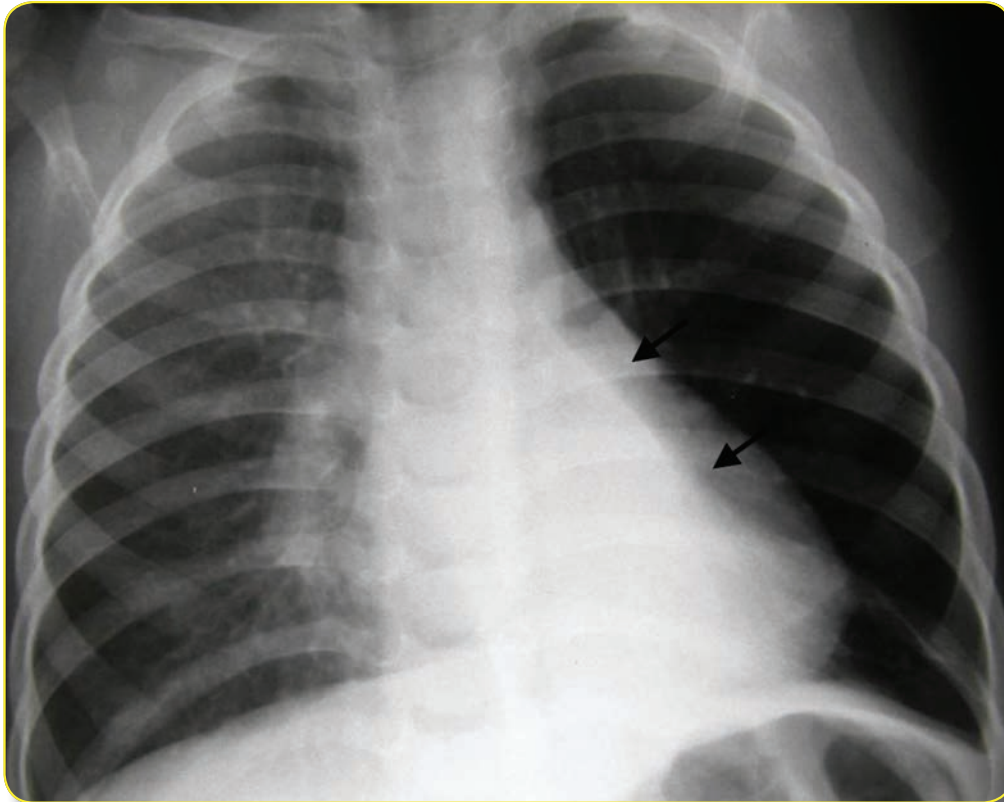
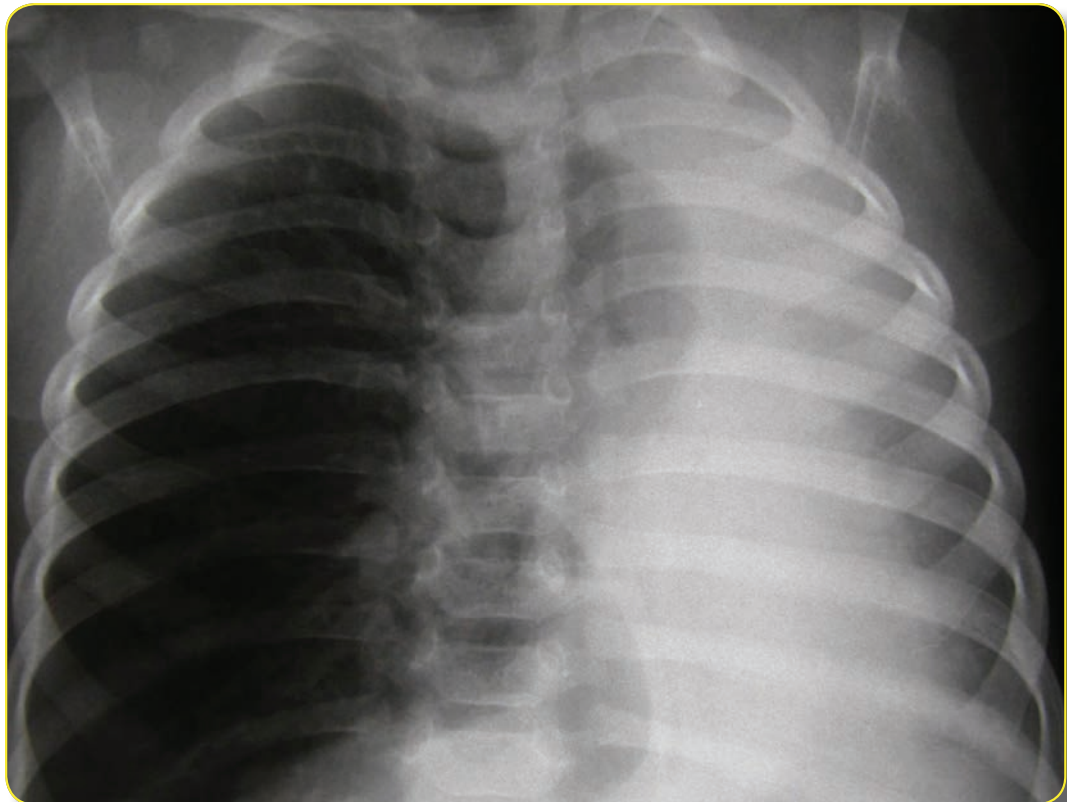


Fig. 22B.
Radiograph taken one month later shows well-defined opacity in the left lower lobe representing atelectasis (arrows) and hyperinflation of the left upper lobe.

Fig. 22C.
Atelectasis has progressed to collapse of the entire left lung in the same child one week later.



Pediatric Intrathoracic Tuberculosis (cont...)

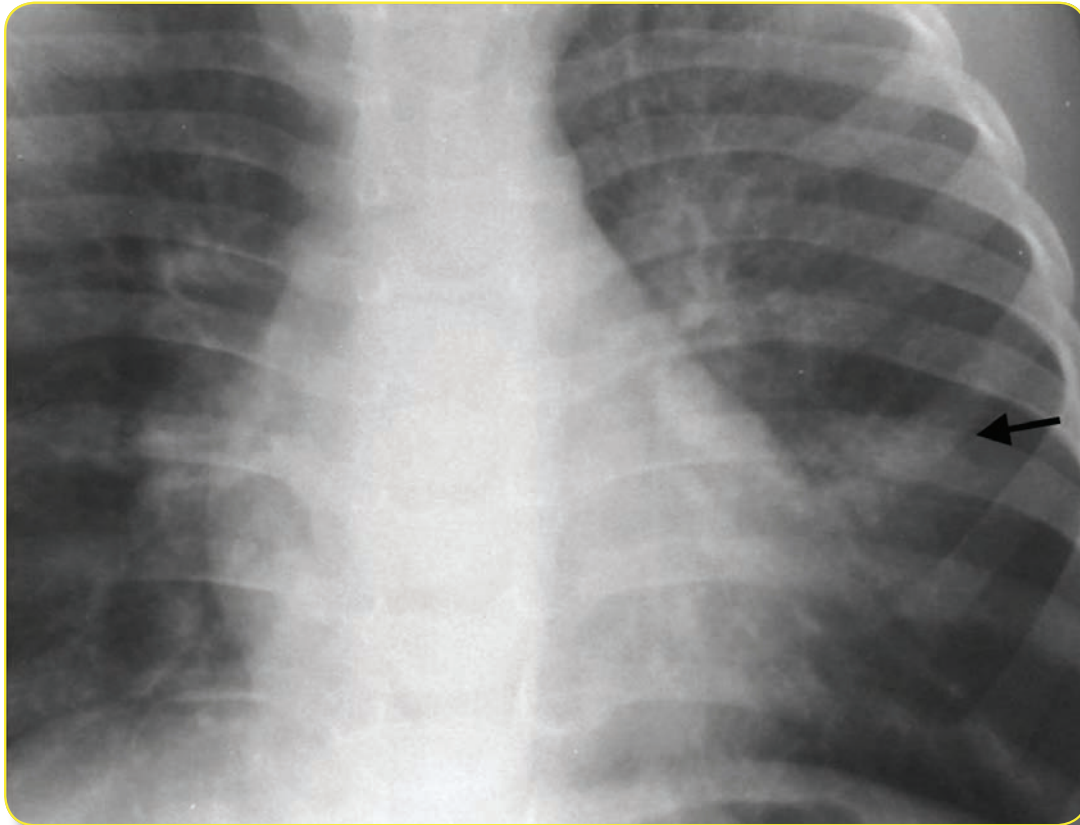
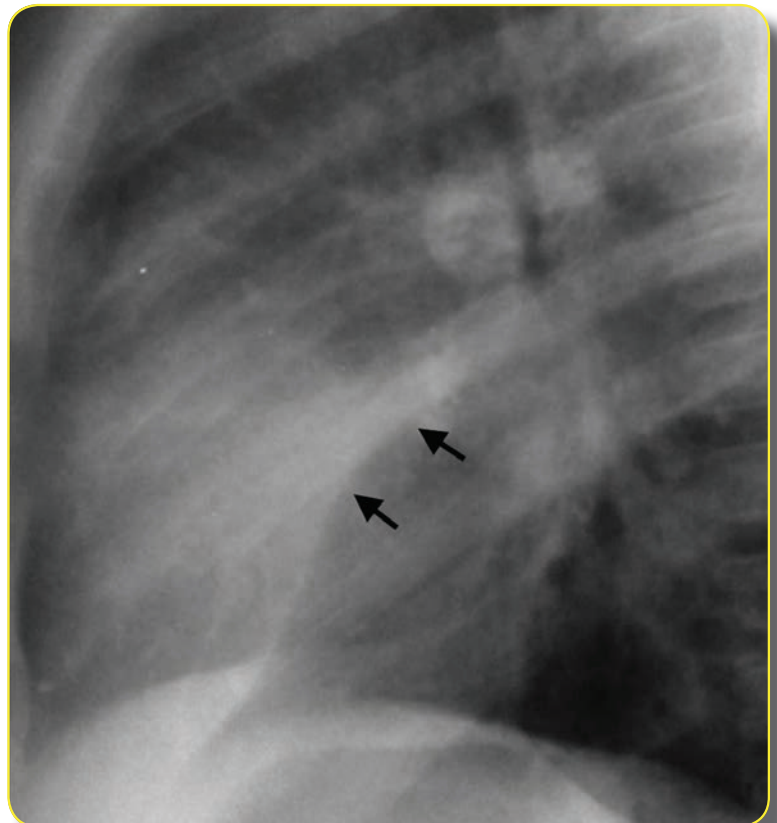


Fig. 23A.
Mild atelectasis
with TB.
Radiograph in
a child shows
vague haziness in
the left mid lung
(arrow).

Fig. 23B.
Lateral view of the
same child reveals
elongated opacity in
the lingula with bowing
of the oblique fissure
toward the opacity
indicating volume loss
(arrows). Nodular
opacity in the left hilar
region on both PA and
lateral views suggests
lymphadenopathy.



Pediatric Intrathoracic Tuberculosis (cont...)

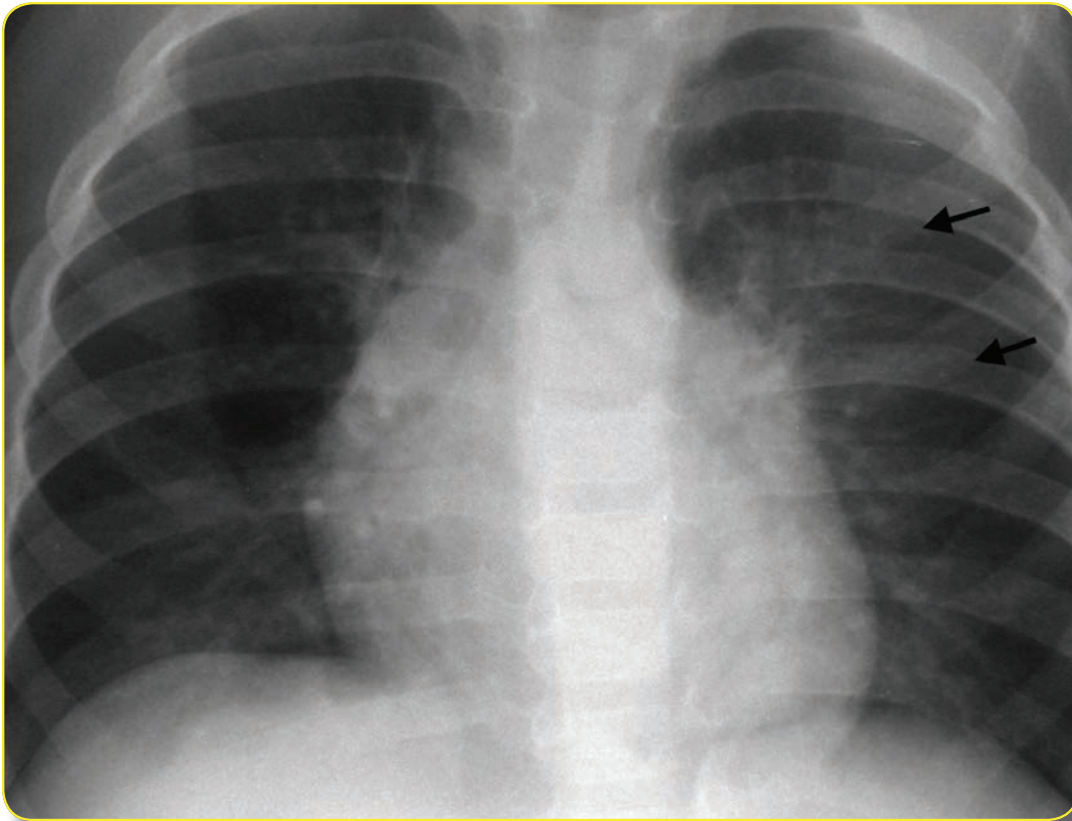
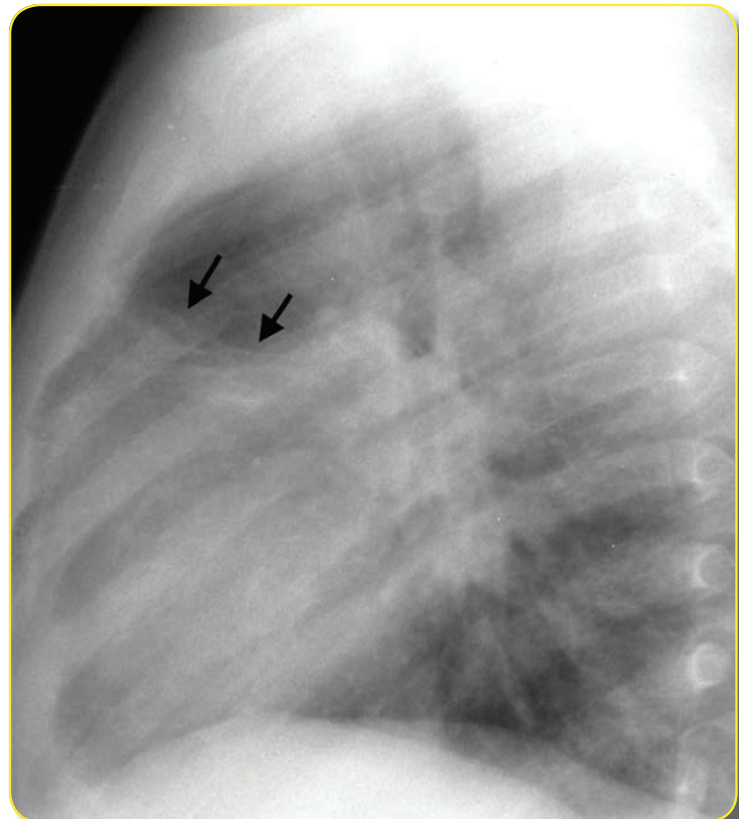


Fig. 23C.
Another child with ill-defined hazy opacity in the left upper lung (arrows)

Fig. 23D.
Linear subsegmental atelectasis is apparent on the lateral view of this child.



Pediatric Intrathoracic Tuberculosis (cont...)

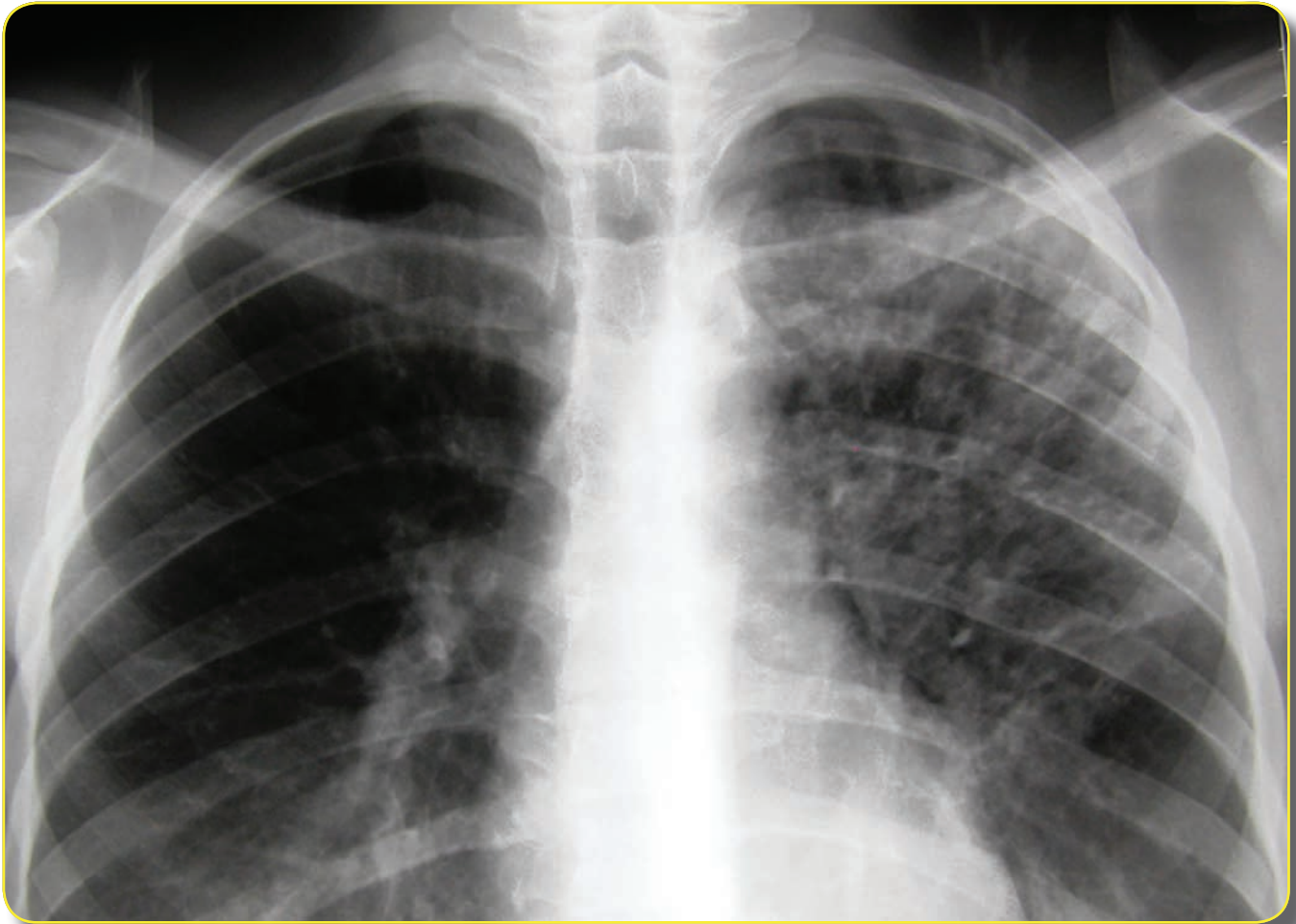


Fig. 24.
Endobronchial spread of TB in an adolescent. Note the extensive linear and nodular opacities in the left upper lobe ("bronchopneumonia" pattern) caused when infected material ruptures into a bronchus.

Pediatric Intrathoracic Tuberculosis (cont...)

Tuberculous pneumonia

Pulmonary parenchymal involvement in TB occurs in children but is less common. Alveolar disease varies from small areas of homogeneous consolidation to large, dense lobar consolidations or multifocal opacities (Fig. 25). Lung involvement can occur in any lobe and does not have a predilection for the lung apices as in the adult reactivation form of tuberculosis. Cavitation is very uncommon, usually only seen in adolescents with reactivation disease and occasionally in infants with extensive disease.

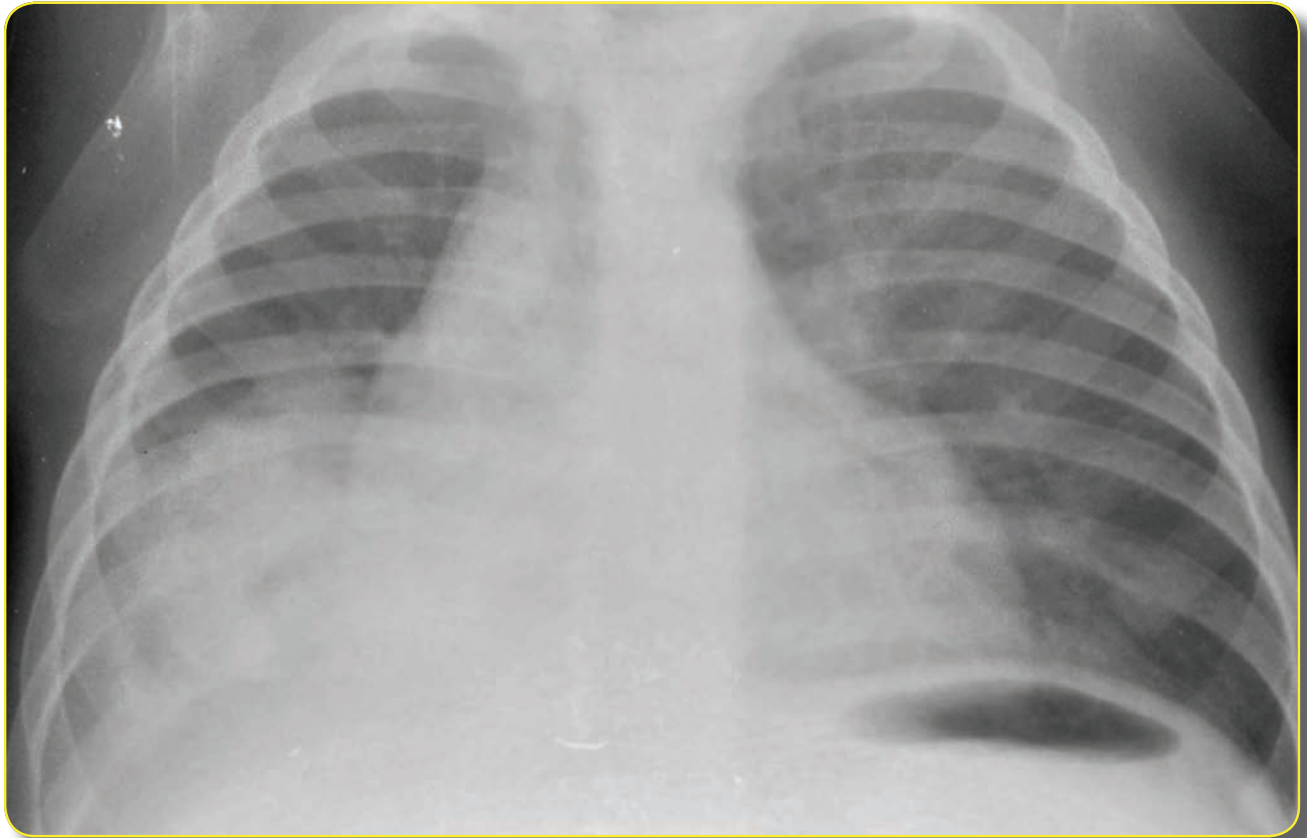


Fig. 25.
Tuberculous pneumonia. The large area of consolidation in the right lower lung is caused by progressive primary TB pulmonary disease.

Miliary Tuberculosis

Miliary TB classically occurs as small, diffuse, nodular opacities evenly distributed throughout all lung fields to the periphery, characteristic of hematogenous dissemination (Fig. 26). Although the name "miliary" implies that the nodules are tiny like millet seeds, the size of the nodules in miliary disease in children may vary from 1-2 mm nodules to large coalescing ill defined patches (Fig. 27). Early miliary TB may be difficult to see radiographically but becomes more easily visible over the course of a few days. CT may more clearly demonstrate the nodules in subtle cases (Fig. 28) and has been described to show ground-glass opacification with early miliary disease.^{18,19} High resolution CT in children with acute disseminated TB may show variation in size, distribution and concentration of nodular opacities. Coalescence of nodules and interstitial thickening can be variable.²⁰ Tuberculosis should always be suspected when miliary infiltrates are seen.

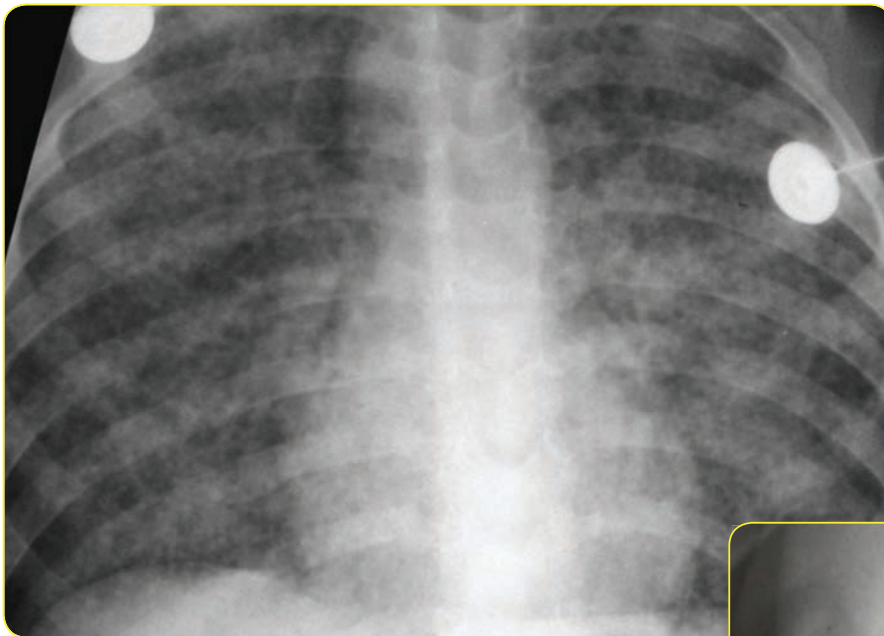


Fig. 26.
Miliary TB.
The lungs are diffusely
studded with small,
uniformly sized
nodules, consistent
with hematogenous
dissemination.

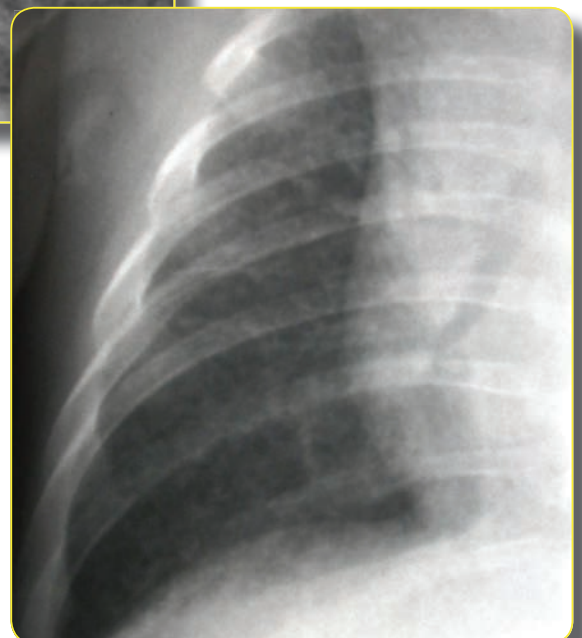


Fig. 27A.
Miliary TB.
Early miliary disease in
this child causes subtle
tiny nodules distributed
evenly through the lung.

Pediatric Intrathoracic Tuberculosis (cont...)

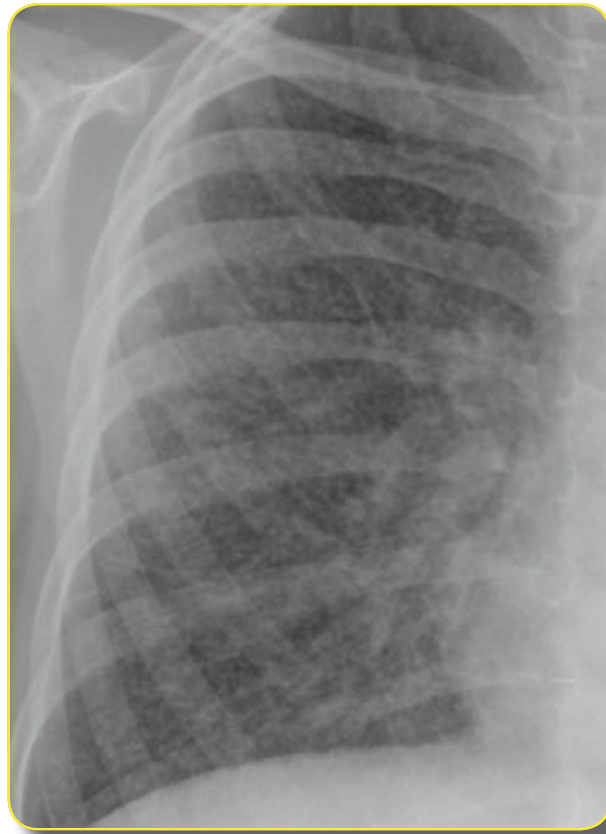
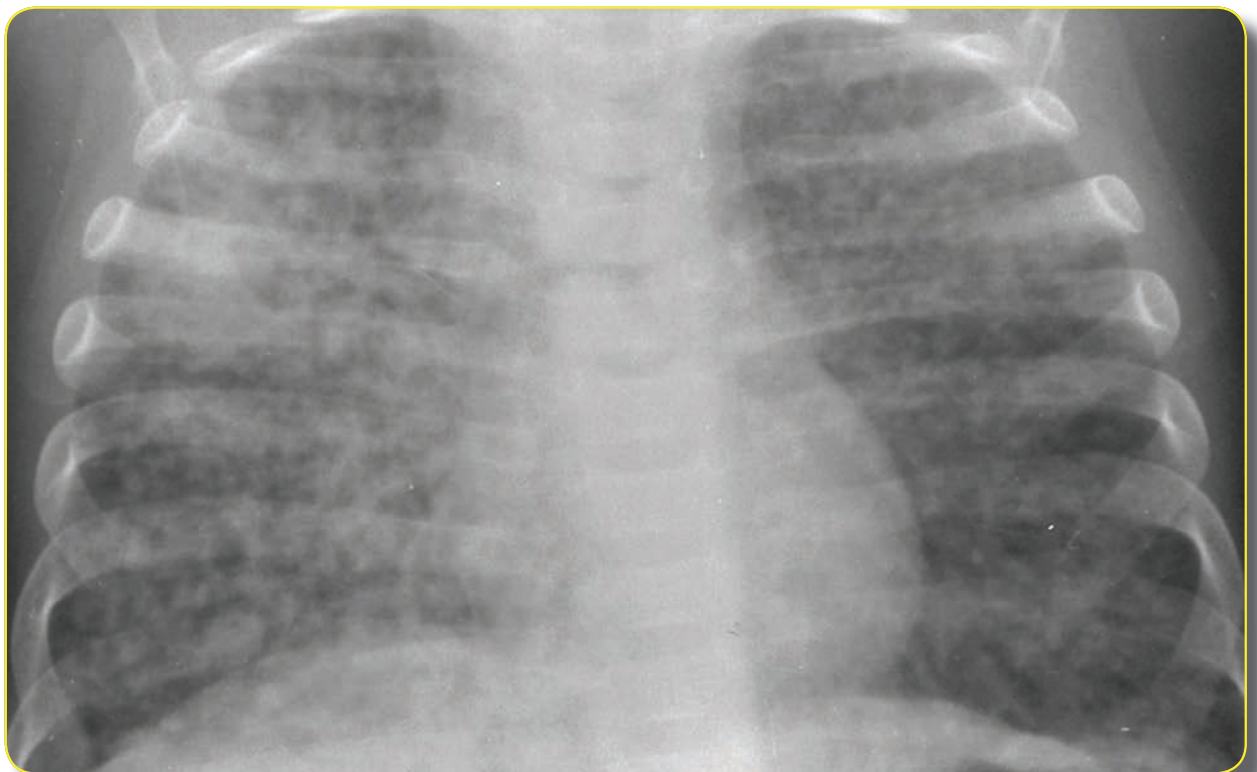


Fig. 27B.
Another child with
more numerous
tiny miliary
nodules.

Fig. 27C.
The nodules
in this child
are slightly
larger than
typical miliary
nodules.



Pediatric Intrathoracic Tuberculosis (cont...)

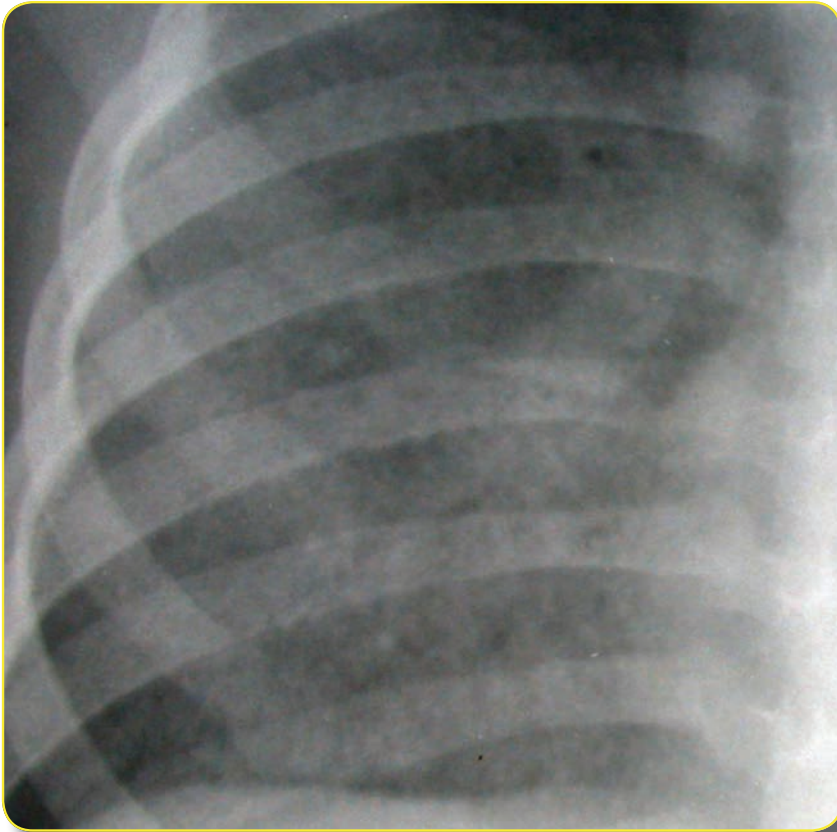


Fig.27D.
Another child with
tiny nodules that are
so numerous that
they appear confluent
and resemble alveolar
disease.

Fig. 28.
Miliary TB.
Tiny miliary nodules
are often more easily
visualized on CT lung
windows.



Pleural effusions

Pleural effusion is an uncommon presenting finding in children with tuberculosis, reported in 1.8% of pediatric cases in the United States between 1993-2003²¹ and 3.9% of cases reviewed in Cape Town, South Africa.²² More commonly pleural effusion in children is a result of other bacterial pathogens which cause pneumonia. Tuberculous pleural effusions are rare in young children but are more frequent in adolescents and in boys (Fig. 29).²³ Most TB pleural effusions are unilateral (92%) and are typically associated with parenchymal involvement (69%)(Fig. 30).²⁴ The size of the effusion may vary from quite small to very large but typically affects less than 2/3rds of the hemithorax.²⁵ Culture and AFB smear of pleural fluid caused by TB has a low yield and is usually not diagnostic, although analysis of the type of fluid may be useful. The fluid is most commonly transudative secondary to a hypersensitivity response. Resolution usually occurs within 1-4 weeks although a small amount of fluid may persist for longer.²⁴ Punch biopsy of the pleura examining histopathology and culture has been shown to have a higher yield than pleural fluid cultures for TB. Chest ultrasound and/or CT can characterize pleural fluid as free flowing or septated and loculated (Fig. 31). Loculated pleural fluid collections usually represent exudates and are much more likely to be caused by other types of bacterial pneumonia. Pleural effusion can rarely be a complication of intra-abdominal tuberculosis.

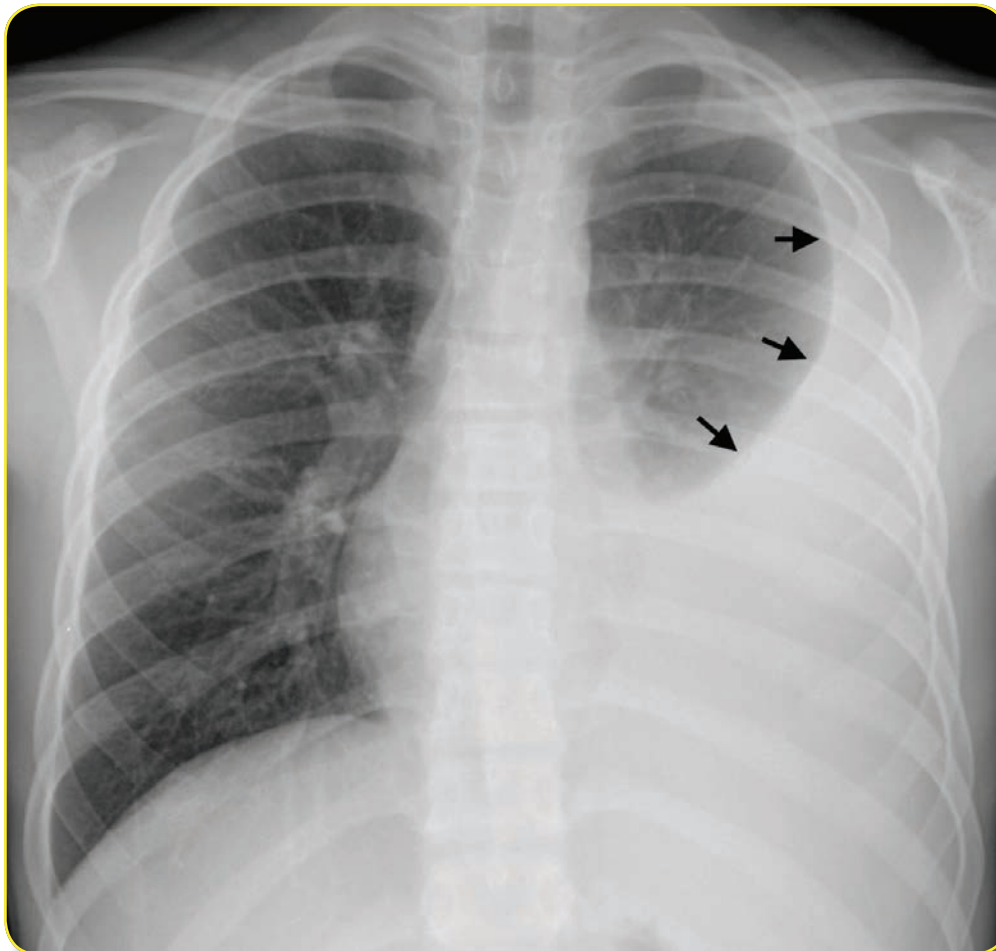


Fig. 29A.
Pleural effusion in an adolescent with TB. The large left sided pleural fluid collection shows the typical "meniscus" sign that indicates a non-loculated pleural effusion (arrows). The effusion hides any consolidation that might be present in the underlying lower lung. The effusion was initially presumed to represent a bacterial empyema.

Pediatric Intrathoracic Tuberculosis (cont...)

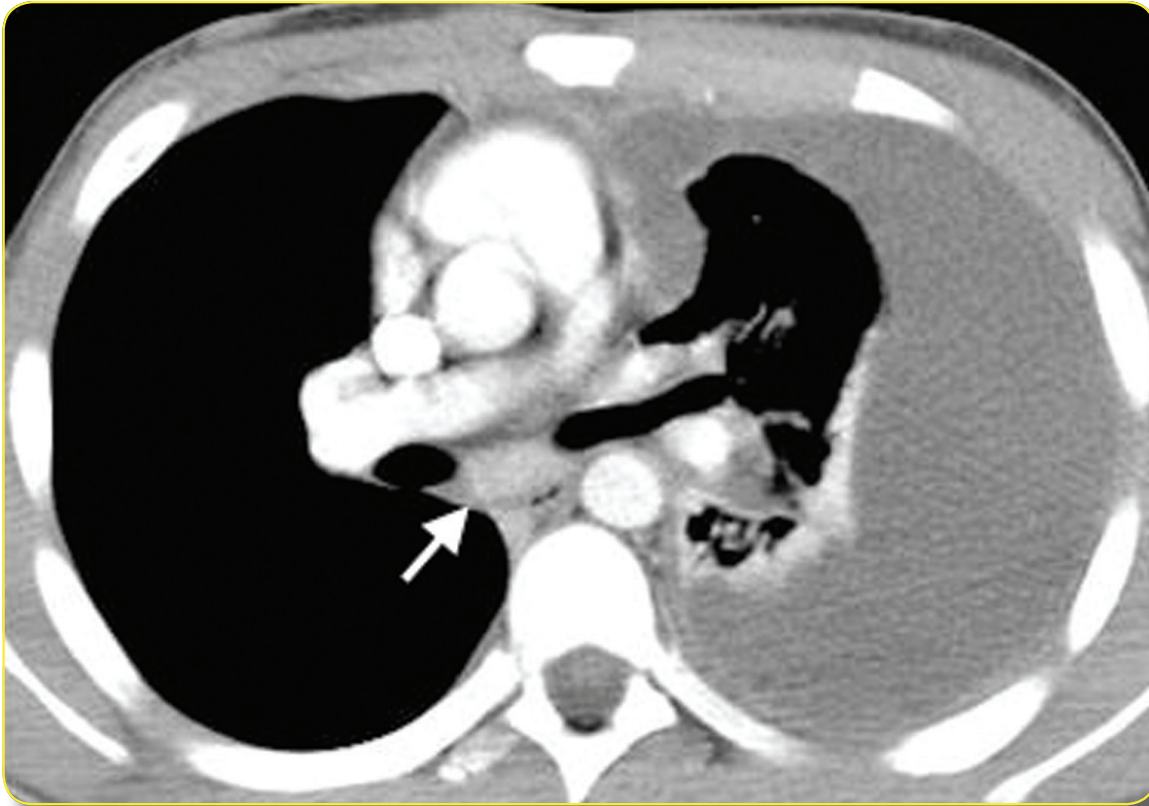
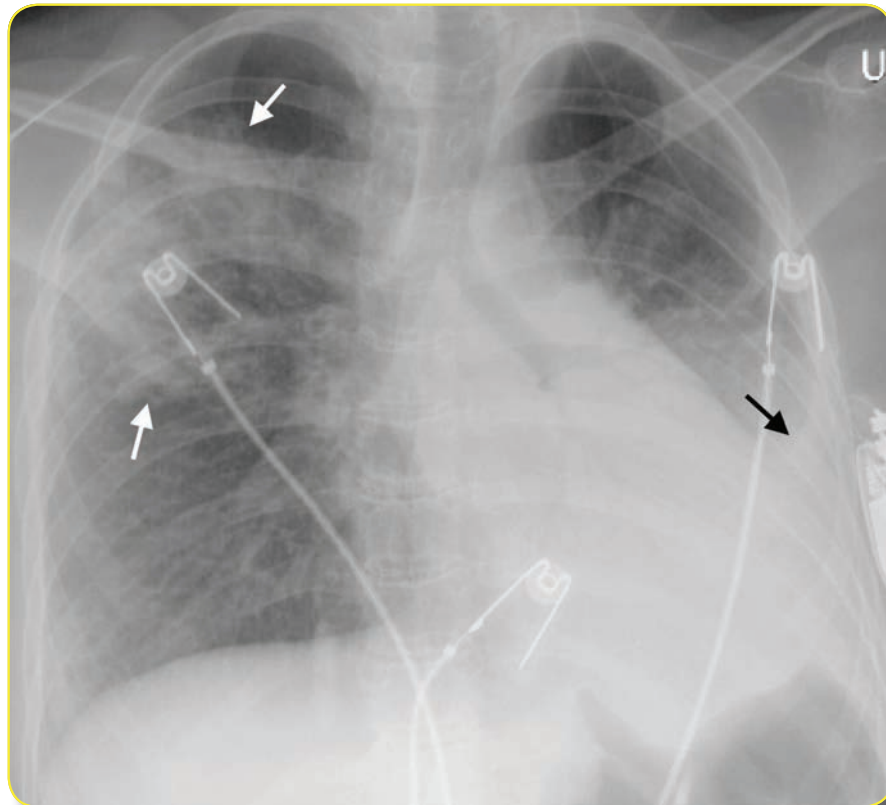


Fig. 29B.
CT of the same patient shows the large effusion with a single enlarged subcarinal lymph node (arrow). The diagnosis of TB was made upon thoracentesis.

Fig. 30A.
Pulmonary tuberculosis with pleural effusion. Radiographic findings include a moderate size left pleural effusion (black arrow) and patchy air space opacities in the right upper lobe (white arrows).



Pediatric Intrathoracic Tuberculosis (cont...)

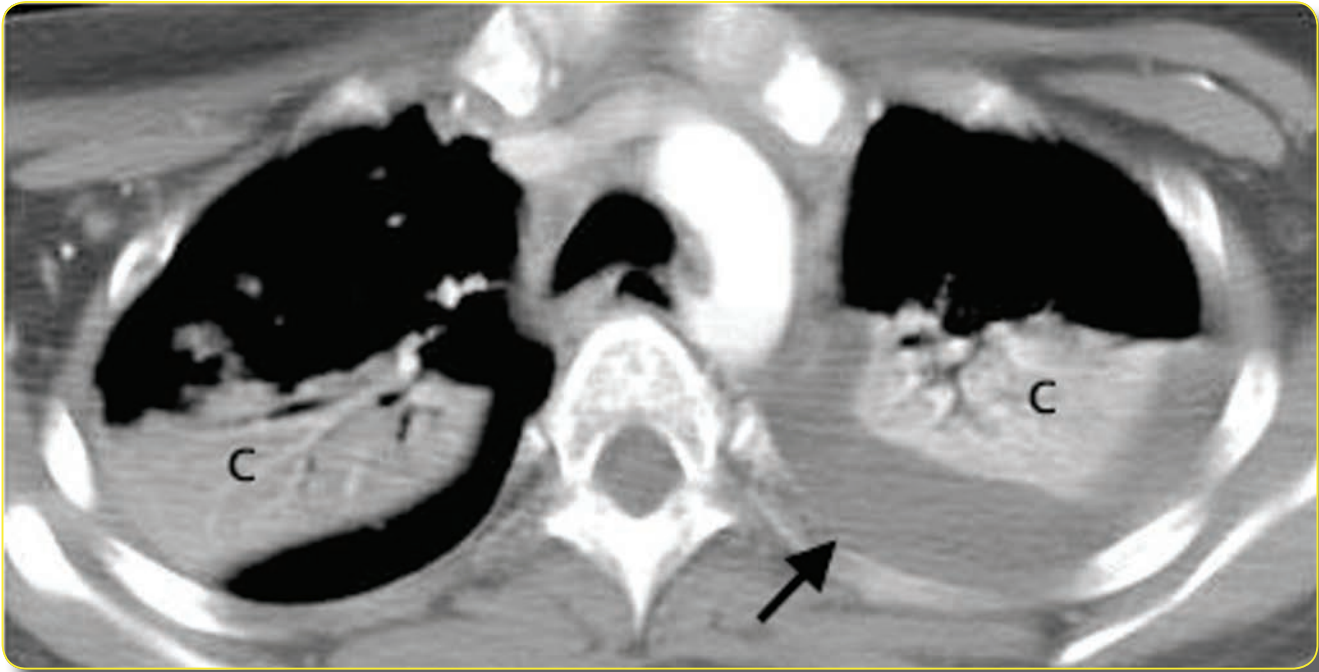


Fig. 30B.
CT of the same patient better defines the pleural effusion (arrow) and bilateral lung consolidations (C) on soft tissue windows.

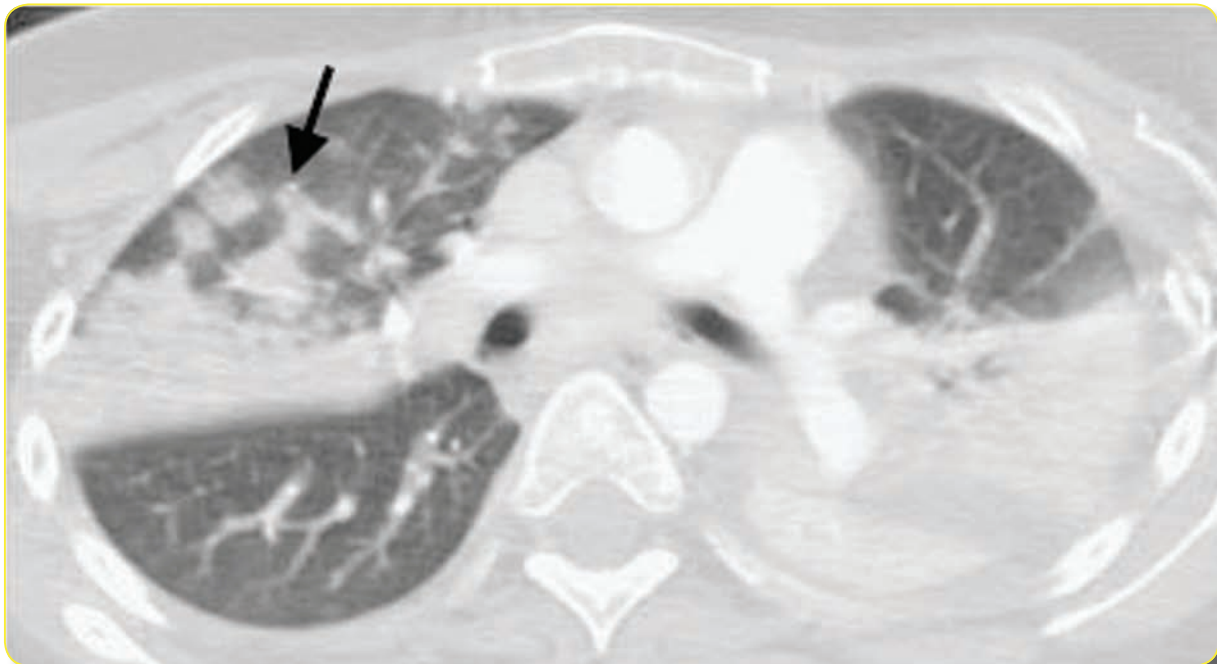


Fig. 30C.
CT with lung windows shows the patchy, slightly nodular pattern of the right upper lobe opacities (arrow).

Pediatric Intrathoracic Tuberculosis (cont...)

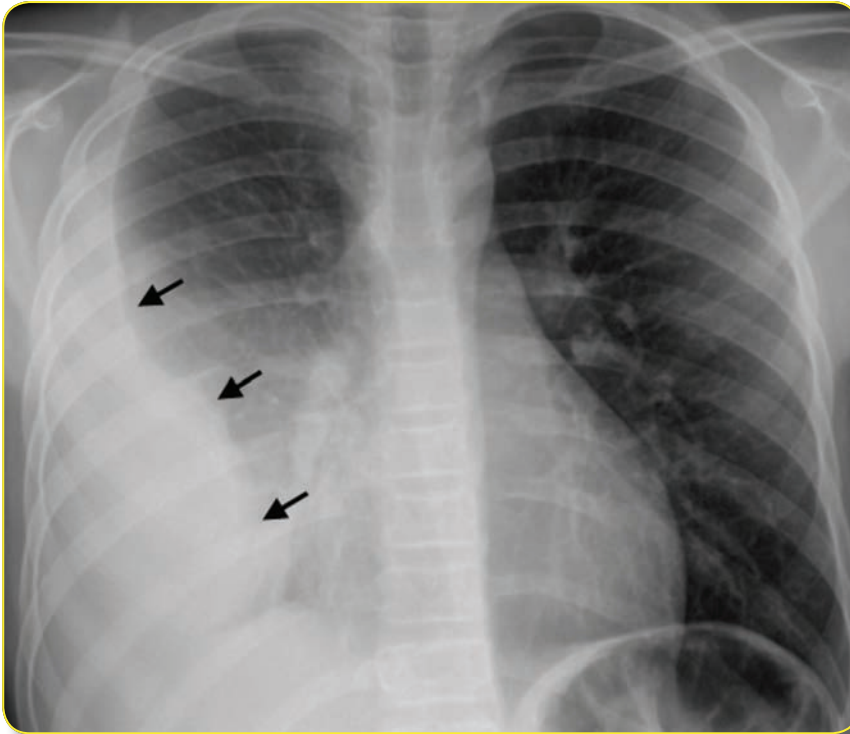


Fig. 31 A.
TB with loculated pleural effusion. PA radiograph shows that the right pleural effusion compresses the lung in an uneven manner (arrows), suggesting loculations within the effusion.

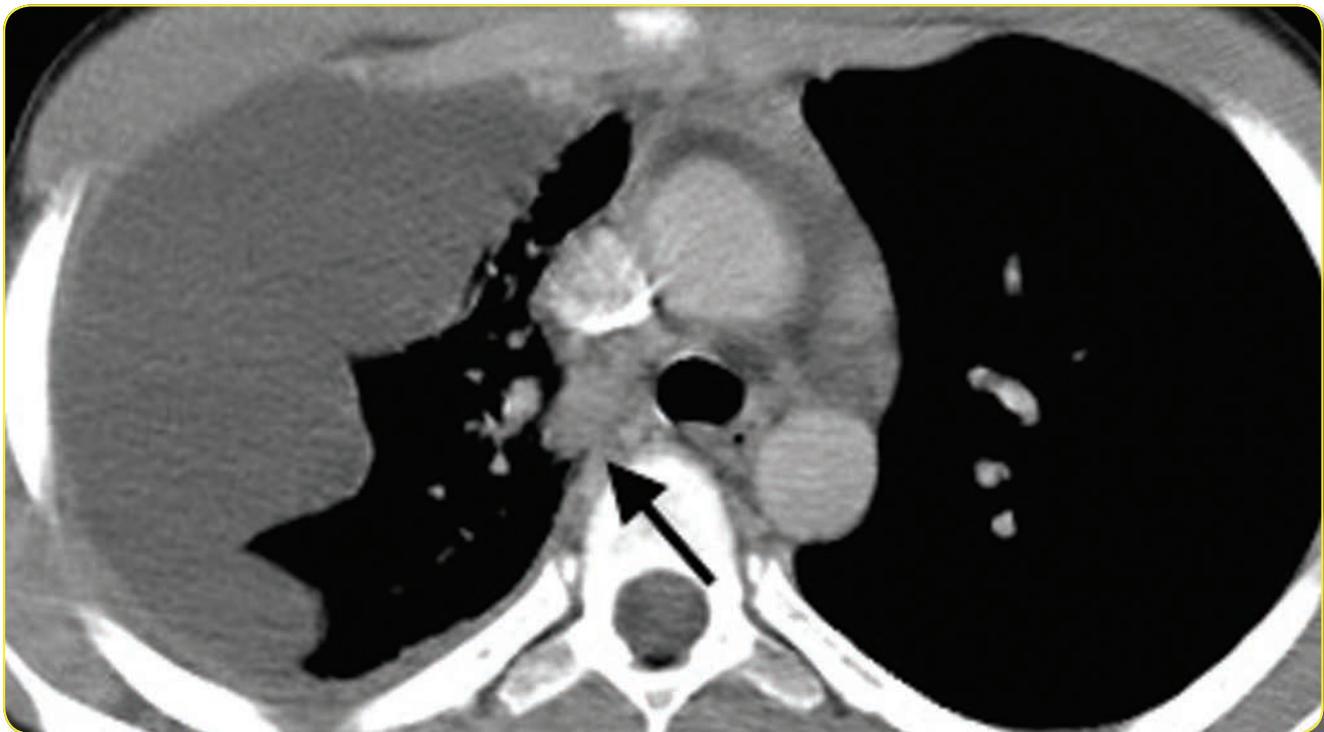


Fig. 31B.
On CT of this patient, the irregular margin of the pleural surface is more evident. The effusion was accompanied by mediastinal lymphadenopathy (arrow).

Pediatric Intrathoracic Tuberculosis (cont...)

Air filled cysts

Cavities are air-filled cysts that occur in an area of lung parenchymal destruction with a persistent bronchial connection. Cavities generally arise within an area of alveolar consolidation and persist after the consolidation resolves (Fig. 32).

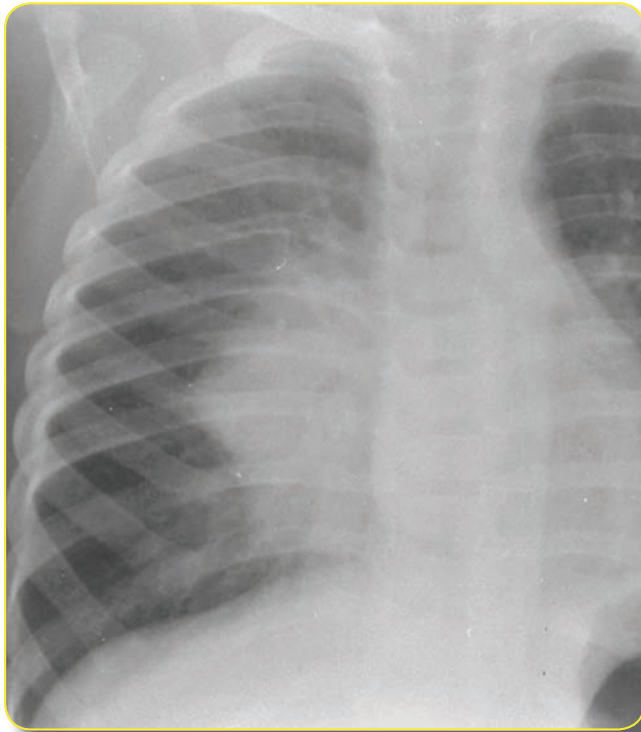
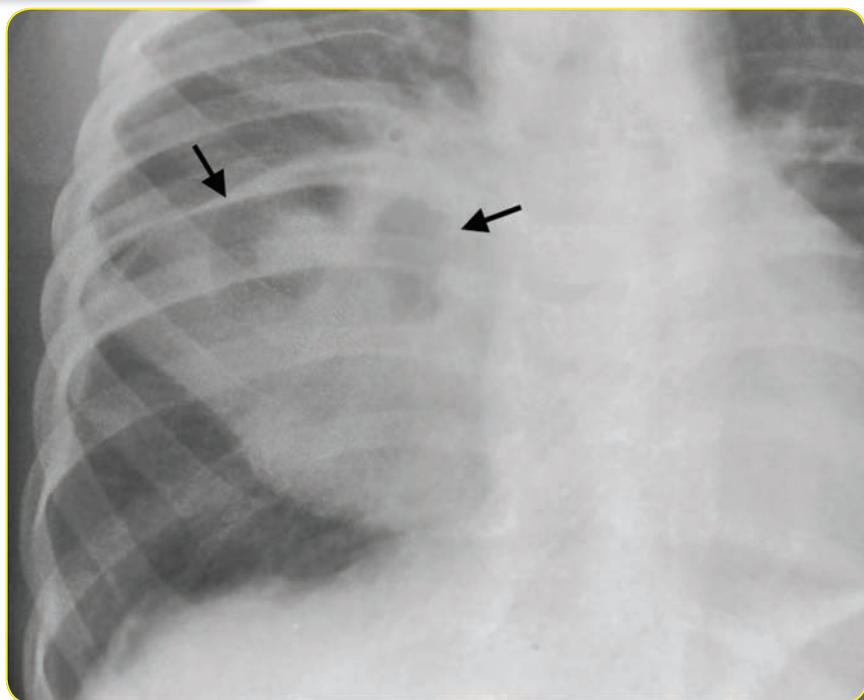


Fig. 32A.
Primary TB with cavitation.
The initial radiograph on this child shows a large area of consolidation in the right parahilar region.

Fig. 32B.
Subsequent radiographs reveal gradual development of multiple air-filled cavities within the consolidation (arrows).



Pediatric Intrathoracic Tuberculosis (cont...)

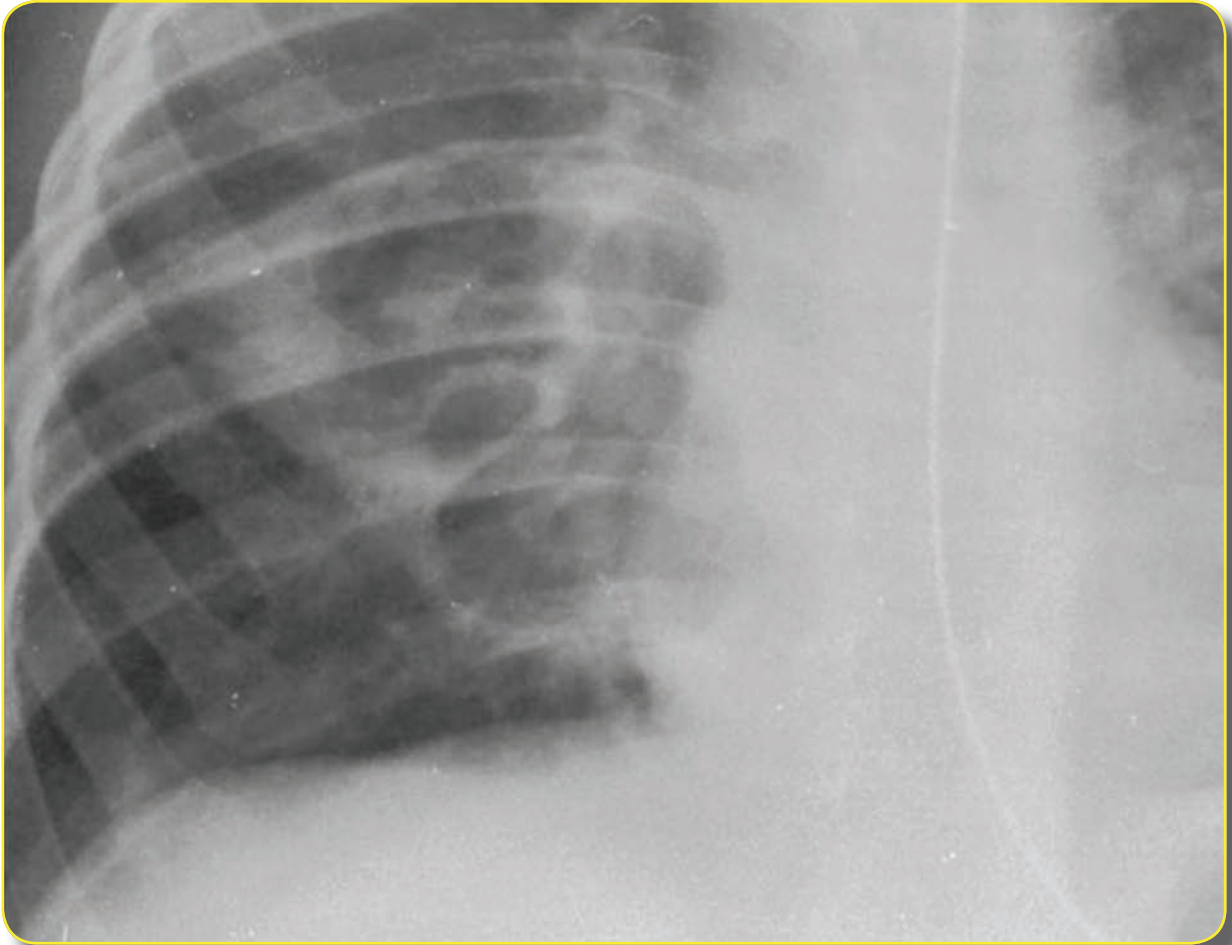


Fig. 32C.
Follow up radiographs show progression of the air-filled cavities.

Pediatric Intrathoracic Tuberculosis (cont...)

Alveolar opacification and cavitation occur occasionally in infants and in immunosuppressed children, including those infected with HIV.^{1,2,5,26} Cavitation is seen with increased frequency in older children and teens compared to younger children, in most cases representing reactivation disease typical of adult TB disease (Fig. 33).

Cavities should be distinguished from pneumatoceles that are more common in pediatric patients (Fig. 34). Pneumatoceles are thin-walled cysts that probably result from partial, ball-valve bronchial occlusion that leads to temporary progressive over-inflation of local alveolar groups. Most pneumatoceles resolve within days to weeks as the disease that caused them subsides, but the time to resolution is variable (Fig. 35). Cavities differ in that they have thicker walls and heal over months to years often resulting in permanent scarring.

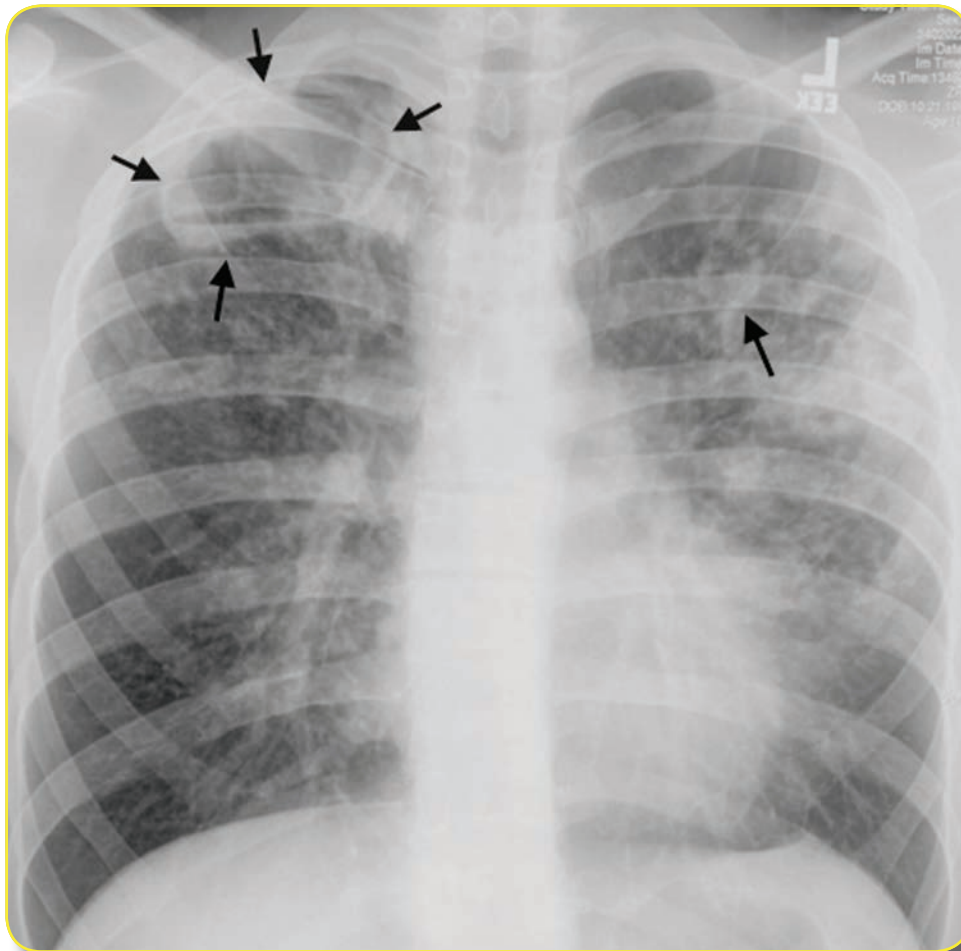


Fig. 33.
16 year old with TB.
Note the patchy and nodular bilateral upper lobe opacities and bilateral air-filled cavities (arrows). The findings are characteristic of the reactivation form of tuberculosis.

Pediatric Intrathoracic Tuberculosis (cont...)

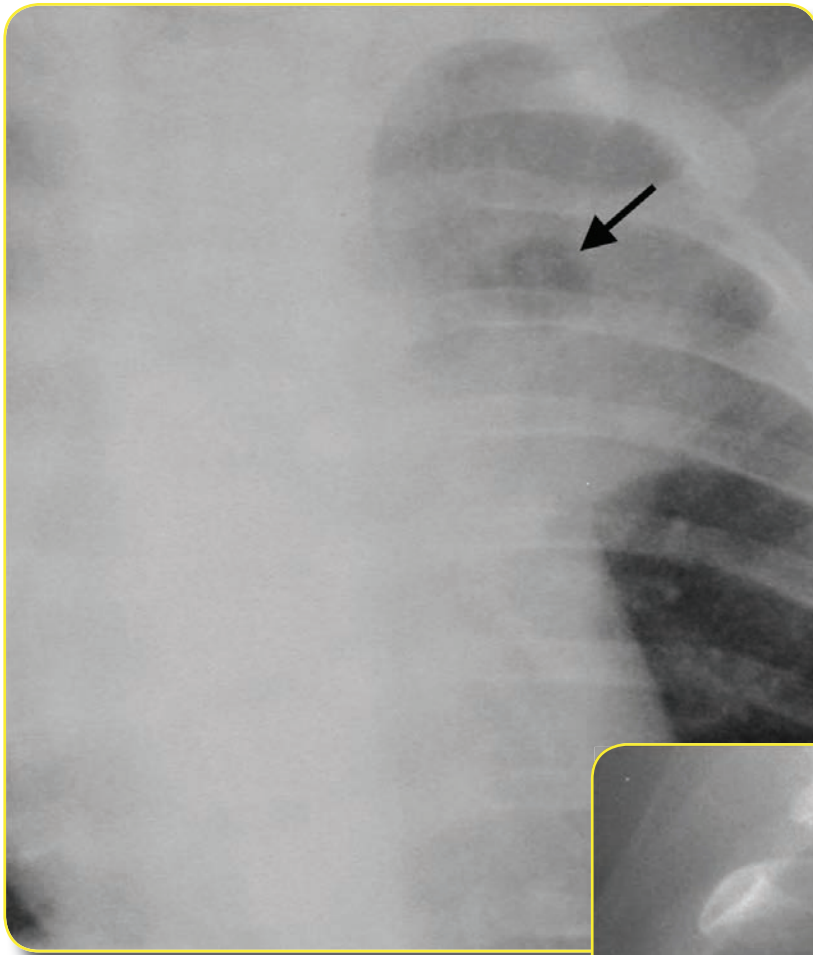


Fig. 34A.
Pneumatoceles in TB.
A small air-filled cyst that developed within the tuberculous lung focus in this young child is a pneumatocele (arrow). The thin wall is obscured by the surrounding lung consolidation.

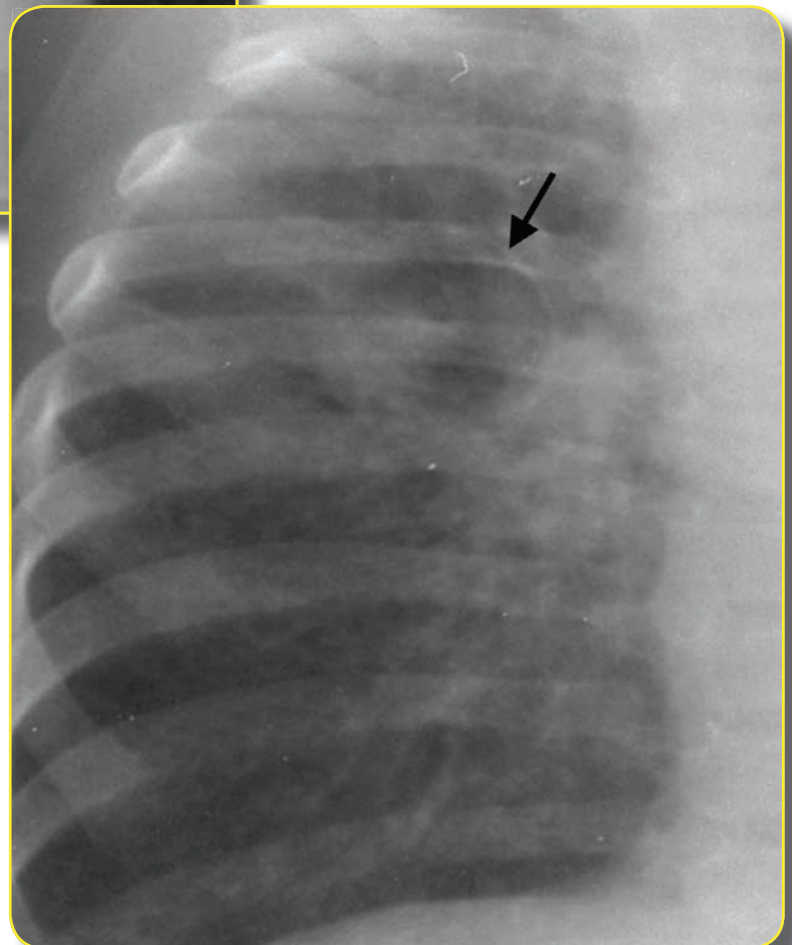


Fig. 34B.
The isolated pneumatocele in another child shows the characteristic thin wall of these air-filled cysts (arrow).

Pediatric Intrathoracic Tuberculosis (cont...)

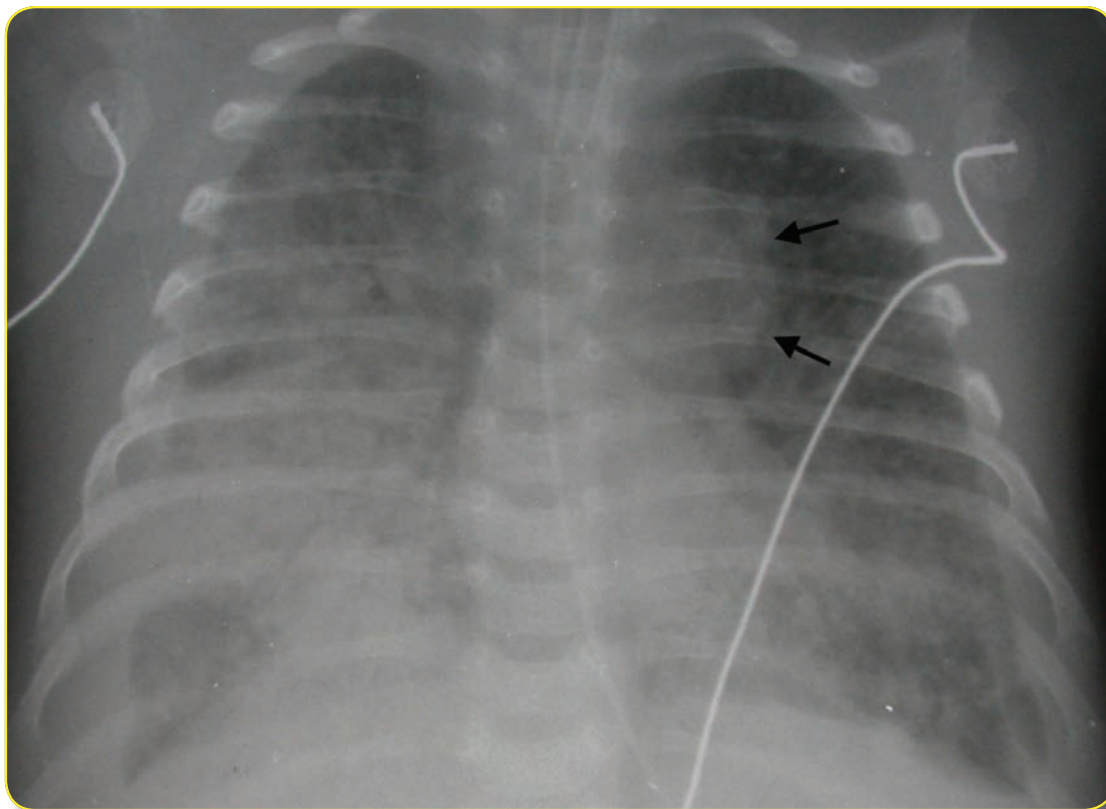
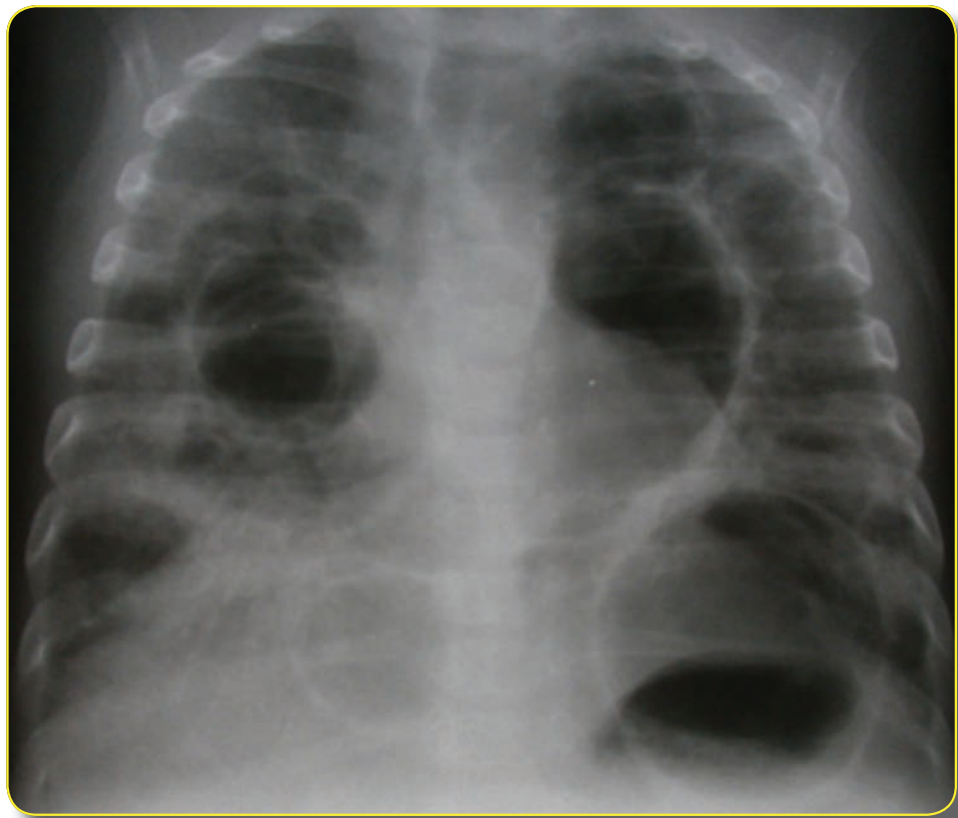


Fig. 35A.
Congenital TB.
This 5 week old infant presented initially with multiple areas of lung consolidation, small nodular lung opacities and bilateral pleural effusions. A left hilar mass consistent with lymphadenopathy suggested the diagnosis of TB (arrows).

Fig. 35B.
Several weeks later, the lung consolidations resolved and were replaced by large air-filled cysts that persisted until the time of discharge



Pediatric Intrathoracic Tuberculosis (cont...)

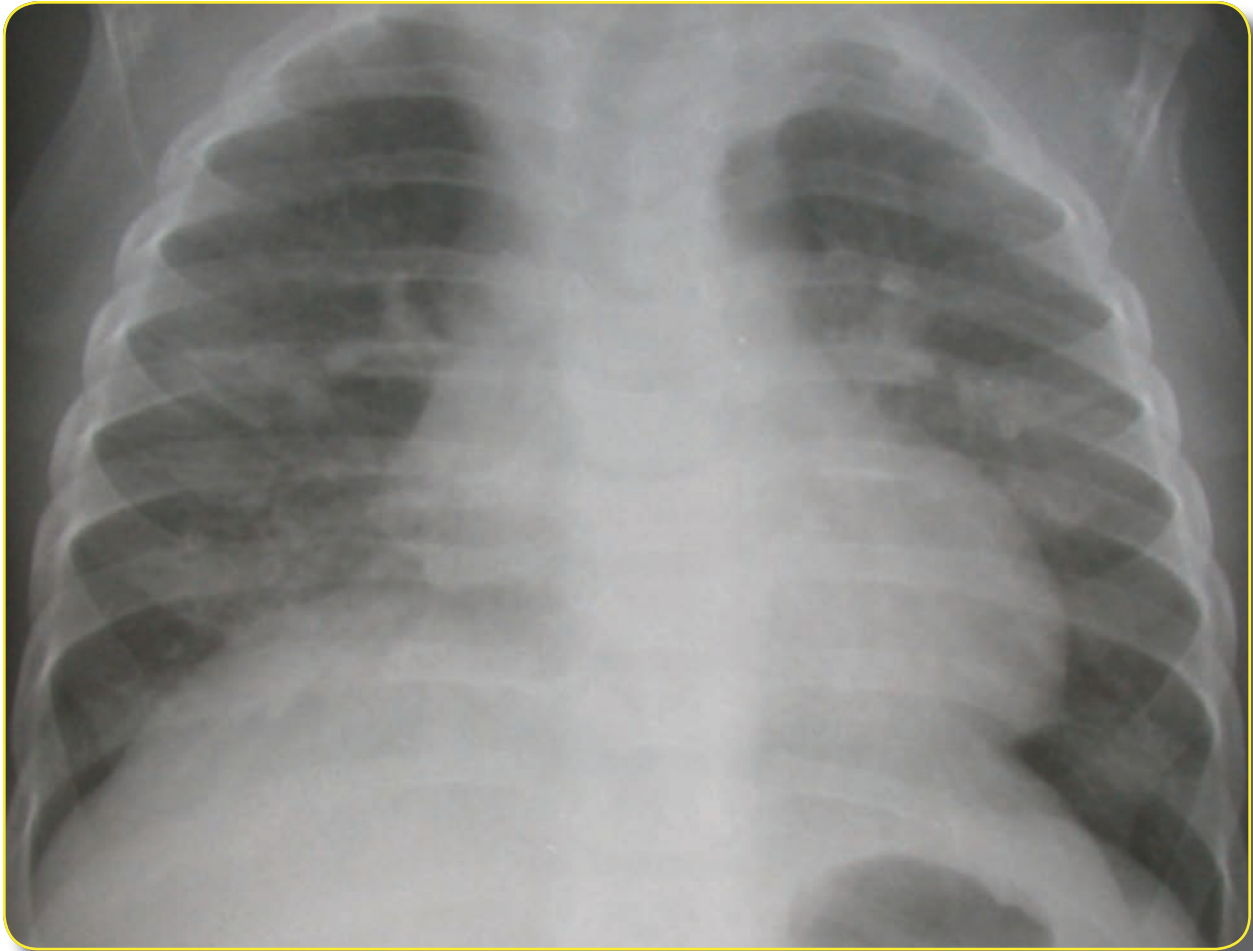


Fig. 35C.
A radiograph obtained at the time of a follow-up clinic visit several months later revealed complete resolution of the cysts with little, if any visible scarring, suggesting that the cysts represented pneumatoceles.

Pediatric Intrathoracic Tuberculosis (cont...)

Upper lobe consolidation and cavitation are more common in postprimary pulmonary TB. These patients may have evidence of prior pulmonary TB and apical pleural thickening. Lymphadenopathy and pleural effusions are not usually seen in patients with postprimary disease.²⁷ Three possible mechanisms have been proposed for development of cavitary TB in children: 1) classical upper lobe, unilateral postprimary TB; 2) progressive primary TB with multiple bilateral cavitary lesions; and, 3) cavitary lesions secondary to mediastinal lymph nodes causing airway compression with distal collapse and consolidation.²⁸

Endobronchial TB may be a complication of cavitary disease, representing spread via the airways following caseous necrosis into bronchial walls. The tree-in-bud appearance of centrilobular nodules and branching centrilobular areas of opacity is caused by bronchiolar wall thickening and filling of bronchioles with fluid, pus, or mucus (Fig. 36). The finding in patients with TB is indicative of endobronchial spread of infection.

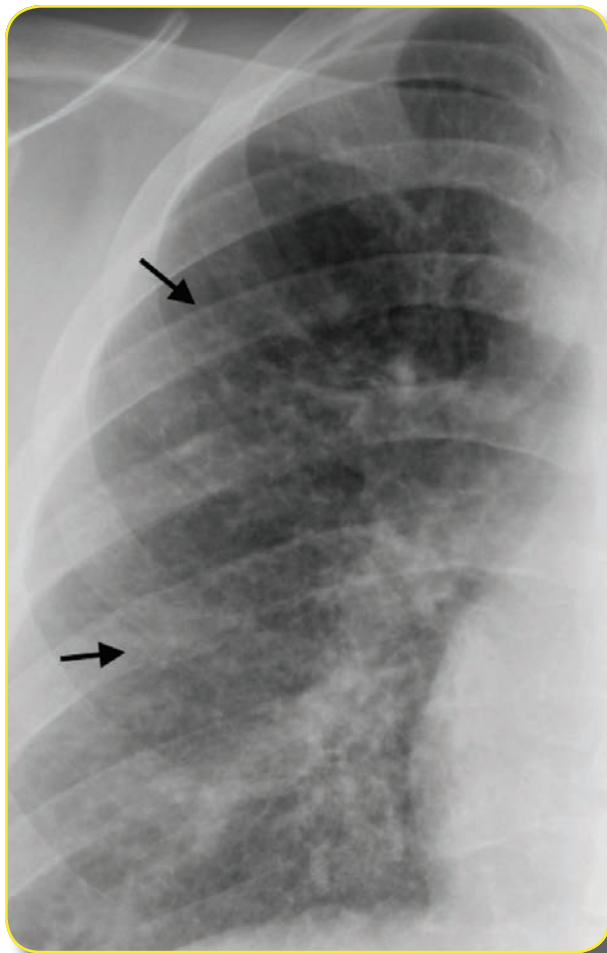


Fig. 36A.
Pulmonary TB in adolescent with gastrointestinal malignancy. The chest radiograph shows a mild reticulonodular pattern that is difficult to characterize (arrows).

Pediatric Intrathoracic Tuberculosis (cont...)

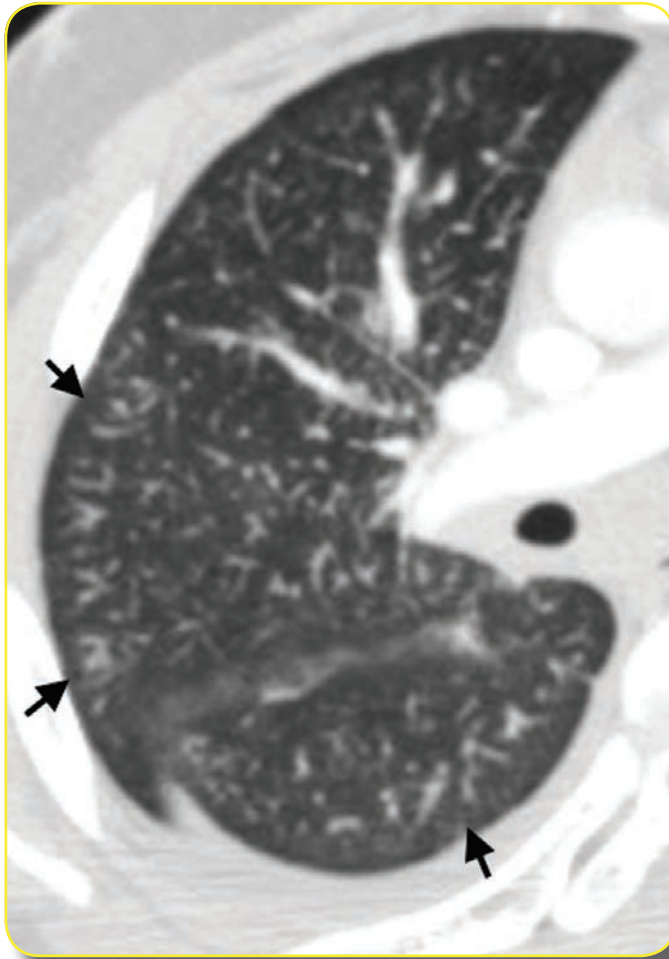


Fig. 36B.
Chest CT shows a “tree-in-bud” pattern that is not specific but can be seen with TB (arrows). Bronchoalveolar lavage revealed acid-fast bacilli in this patient.

Congenital Tuberculosis

Congenital tuberculosis is a rare form of primary disease caused by prenatal transmission of TB from the mother to the fetus through the umbilical vein or amniotic fluid. For this to occur, hematogenous spread, disseminated disease or uterine involvement during pregnancy would be the most likely mechanisms. Infants with congenital TB may have clinical symptoms at birth but usually present within the first 2-3 weeks of life. Disease after 1 month of age is more likely to have been acquired post-natally. Chest radiographic findings may resemble other more common types of neonatal pneumonia. Findings of intrathoracic lymphadenopathy, evidence of liver involvement (usual site of entry), or a miliary pattern of pneumonia are all supportive of tuberculosis. Unless the mother has evidence of uterine, placental or disseminated TB disease, it can be difficult to distinguish congenital transmission from respiratory transmission soon after birth. In either case, TB in the neonatal period is often a rapidly progressive, disseminated, extensive and life threatening disease (see Fig. 35).

Healed intrathoracic disease

Abnormal chest radiograph findings regress more slowly in patients with tuberculosis than in other more common types of pneumonia. Even with treatment, little change may occur in the first 3 months after the initial diagnosis. The primary complex may remain visible for 6-8 months and sometimes as long as 2 years.³ Frequent radiographs are not necessary unless the clinical condition deteriorates or raises concerns about complications. There are no evidence-based guidelines for follow up radiographs for children with TB, but some experts recommend films at beginning of treatment, 2 months after initiation, at the end of treatment and 2 months after completion of medication.²⁹ Other experts recommend films at the time of diagnosis and the conclusion of therapy unless clinical symptoms dictate otherwise. The severity of the disease and immune response of the patient influence the degree of radiographic resolution. Thirty to 40% of pediatric patients may still have visible mediastinal lymphadenopathy at the conclusion of therapy.^{1,3,8}

Calcification is indicative of healed disease and is a relatively rare finding in children treated for TB (Fig. 37). Calcification of the pulmonary focus and/or lymph nodes is more common in cases that were not diagnosed or treated. Uncomplicated primary disease often heals with no signs of fibrosis, scarring or calcification.³⁰ Calcification may form in the lymph nodes or the Ghon focus between 6 months to 4 years after infection.^{1,2,5} CT can detect calcification not visible on plain radiographs and has been reported in 15-20% of children with healed TB.^{12,31,32} One study published in 1970 found partial or complete clearing of calcifications in the lungs and lymph nodes in many children over a 10-17 year period of follow up.³²

Pediatric Intrathoracic Tuberculosis (cont...)

Bronchiectasis can result from TB pneumonia. The earliest radiographic finding of bronchiectasis is bronchial wall thickening resulting in a “tram track” pattern, followed later by bronchiolar dilation and eventually a cystic honeycomb pattern. Chest CT is a much more sensitive examination for the detection of bronchiectasis in the earlier stages.³³

Healing of cavitary lesions may result in fibrosis, volume loss and anatomic distortion. Cavitation caused by caseating pneumonia often leads to fibrosis with resolution and is more common among teens and adults.

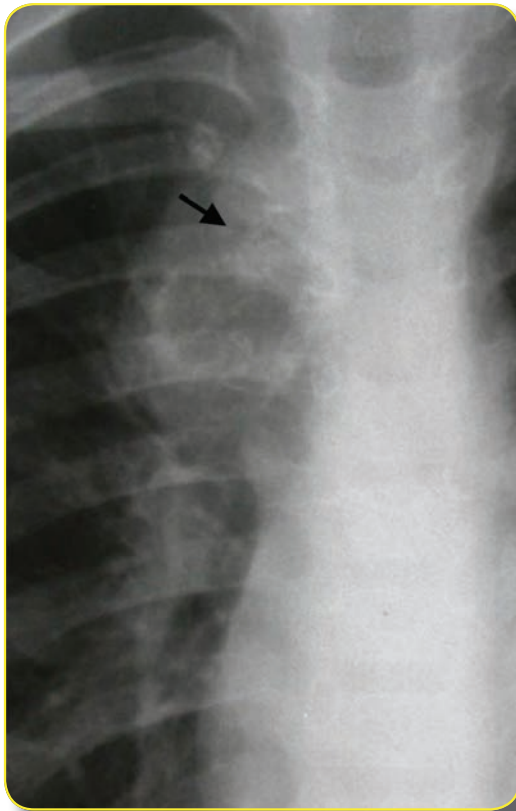


Fig. 37A.
Calcified lymph nodes with TB. Early calcifications in this right paratracheal lymphadenopathy are difficult to see on radiographs (arrow).

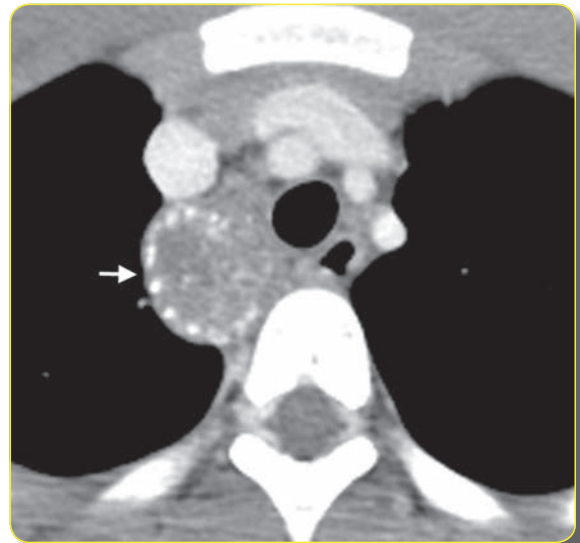
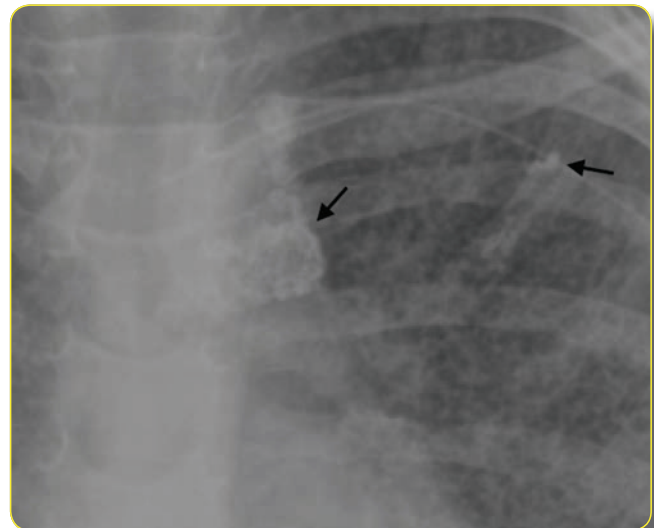


Fig. 37C.
Another child with peripheral calcifications in a large retrocaval lymph node (arrow).

Fig. 37B.
A different patient with miliary TB shows calcifications in a left hilar lymph node and small left upper lobe granuloma (arrow).



Pediatric Extrapulmonary Tuberculosis

Pediatric Extrapulmonary Tuberculosis

Central Nervous System TB

Tuberculosis can involve the meninges or the parenchyma of the cerebrum, cerebellum, brainstem, or spinal cord. Tuberculous meningitis is generally more common in children than adults, especially infants.³⁴ Like most forms of extrapulmonary TB, spread to the brain and meninges is typically hematogenous. Up to 50% of patients with miliary TB may have central nervous system involvement. Local spread from the middle ear, mastoid or the calvarium occasionally can occur. The most common clinical manifestation is diffuse meningitis. But focal disease, infarction and hydrocephalus are possible complications. An intense inflammatory response, which may paradoxically worsen during the first month of therapy, contributes to morbidity and complications.

Brain CT findings of tuberculous meningitis are subtle to absent in many cases. Intense basal contrast enhancement is the most common finding on CT and MRI in early cases (Fig. 38 A,B). The findings on head CT most suggestive of tuberculous meningitis (TBM) is marked contrast enhancement outlining the basal cisterns or basal enhancement.³⁵ A study of 37 children with culture confirmed TBM reported 89% with basal enhancement, 68% with hydrocephalus, 62% with parenchymal infarcts and 13.5% with tuberculoma.³⁶ These authors summarized 17 studies reporting CT findings in children with TBM. The results are compared in Table 2. Basilar enhancement is not specific for TBM and can be seen in other disease processes like fungal meningitis, sarcoidosis and syphilis.^{37,38} The findings are more difficult to see on non-contrast CT scans, however in some cases, hyperdensity is visible in the basal cisterns, representing high density exudates (Fig. 38C). This finding has been reported to be highly specific for TBM.³⁷

Pediatric Extrapulmonary Tuberculosis (cont...)

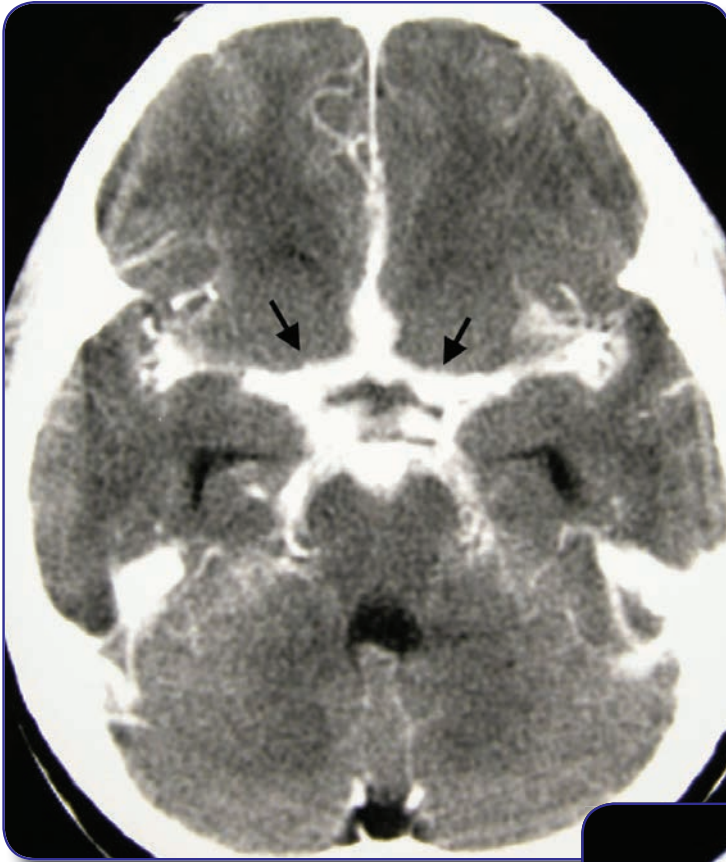


Fig. 38A.
TB meningitis.
Contrast-enhanced
CT image shows
pronounced
enhancement in the
basal cisterns (arrows)
in this child with TB
meningitis.

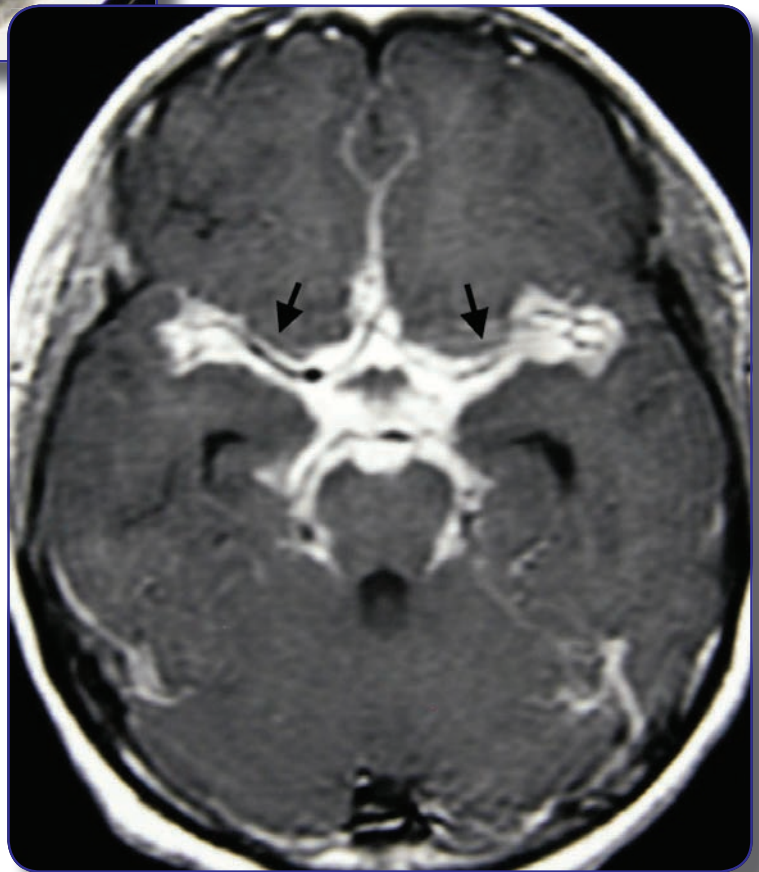


Fig. 38B.
Gadolinium-enhanced
MRI image of the
same child shows
similar basilar
enhancement. The
dark flow void of the
vessels of the circle
of Willis surrounded
by the inflammatory
exudates creates
a double line of
enhancement
(arrows).

Pediatric Extrapulmonary Tuberculosis (cont...)

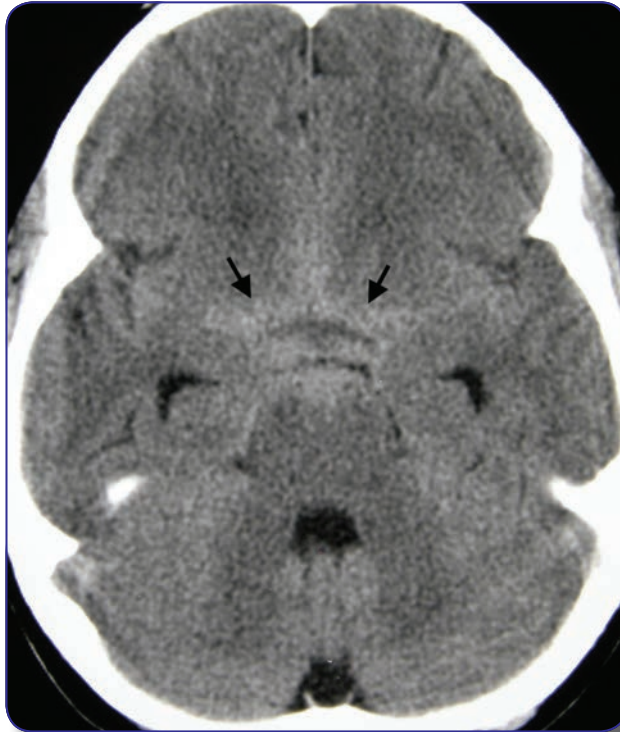


Fig. 38C.
Non-contrast enhanced CT image shows high attenuation surrounding the basal cisterns and Circle of Willis (arrows), representing dense tuberculous exudates.

TABLE 2
Comparison of CT findings in children with TB meningitis

Study	Total Patients	Children #	Hydrocephalus (%)	Basal enhancement (%)	Infarcts (%)	Tuberculoma (%)
Artopoulos ³⁹	9	9	100	11	44	56
Bhargava ⁴⁰	60	36	83	82	28	10
Farinha ⁴¹	33	33	94	93	33	15
Kingsley ⁴²	25	12	72		67	
Kumar ⁴³	94	94	81	83	19	24
Leiguarda ⁴⁴	65	65	89	69	38	27
Patwari ⁴⁵	136	136	32		13	27
Waeker ⁴⁶	30	30	100	37	37	
Andronikou ³⁶	37	37	68	89	62	13.5
Altunbasak ⁴⁷	52	52	98	52	25	
De ⁴⁸	21	21	76	67	50	10
Kemaloglu ⁴⁹	156	156		46	22	4
Ozates ⁵⁰	289	214	80	15	14	4
Tung ⁵¹	7	7	100	14	29	
Upadhyaya ⁵²	59	59	100		6	8
Schoeman ⁵³	198	198	83	75	38	11

Adapted from Andronikou S. *Pediatr Radiol.* 2004 34(11):876-85. ³⁶

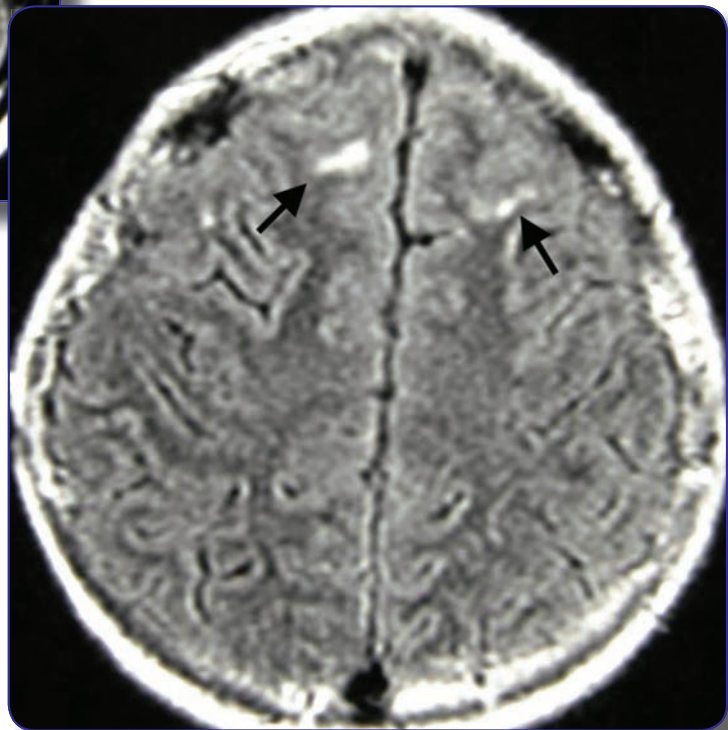
Pediatric Extrapulmonary Tuberculosis (cont...)

Objective radiographic CT and MRI criteria for the presence of basal enhancement in children with TBM may have high sensitivity and specificity when more than one criterion is present.⁵⁴ The useful findings include: 1) filling of the CSF spaces around the vessels with contrast, 2) double lines of enhancement in the middle cerebral artery cisterns, 3) enhancement along the frontal lobe and uncus of the temporal lobe at the supracellar cistern, 4) enhancement of the infundibular recess of the third ventricle, 5) nodular enhancement of the vessels, and 6) asymmetrical vascular enhancement.^{37,54} Early follow up head CT within 1-4 weeks of initial CT may be of value in detecting new findings including hydrocephalus, cerebral infarcts and basal enhancement which may be of diagnostic and/or prognostic benefit.⁵⁵ MRI is more sensitive for detection of infarcts and is generally of more value (Fig. 39).⁵⁶



Fig. 39A.
Brain infarcts
secondary to
TB meningitis.
Contrast enhanced
MRI images show
scattered focal areas
of enhancement
secondary to post-
infectious infarcts
(arrows).

Fig. 39B.
Infarcts shown in
contrast enhanced
MRI.



Pediatric Extrapulmonary Tuberculosis (cont...)

Tuberculoma is the most common form of localized TB CNS disease. The tuberculous mass usually measures less than 2 cm in diameter and is rarely calcified (Fig. 40). Tuberculomas can mimic neoplasms. CNS abscess is uncommon with TB. Intravenous contrast is important on CT and MRI scans to show enhancement patterns. TB lesions are usually of low density with ring enhancement (Fig. 41), and the cerebral hemisphere is the most common location. These lesions exhibit mass effect with surrounding edema, but no mural nodules are present.⁵⁷

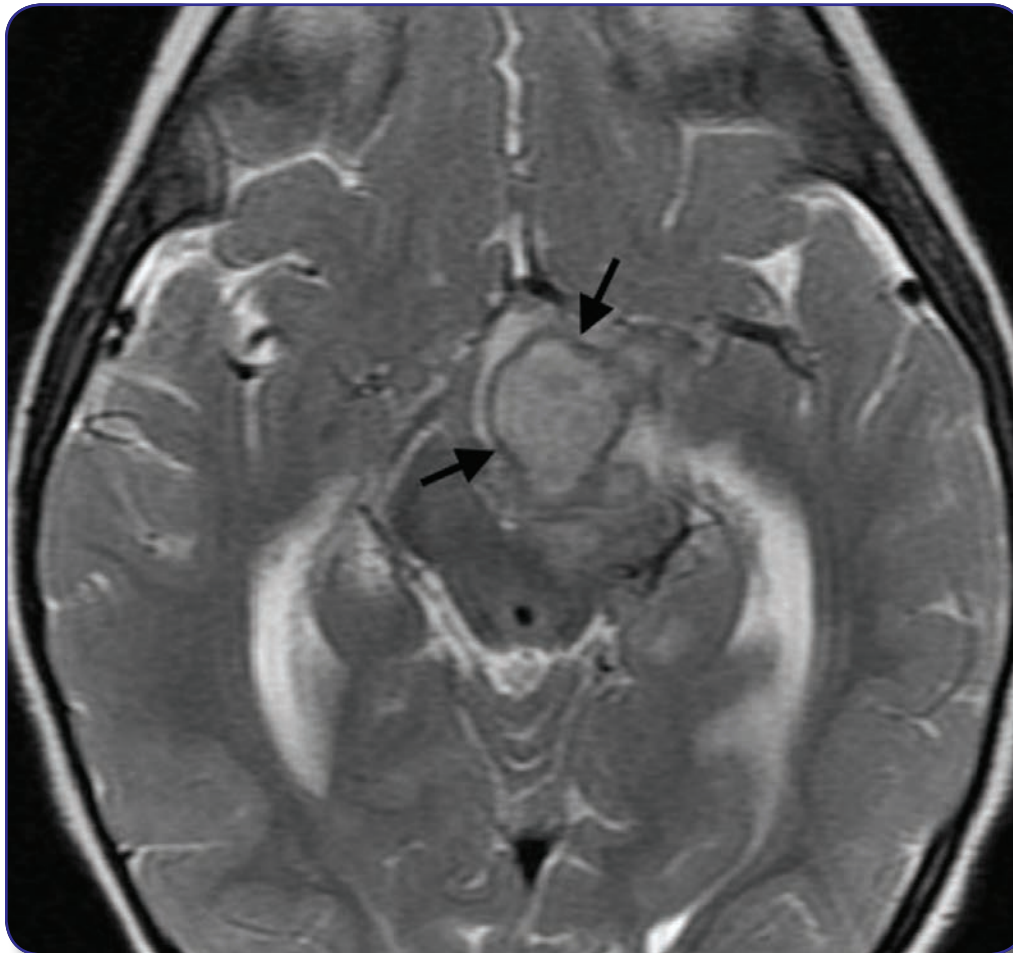


Fig. 40A.
Axial T2 weighted MRI image shows loculated fluid collection in the left mesial temporal and hypothalamic regions with mass effect on the third ventricle and midbrain (arrows)

Pediatric Extrapulmonary Tuberculosis (cont...)

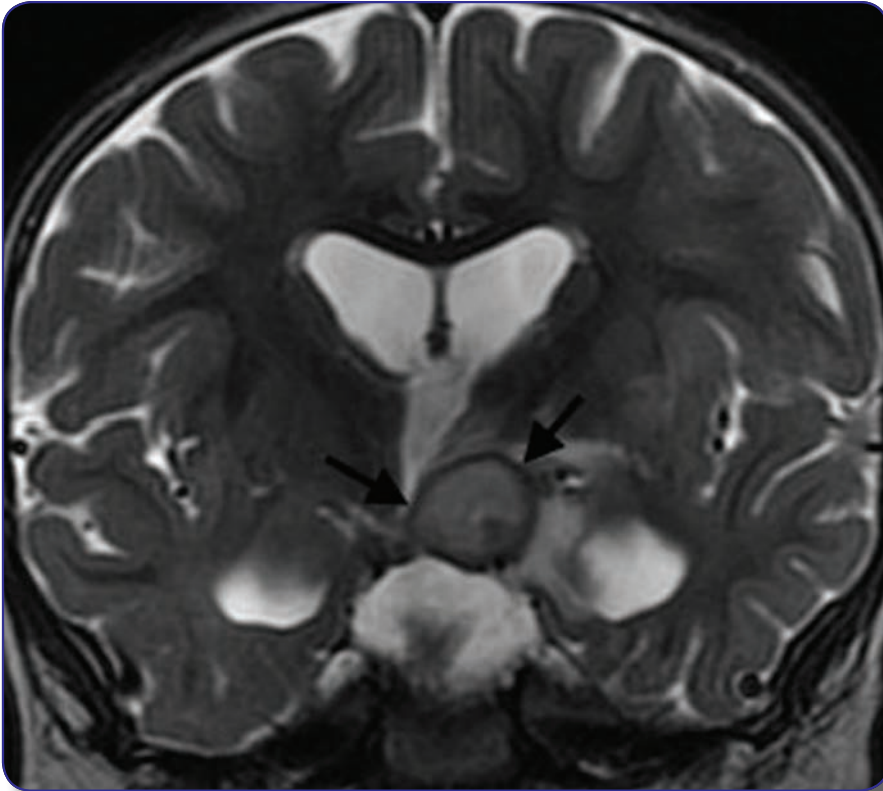
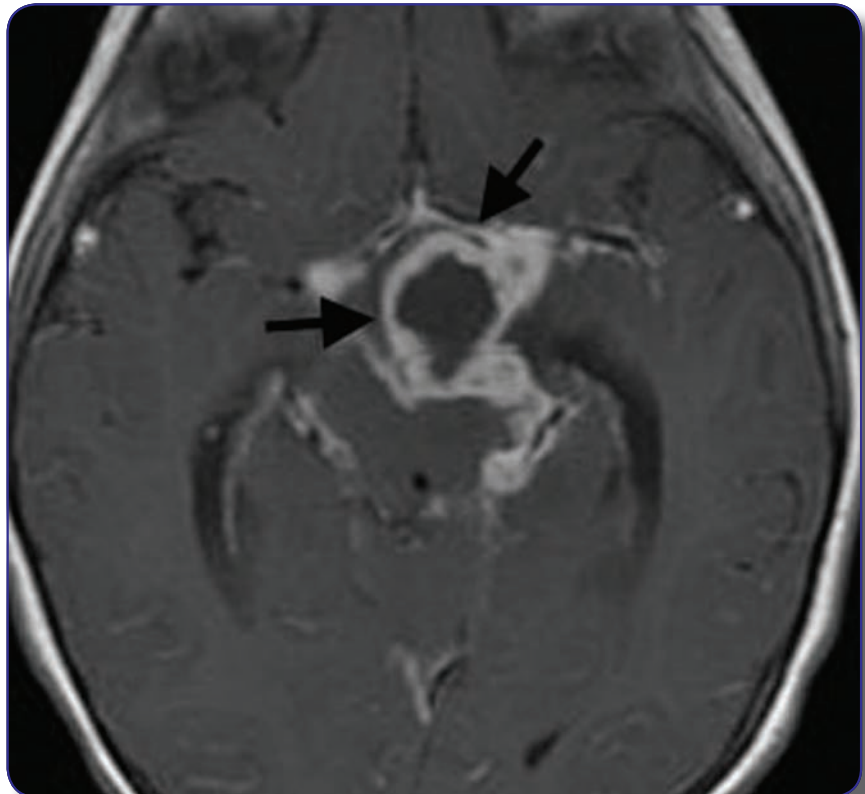


Fig. 40B.
Coronal T2
weighted image of
same lesion.

Fig. 40C.
Contrast-enhanced
axial image shows
intense leptomeningeal
enhancement in the basal
cisterns and midbrain,
surrounding the non-
enhancing loculated
abscess (arrows).



Pediatric Extrapulmonary Tuberculosis (cont...)

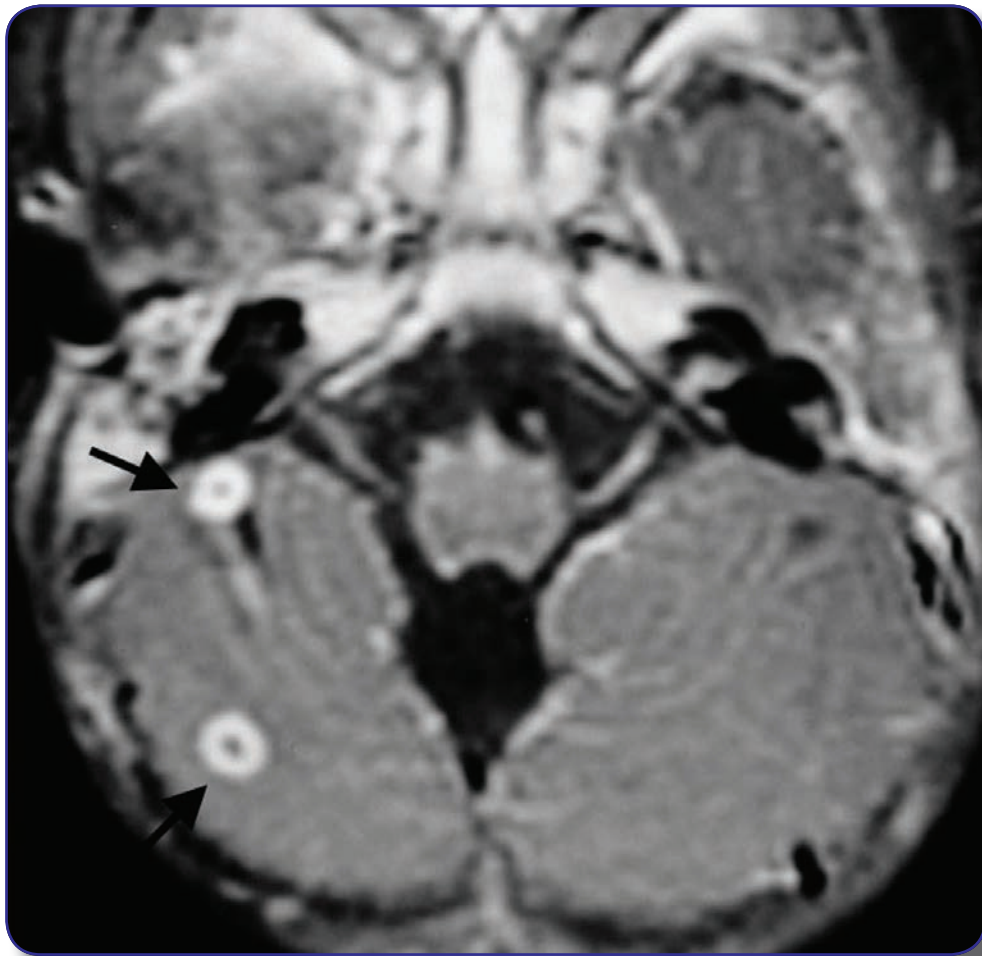


Fig. 41.
Tuberculomas.
Multiple small ring enhancing lesions in the cerebellum represent tuberculomas (arrows).

Pediatric Extrapulmonary Tuberculosis (cont...)

Tuberculous otomastoiditis can be a result of hematogenous spread or direct extension from the upper respiratory tract (Fig. 42). CT or MRI demonstrates opacification of the mastoid air cells and the middle ear space. Damage to the middle ear structures may occur.

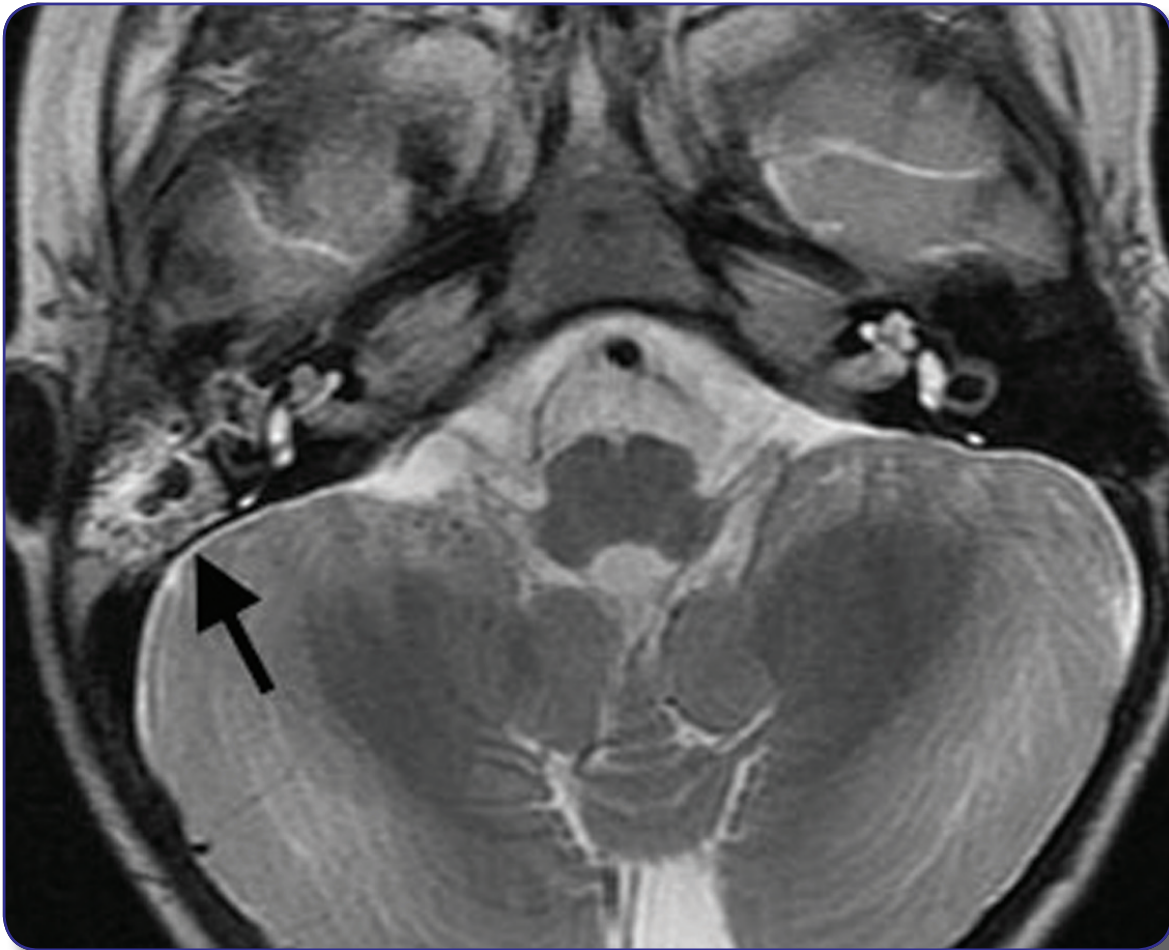


Fig. 42A.
Tuberculous otomastoiditis.
T2-weighted MRI shows inflammatory edema in the right mastoid air cells, with a central non-enhanced area representing an abscess (arrow).

Pediatric Extrapulmonary Tuberculosis (cont...)

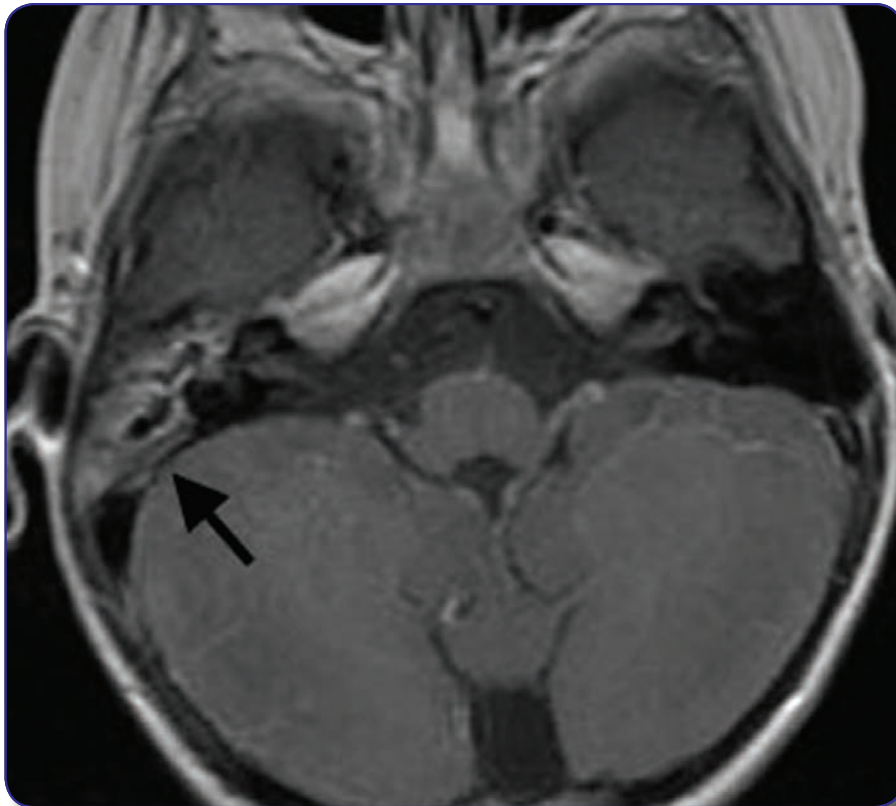
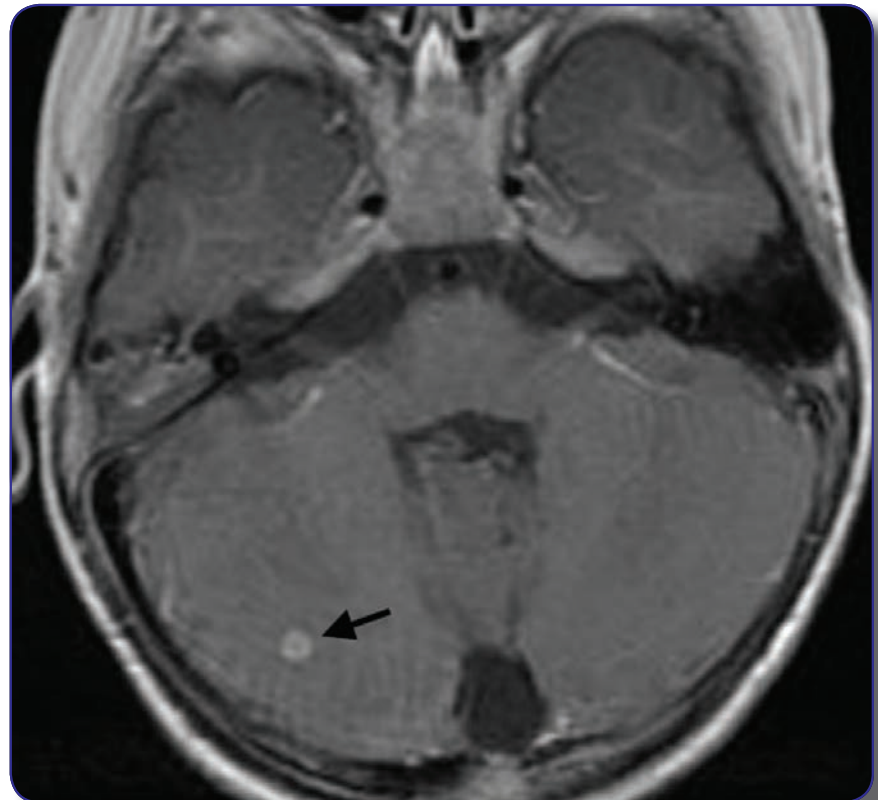


Fig. 42B.
Gadolinium-enhanced
MRI images show
enhancement in the
mastoid air cells
(arrow).

Fig. 42C.
A ring enhancing
lesion in the
cerebellum
(arrow).



Abdominal Tuberculosis

Abdominal TB is less common in children than adults. The majority (64%) of children with abdominal tuberculosis also have pulmonary disease.⁵⁸ Lymphadenopathy can occur throughout the abdomen with para-aortic, mesenteric, and periportal lymph nodes most commonly involved (Fig. 43). Peripheral lymph node enhancement can occur, similar to that seen in thoracic tuberculous lymphadenopathy. Calcification is more likely in abdominal tuberculous than in thoracic lymph node disease in children. Abdominal and pelvic CT and MRI are equally effective for identifying abnormal lymph nodes in the abdomen and pelvis. Intravenous contrast enhancement is necessary to distinguish lymphadenopathy caused by tuberculosis from normal intra-abdominal structures.

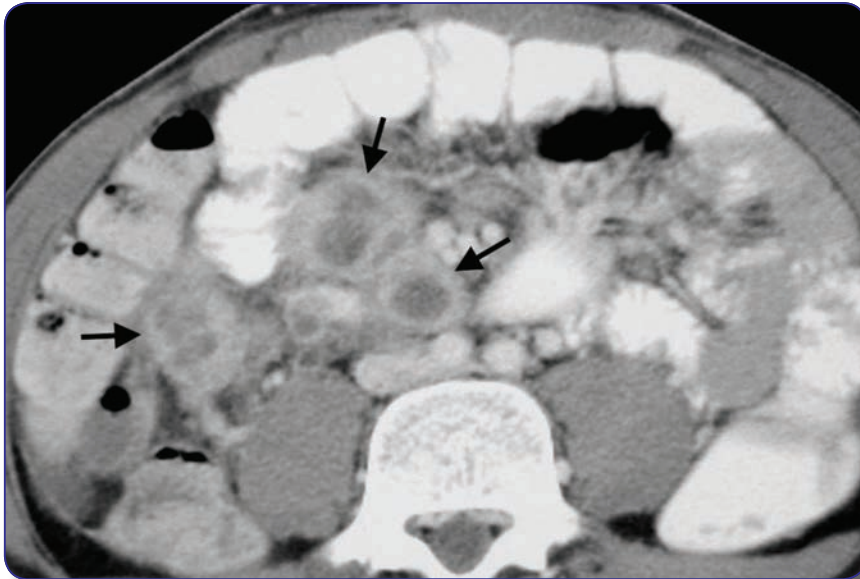


Fig. 43A.
Abdominal TB lymphadenopathy. Multiple enlarged mesenteric lymph nodes show peripheral enhancement typical of tuberculous lymphadenopathy (arrows).

Fig. 43B.
A larger lesion in the right lower quadrant of the same patient has a low attenuation center and a thin rim of peripheral enhancement, suggestive of an abscess (arrow).



Pediatric Extrapulmonary Tuberculosis (cont...)

Solid organ lesions are usually granulomas or microabscesses and appear as either calcified or low attenuation lesions on CT. Lesions in the liver or spleen on MRI are low intensity on T1 weighted images and high intensity on T2 weighted sequences. Both CT and MRI may show mild enhancement around the periphery of the lesions. High frequency ultrasound is a sensitive method for detecting small tuberculous lesions in the liver or spleen. The lesions are hypochoic and multiple (Fig. 44).

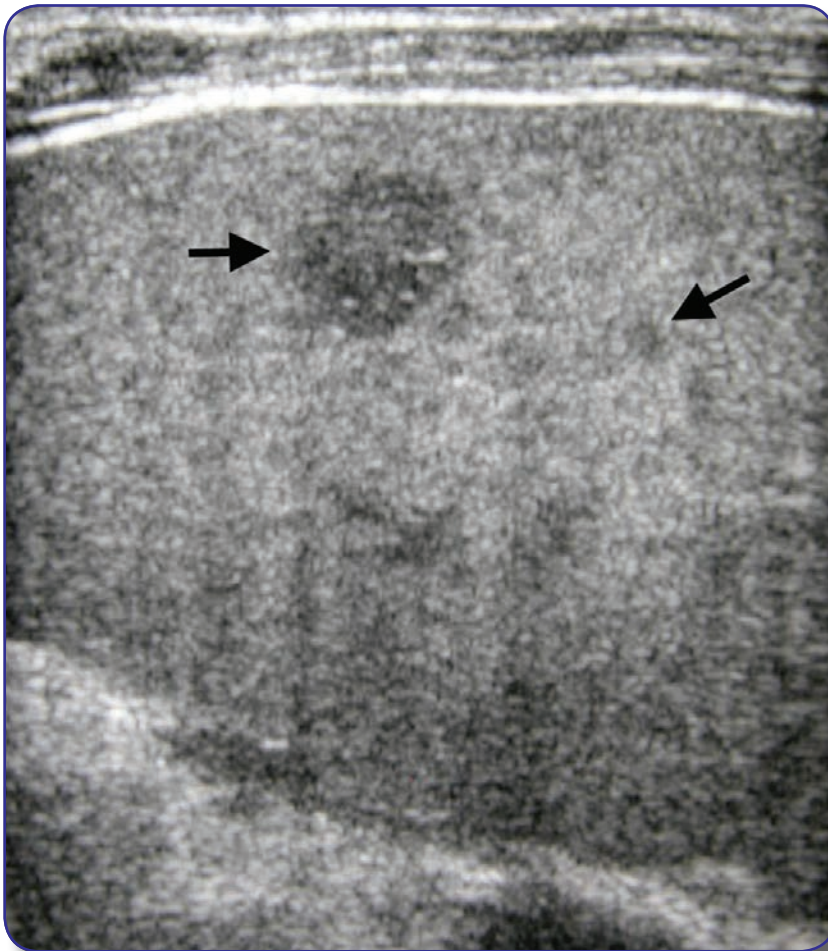


Fig. 44.
Splenic lesions.
The hypochoic,
round lesions of
varying sizes seen
on ultrasound may
represent granulomas
or microabscesses
(arrows).

Pediatric Extrapulmonary Tuberculosis (cont...)

Less common types of abdominal involvement include tuberculous peritonitis and ileocolitis. Peritonitis is accompanied by ascites that may have high attenuation values on CT (Fig. 45). Ultrasound identifies the fluid but the findings cannot distinguish TB peritonitis from other causes of ascites and peritonitis. Bowel involvement usually occurs in the ileocecal region and is manifest by bowel wall thickening or inflammatory phlegmon (Fig. 46).⁵⁹

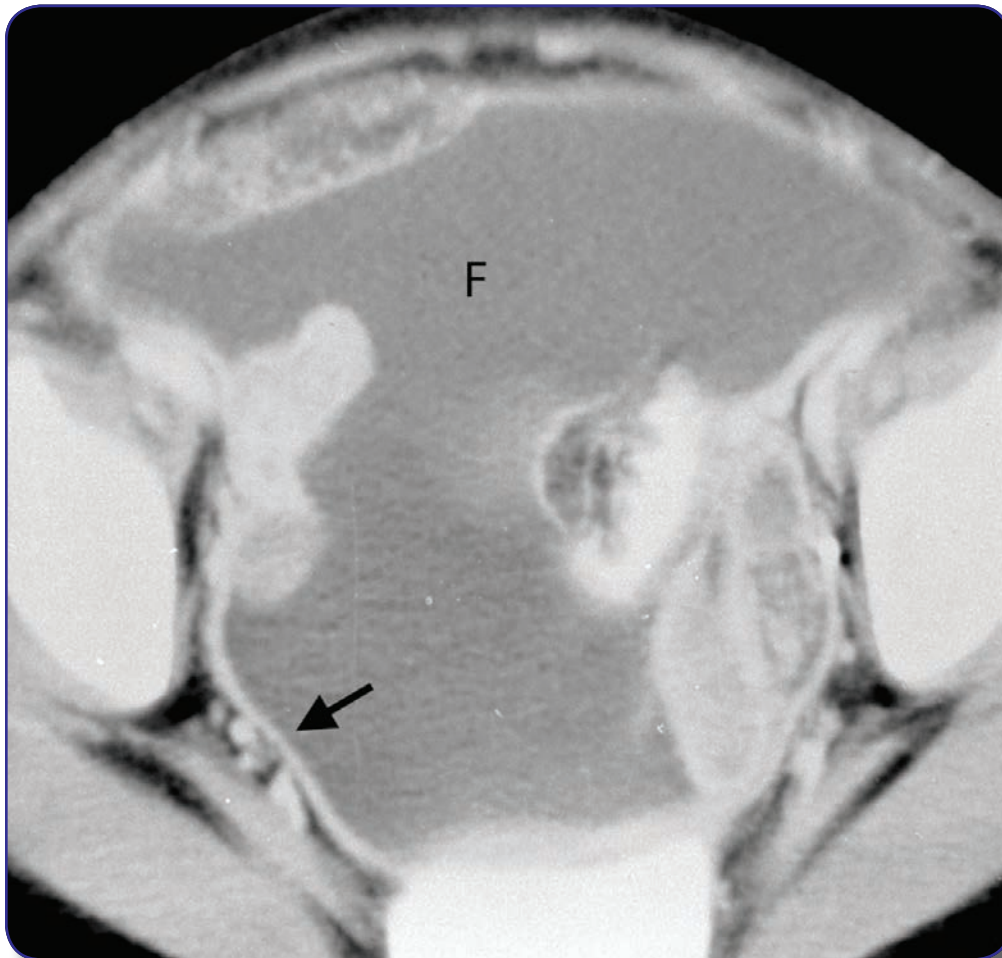


Fig. 45A.
Tuberculous
peritonitis.
Contrast-enhanced
CT shows a large
amount of free
intra-peritoneal fluid
(F). Enhancement
of the peritoneal
surface indicates
peritonitis (arrow).

Pediatric Extrapulmonary Tuberculosis (cont...)

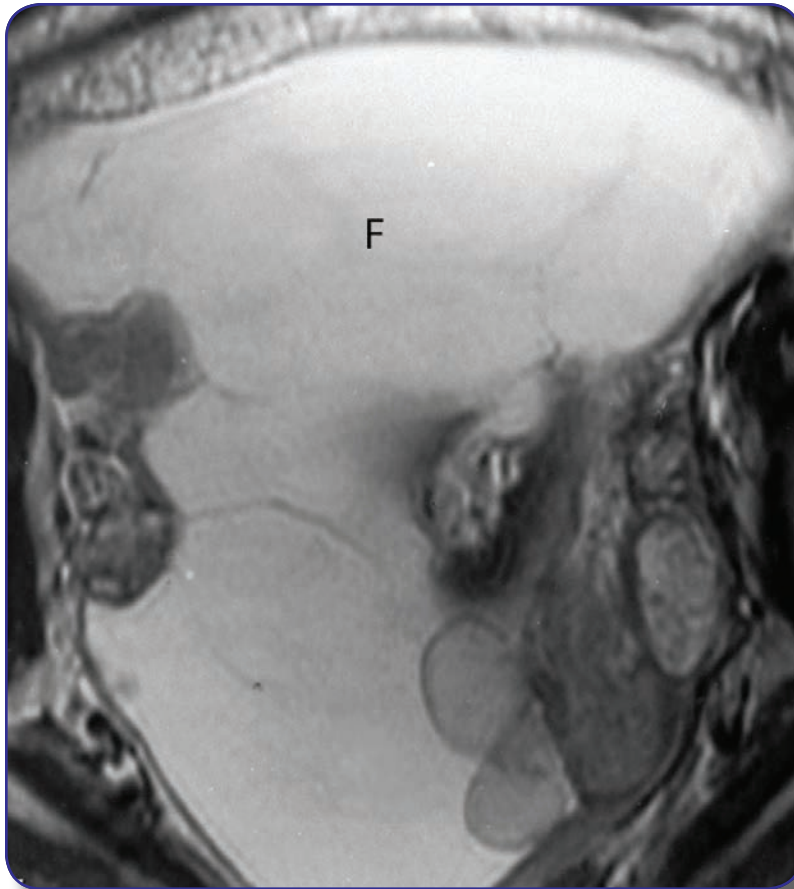
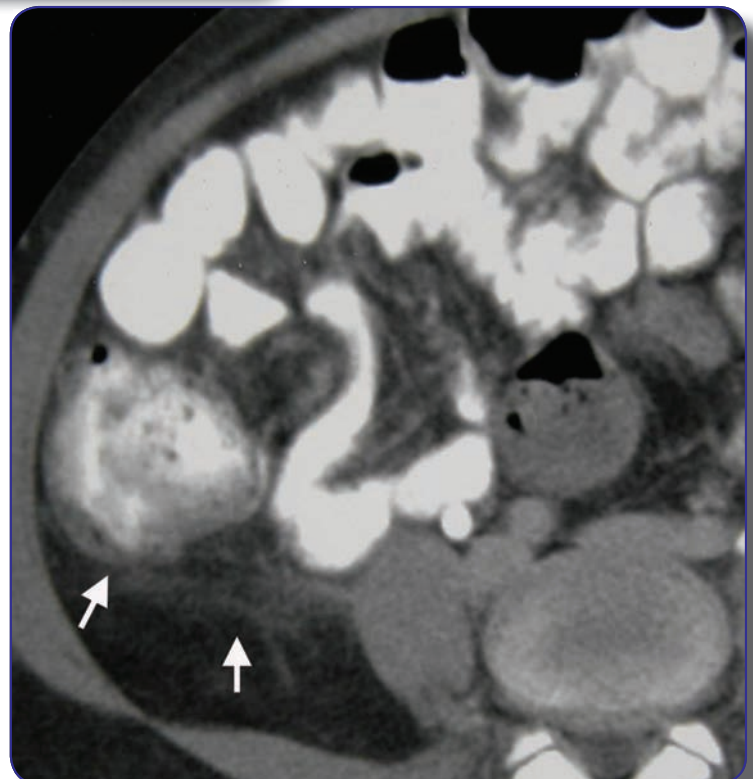


Fig. 45B.
T2-weighted MRI
shows the high
signal intensity
peritoneal fluid.

Fig. 46.
Bowel
involvement
with TB. Note
thickening of the
wall of the cecum
and stranding
in the adjacent
intra-abdominal
fat indicating
edema (arrows).



Pediatric Extrapulmonary Tuberculosis (cont...)

Musculoskeletal Tuberculosis

Skeletal involvement in children is uncommon, occurring in 1-2% of all pediatric TB cases. Hematogenous dissemination to bone is the origin of the infection, but the primary pulmonary site is usually occult. Tuberculous bone lesions start as caseating granuloma, then progress to trabecular and cortical destruction. Subperiosteal spread and soft tissue involvement are late findings. The spine is a common site of bone involvement. The infection is hematogenously deposited in the anterior aspect of the vertebral body and often spreads to the disc, subligamentous space and soft tissues (Fig. 47). The posterior elements are seldom involved. Eighty-five percent of patients with spinal TB will have multiple contiguous vertebrae involvement. MRI of the spine is critical in children with spinal tuberculosis, because paravertebral and epidural abscesses are common and can lead to cord compression (Fig. 48). Infection can also spread along the iliopsoas muscle into the groin or chest. After healing, kyphotic gibbus deformity can remain^{60,61} but this complication is uncommon in developed countries (see Fig. 47C).

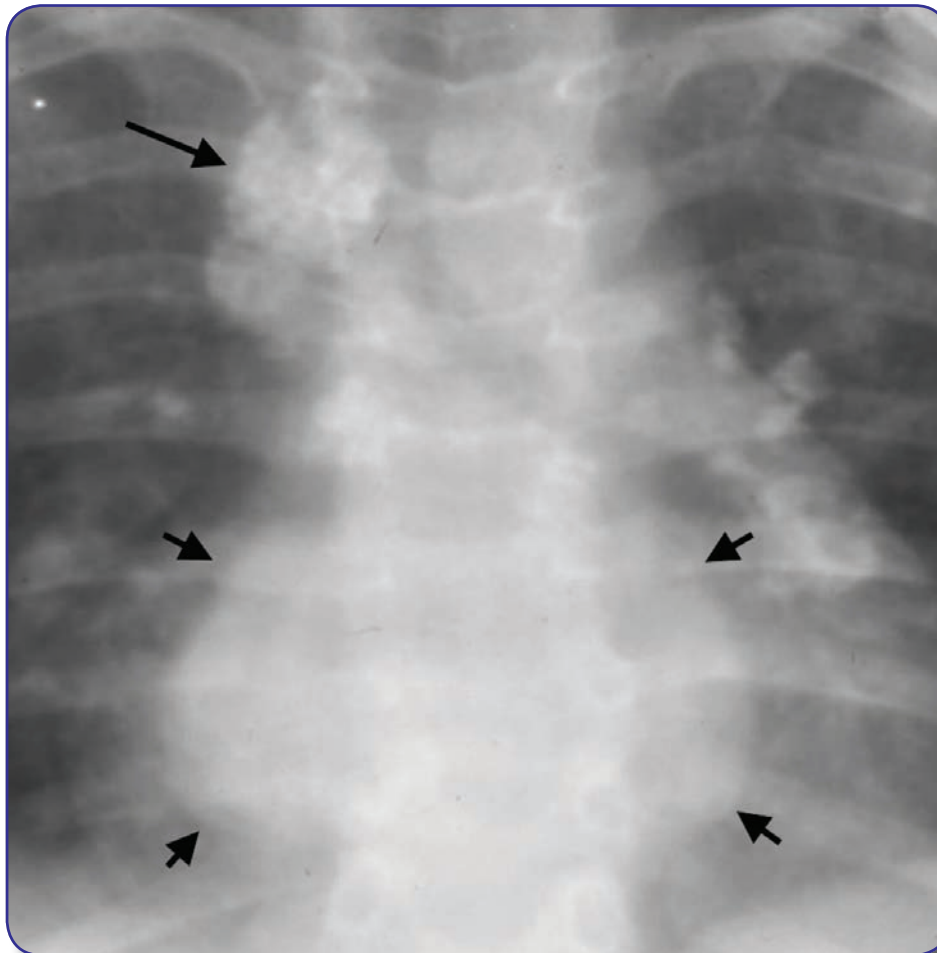


Fig. 47A.
TB spondylitis.
AP radiograph of the thoracic spine shows bilateral paraspinal soft tissue masses (short arrows) surrounding a narrowed disc space. Note the calcified mediastinal lymph nodes (long arrow).

Pediatric Extrapulmonary Tuberculosis (cont...)



Fig. 47B.
Coronal T2-weighted MRI image of this patient shows large subligamentous abscess collections (black arrows) surrounding multiple vertebral bodies with abnormal signal intensity and a narrowed and low signal disc space (white arrows).

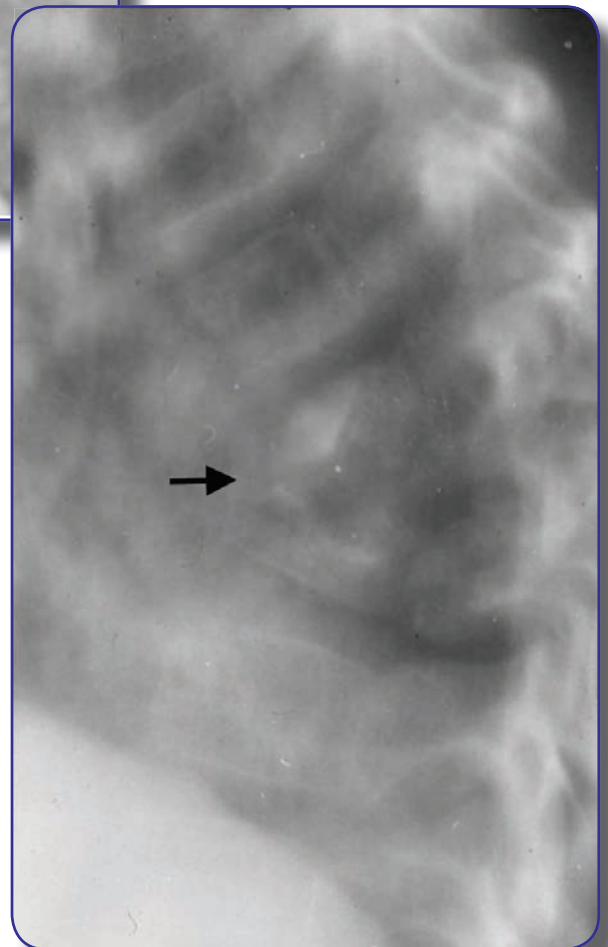


Fig. 47C.
Lateral spine radiograph in this patient shows vertebral endplate destruction and angular kyphosis (gibbus deformity) (arrow).

Pediatric Extrapulmonary Tuberculosis (cont...)

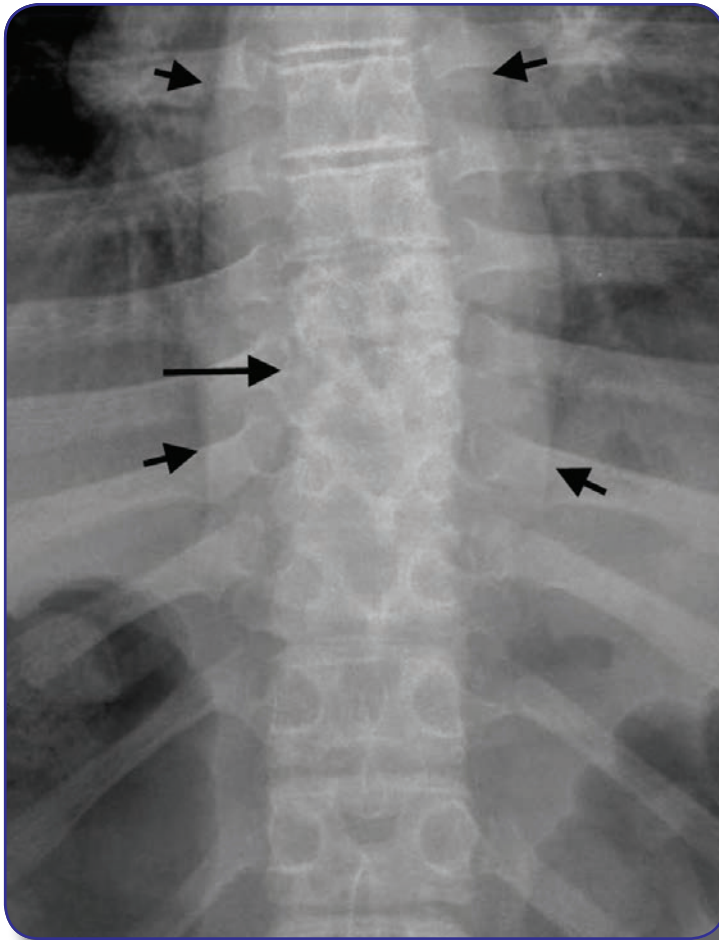


Fig. 48A.
TB spondylitis.
AP radiograph of the lower thoracic spine shows thickening of the paraspinal stripes bilaterally, consistent with paraspinal mass or abscess (short arrows). The T 7-8 and T 8-9 disc spaces are narrowed and the right pedicle of T8 appears partially destroyed (long arrow).

Fig. 48B.
Coronal T2-weighted MRI image shows extensive paraspinal subligamentous abscess and abnormal disc spaces.



Pediatric Extrapulmonary Tuberculosis (cont...)



Fig. 48C.
Sagittal T2-weighted MRI image shows the predominantly anterior location of the paraspinal abscess (arrow). Abscess also involves the disc and vertebral bodies. Note compromise of the spinal canal and mild kyphotic deformity.

Pediatric Extrapulmonary Tuberculosis (cont...)

Joints are the second most frequent location for pediatric musculoskeletal involvement. Tuberculous arthritis is usually monoarticular often involving the hips and knees.⁶² Joint effusions are the most common finding and may be visible in the knees, elbows or ankles on radiographs. Effusions in other joints may be detected with ultrasound. Periarticular demineralization can also occur. Joint narrowing, ankylosis and overgrown epiphyses are characteristic but late findings.

TB osteomyelitis beyond the spine is rare and is usually a solitary lesion (Fig. 49). Like all hematogenously disseminated osteomyelitis in children, tuberculosis infection is initially deposited in the long bone metaphyses and metaphyseal equivalent areas of bone such as the iliac bone adjacent to the sacroiliac joint. In some cases the infection can spread across physis to the epiphysis. The most commonly seen sites include the skull, hands, feet and ribs. Rarely other sites may be involved (Fig. 50). TB bone lesions are most often cystic but permeative lesions have been seen. The typical radiographic appearance of the cystic lesion is usually a well-defined osteolytic lesion with mild surrounding sclerosis and bone expansion. Infiltrative lesions have a “moth-eaten” appearance with ill-defined margins. A similar appearance occurs with other types of infection such as fungal or chronic pyogenic infections or with tumors such as Ewing sarcoma. When the skull is involved, the parietal bone is most frequently affected. Skull lesions are usually discrete, well-circumscribed osteolytic lesions (Fig. 51A). Associated subgaleal swelling is seen in 92% of patients (Fig. 51B).



Pediatric Extrapulmonary Tuberculosis (cont...)

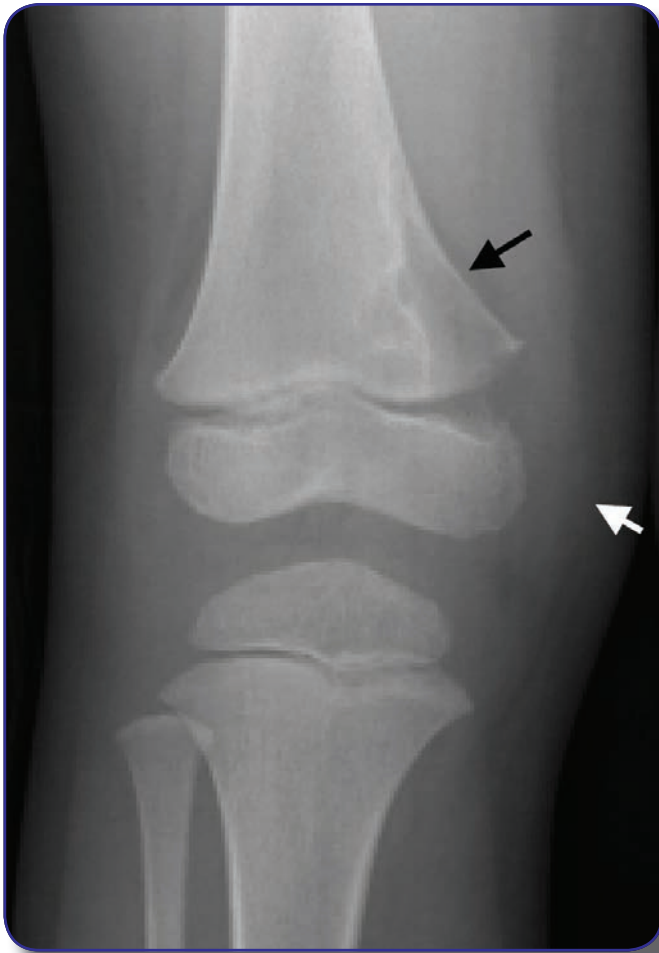
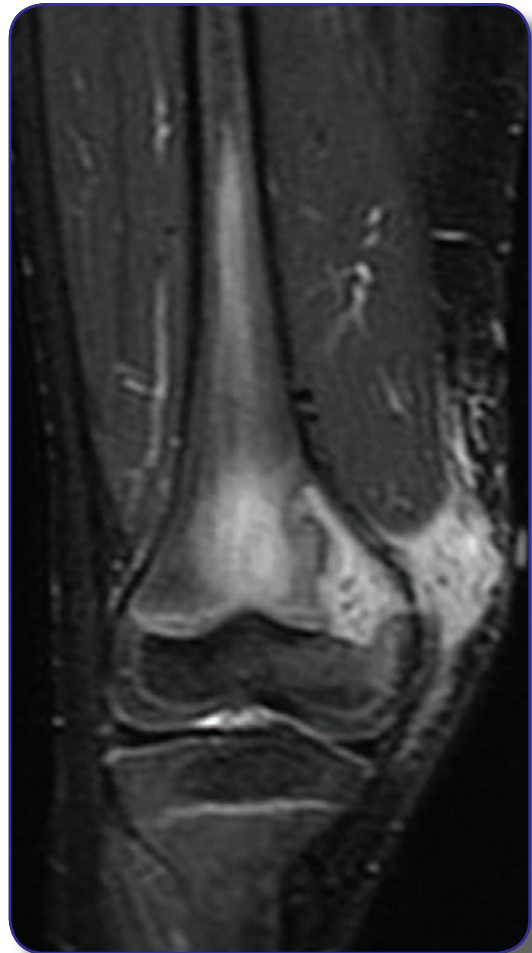


Fig. 49A.
TB osteomyelitis.
A well-defined osteolytic lesion with a thin sclerotic rim is present in the medial aspect of the distal femoral metaphysis (black arrow), associated with widening of the adjacent physis and a large soft tissue mass over the medial knee (white arrow).

Fig. 49B.
Coronal STIR MRI image shows high signal intensity in the bone lesion, which involves the medial growth plate. High signal is also present in the soft tissues.



Pediatric Extrapulmonary Tuberculosis (cont...)

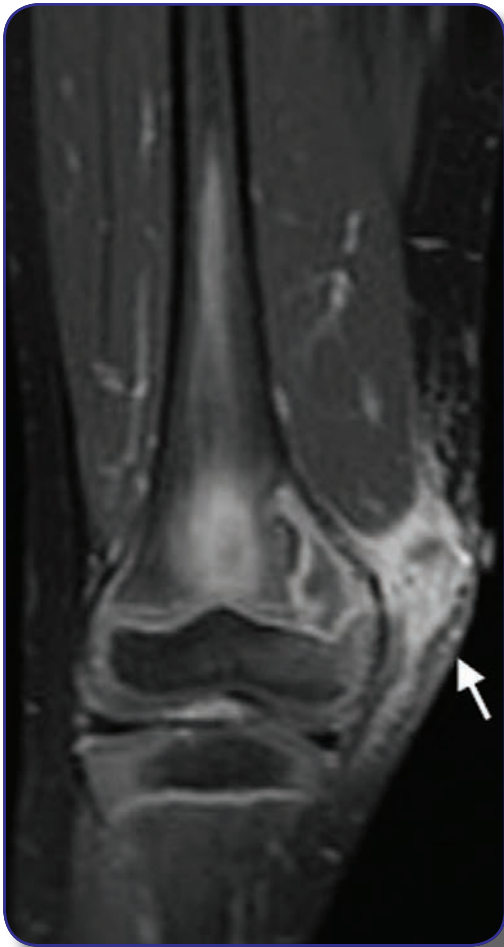
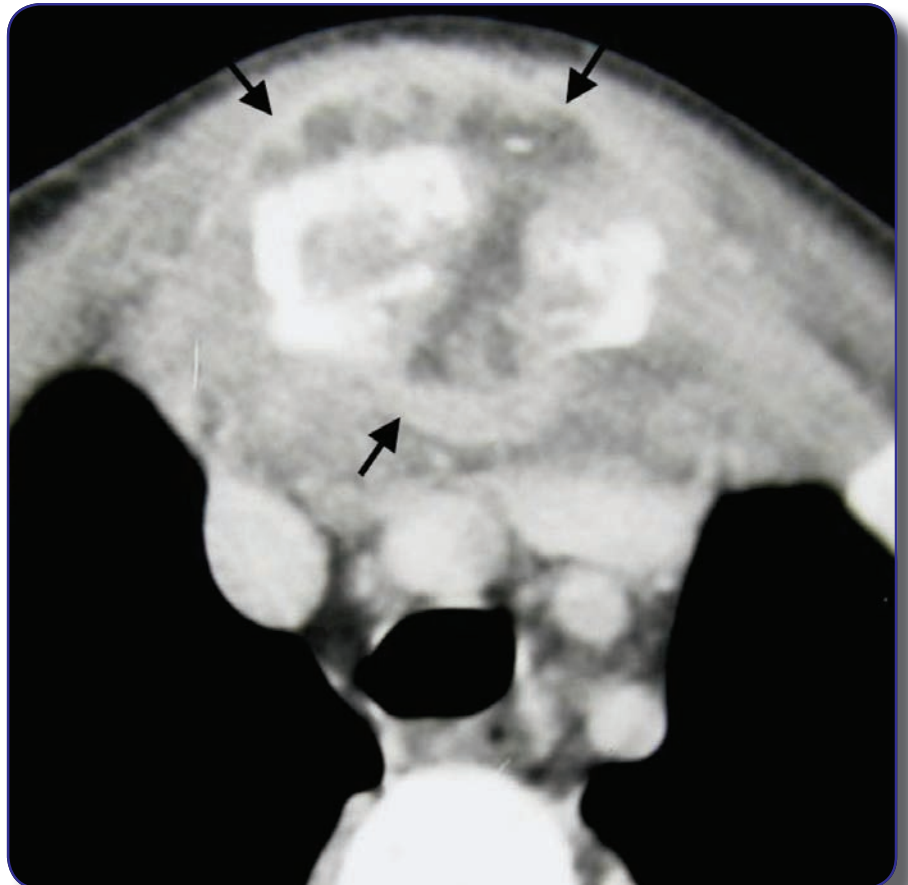


Fig 49C.
Coronal post-
Gadolinium image
shows peripheral
enhancement
surrounding the
abscesses in the
bone and soft
tissues (arrow).

Fig. 50A.
TB of the sternum.
Contrast-enhanced CT image
shows destruction of the
manubrium with surrounding
fluid collections with peripheral
enhancement representing
abscesses (arrows).



Pediatric Extrapulmonary Tuberculosis (cont...)



Fig. 50B.
A lower image of
the same patient
shows a large
retrosternal abscess
with adjacent
anterior mediastinal
lymphadenopathy
(arrow).

Pediatric Extrapulmonary Tuberculosis (cont...)

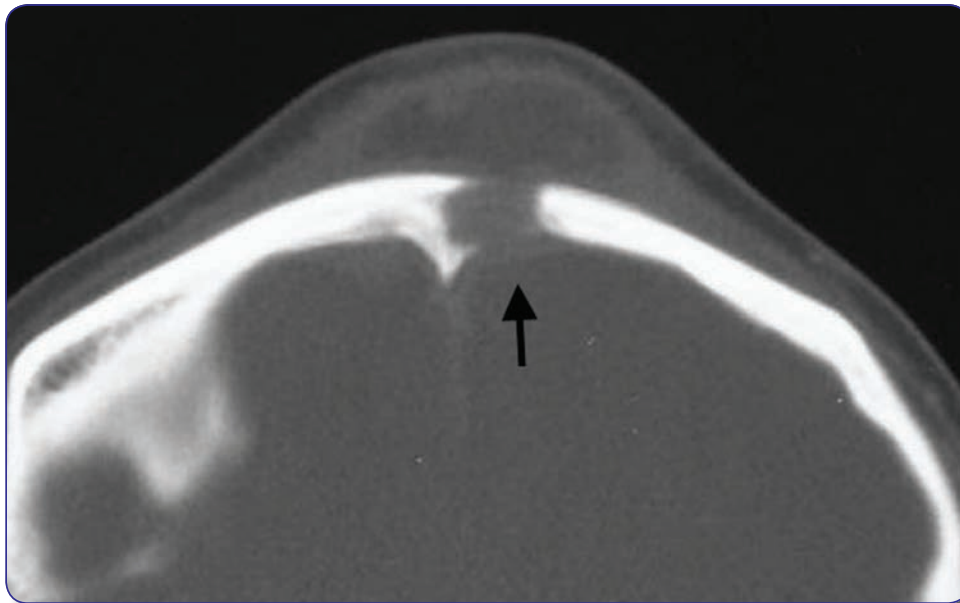


Fig. 51A.
TB of the skull.
CT with bone windows reveals the well-defined margins of the osteolytic defect (arrow).

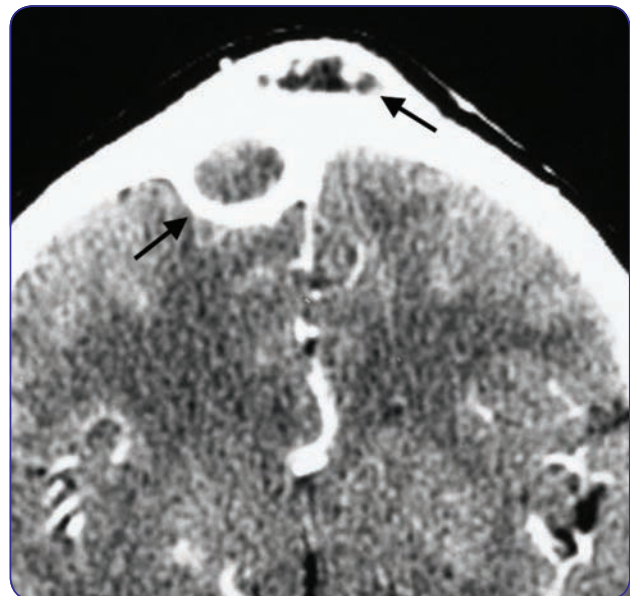


Fig. 51B.
Contrast-enhanced head CT of the same patient shows the enhancing abscesses overlying the defect and in the epidural space (arrows).

Pericardial Tuberculosis

The pericardium is a rare but potentially life-threatening site for extrapulmonary tuberculosis disease. Pericardial effusion is the only visible manifestation of the infection, creating an enlarged and globular cardiac silhouette on radiographs. Echocardiography is the most sensitive method for detection of pericardial fluid, but there are no specific findings in tubercular disease.

Other Diseases That Can Mimic Tuberculosis

Other diseases that can mimic tuberculosis

Tuberculosis has been called the great imitator considering the variety of presentations and clinical manifestations of the disease. Unilateral hilar or paratracheal lymphadenopathy is strongly associated with mycobacterial disease in children. A few other clinical entities may result in similar radiographic findings but are less common depending on the epidemiology in a given region. Conditions including other infections, immune deficiency diseases and neoplastic diseases can cause intrathoracic lymphadenopathy on chest imaging. Childhood lymphoma and leukemia may present with mediastinal lymphadenopathy often with bilateral involvement including multiple nodes in different sites (Fig. 52). TB lymphadenopathy is usually limited to a few nodes within a localized region, but may occasionally involve multiple sites. Although not a common finding with mycoplasma pneumonia, unilateral hilar lymphadenopathy similar to TB has been reported (Fig. 53).⁶³ Severe mycoplasma infections may produce lymphocytic exudative effusions that can be confused with TB.⁶⁴ Other causes of thoracic lymphadenopathy in children such as viral or fungal infections and sarcoidosis are more likely to show bilateral disease than tuberculosis (Fig. 54).

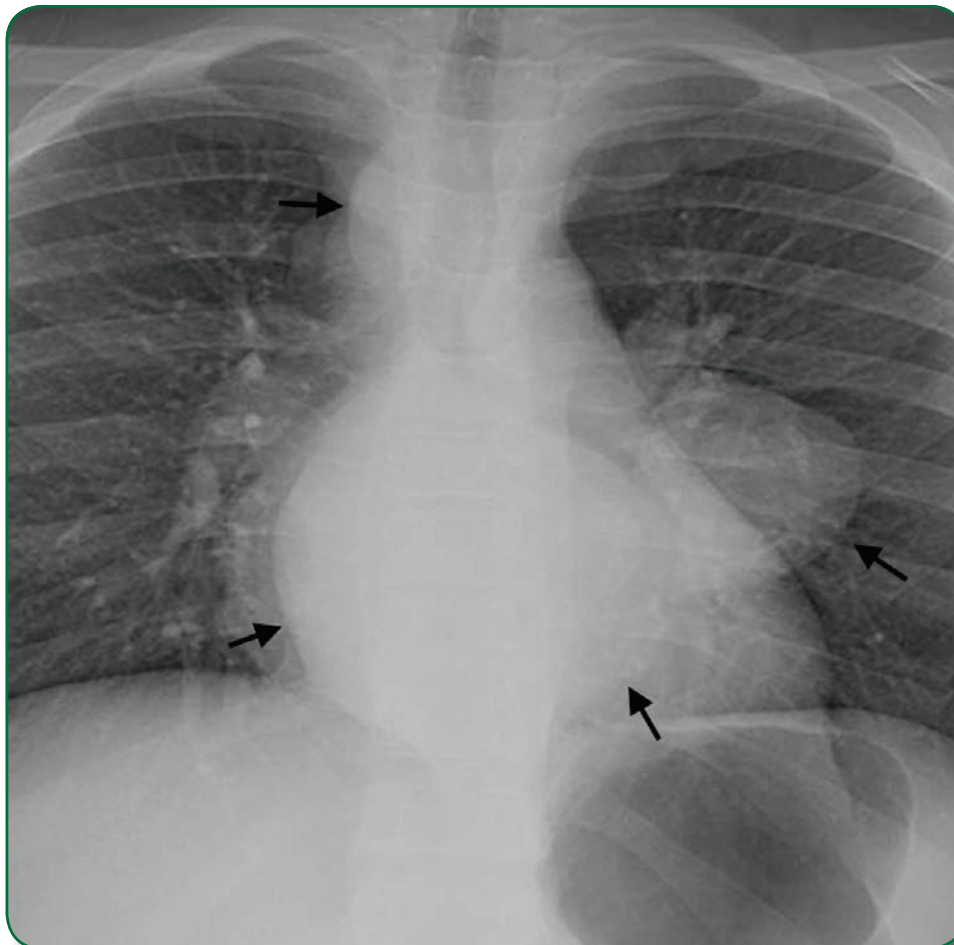


Fig. 52. Lymphoma. Left hilar and bilateral mediastinal masses (arrows) in this adolescent with Hodgkin lymphoma have an appearance similar to lymphadenopathy seen with TB.

Other Diseases That Can Mimic Tuberculosis (cont...)

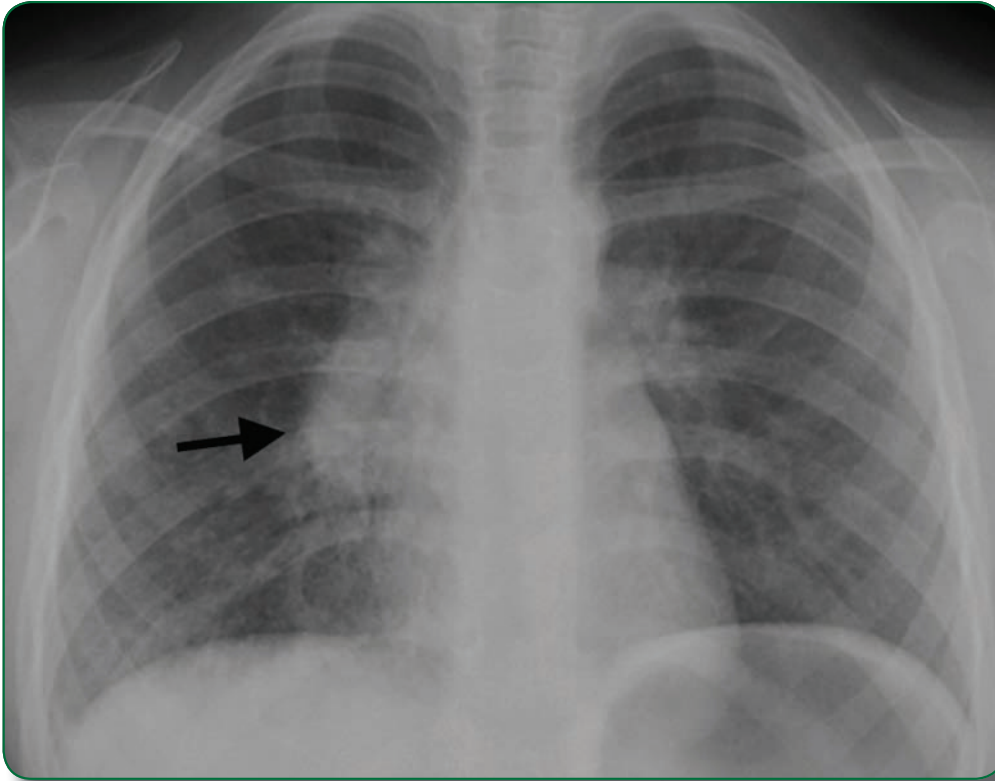
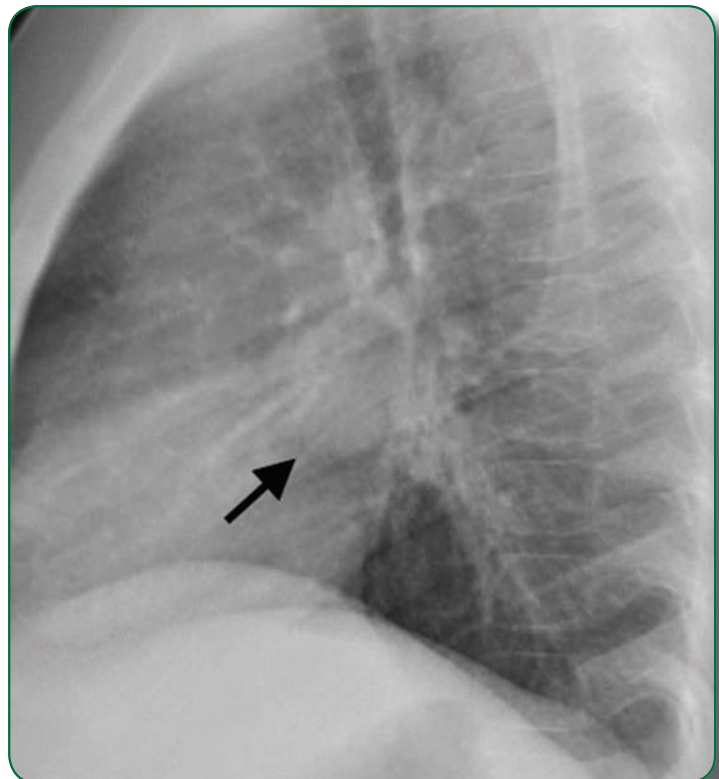


Fig. 53A.
Mycoplasma
infection.
PA radiograph
shows nodular
prominence in
the right lung
hilum (arrow),
consistent with
lymphadenopathy.
The lungs are clear.

Fig. 53B.
Lateral
radiograph
verifies an
enlarged node
in the infrahilar
region (arrow).



Other Diseases That Can Mimic Tuberculosis (cont...)



Fig. 54.
Mediastinal lymphadenopathy with cysticercosis. Multiple enhancing anterior mediastinal lymph nodes in a child with disseminated cysticercosis, resembling TB.

Other Diseases That Can Mimic Tuberculosis (cont...)

Pulmonary consolidative opacities are seen with many lung infections and cannot be distinguished from TB radiographically. Diffuse micronodular or miliary patterns as well as cavitary pneumonias are highly suggestive of TB but can sometimes be caused by other infections. MRSA is an increasingly common cause of multiple cavitary nodules in children (Fig. 55). Pleural effusion, a nonspecific inflammatory response to pneumonia, is more common in adults with TB than in pediatric disease. Adolescents have a higher incidence of TB pleural effusions than younger children. More often, pleural effusions are seen with *Staphylococcus aureus* and *Streptococcus pneumoniae*, especially in areas with a low incidence of TB. Viral, fungal and parasitic infections, nontuberculous mycobacteria, *Pneumocystis jirovecii* and aspiration pneumonia may present with pulmonary findings similar to TB. Severe allergic bronchopulmonary aspergillosis may show nodular pulmonary densities and air space opacities on chest radiograph masquerading as pulmonary TB. On biopsy, acute and chronic inflammation, necrotizing granulomas, giant cells, eosinophilia, and rare hyphal elements are described with aspergillosis.⁶⁵ Thoracic actinomycosis may mimic TB with pulmonary consolidation, pleural effusion, or mediastinal involvement.⁶⁶ Detailed clinical information, other diagnostic tests and cultures are usually necessary to make the final diagnosis. Lymphocytic interstitial pneumonitis (LIP) (Fig. 56) and opportunistic infections can look like TB and cause diagnostic confusion.^{67, 68} Pulmonary blastomycosis, endemic to Canada and the upper Midwest of the United States, has a variety of radiology manifestations that can imitate TB including miliary disease, consolidation, and cavitary lesions. Lymphadenopathy, pleural effusion and calcification are rarely seen with blastomycosis.⁶⁹ Other granulomatous diseases such as histoplasmosis and sarcoidosis can cause hilar lymphadenopathy and sometimes diffuse reticulonodular opacities that are indistinguishable from TB on plain radiographs.⁷⁰

Other Diseases That Can Mimic Tuberculosis (cont...)

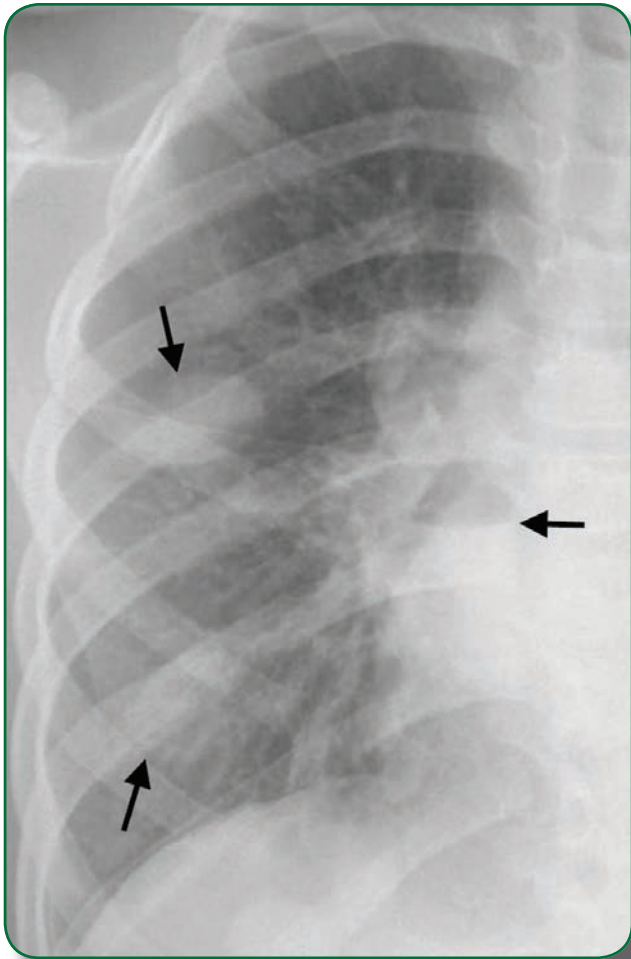
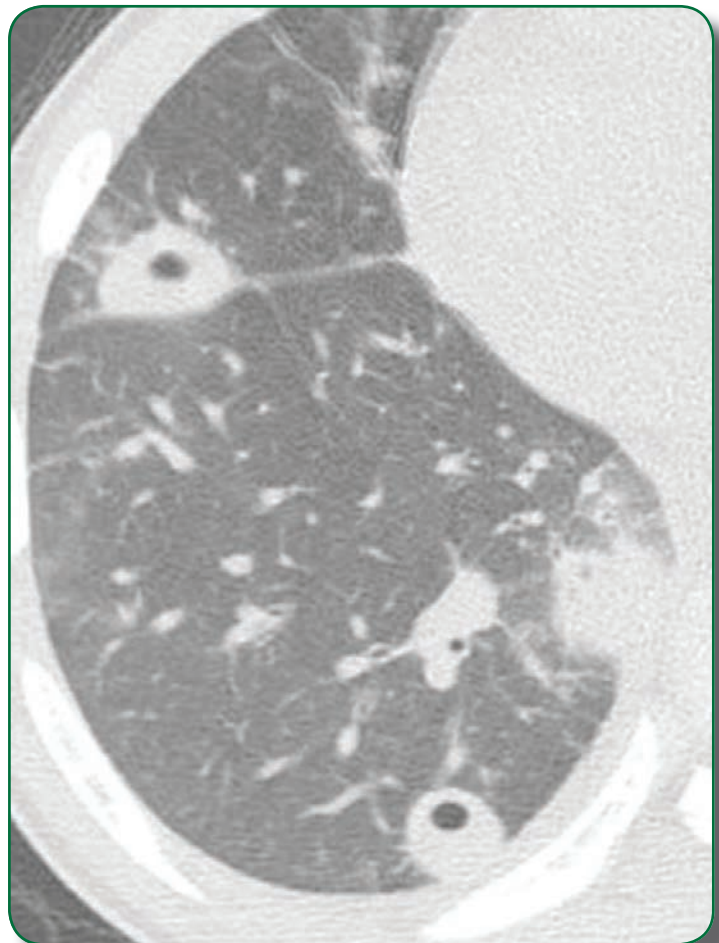


Fig. 55A.
MRSA cavitory
nodules.
Chest radiograph
shows multiple
pulmonary nodules,
one of which
contains an air-fluid
level indicating
cavitation (arrows).

Fig. 55B.
Chest CT on the
same patient shows
cavitation within
nodules that was
not apparent on
radiographs.



Other Diseases That Can Mimic Tuberculosis (cont...)

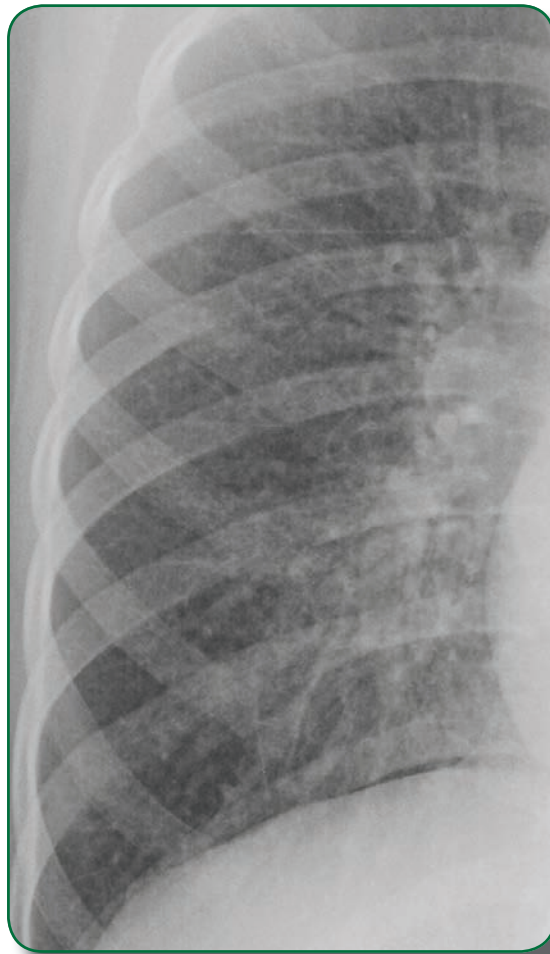


Fig. 56.
Interstitial disease
mimics miliary TB.
The fine reticulonodular
pattern in the lung of
this adolescent with
lymphocytic interstitial
pneumonitis (LIP)
could be mistaken for a
miliary pattern of TB.

Other Diseases That Can Mimic Tuberculosis (cont...)

Noninfectious conditions such as cystic fibrosis, dyskinetic cilia syndrome and chronic granulomatous disease may lead to long term or recurrent infections and inflammatory conditions resulting in findings confused with TB (Fig. 57). Reticulonodular patterns can be seen with Langerhans cell histiocytosis, rheumatoid lung disease, pulmonary fibrosis or rarely lymphatic spread of cancer. Wegener granulomatosis, a systemic vasculitis, can present with diffuse, nodular pulmonary granulomatous disease sometimes mistaken for TB. Epidemiologic information, clinical findings, cultures, biopsy and pathologic examination may be required to elucidate the final diagnosis.

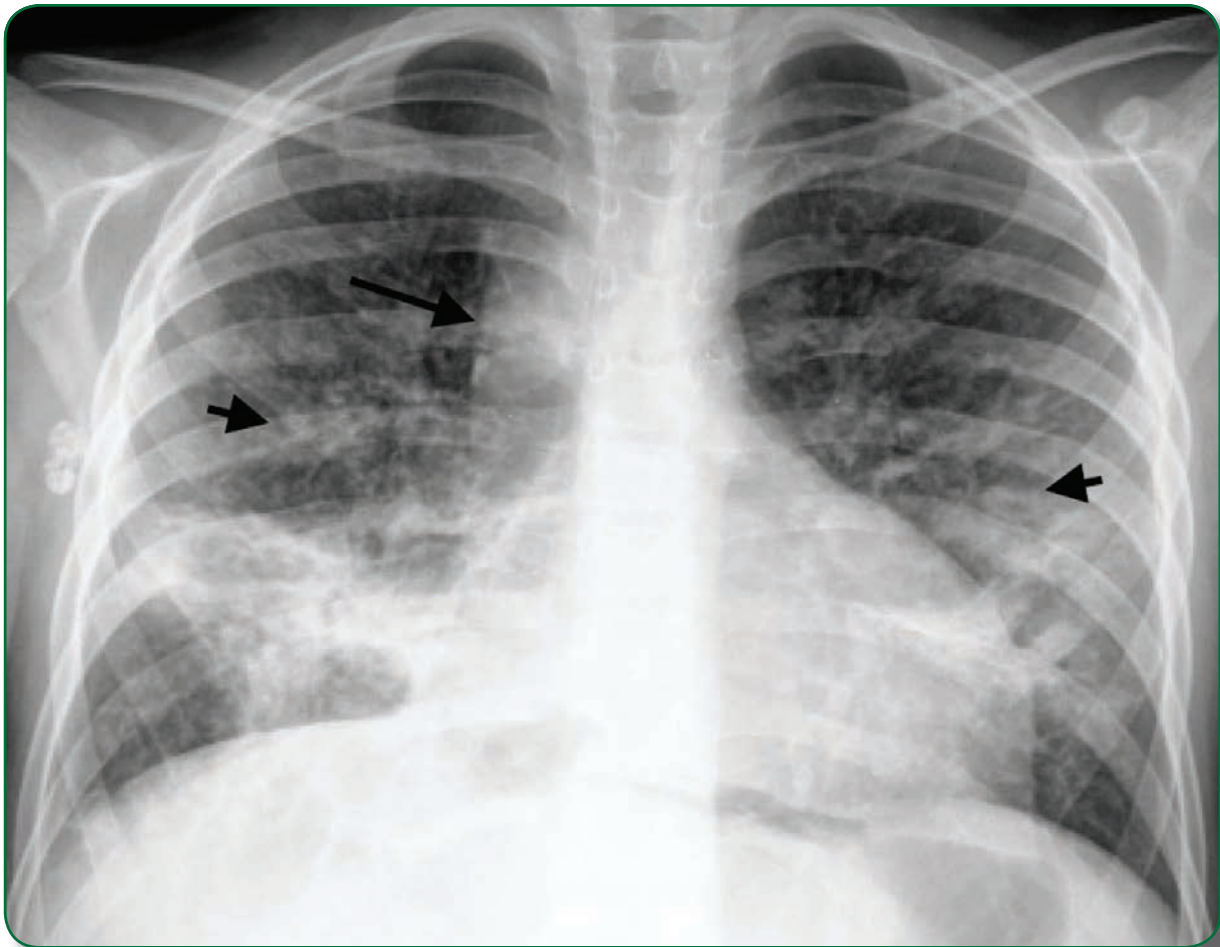


Fig. 57.

Chronic granulomatous disease.

Chest radiographs show small, bilateral pulmonary nodules (short arrows), right paratracheal lymphadenopathy (long arrow), and bilateral areas of atelectasis, similar to what might be seen with TB.



Clinical Cases

Clinical Cases

CASE 1.

A 12-year-old Hispanic male was exposed to his father who had AFB smear positive pulmonary TB. The child's tuberculin skin test measured 6 mm induration (> 5 mm is considered positive among household contacts). The patient had no symptoms and a normal physical examination. See initial chest radiograph (Fig. 58). The primary physician read the initial radiograph as normal and started isoniazid for LTBI. Look for the subtle abnormal finding on the chest radiograph (Fig. 59).

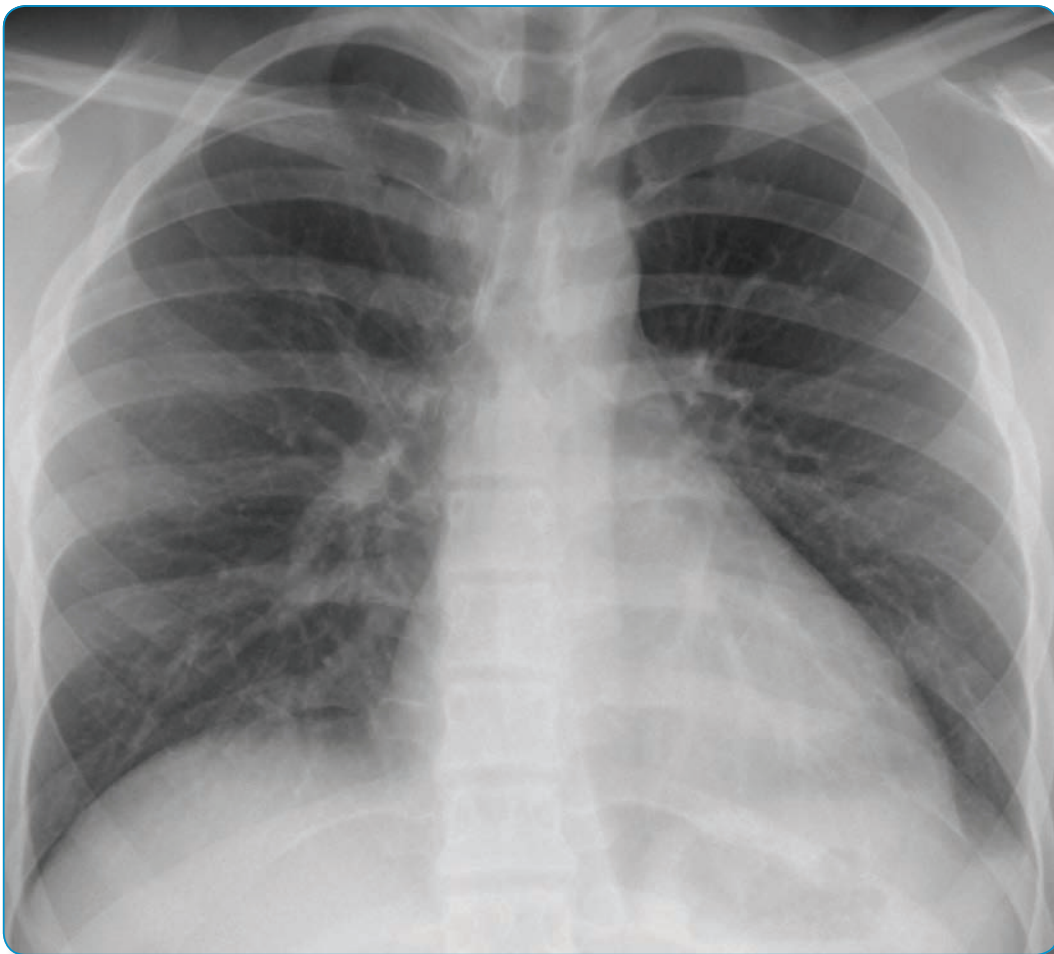


Fig. 58. Case 1.

Clinical Cases (cont...)

Upon follow up 6 weeks later the child was ill with fever, cough and weight loss. A repeat chest radiograph showed a large pleural effusion (Fig. 60). The patient required hospitalization, video-assisted thorascopic surgery (VATS) and a chest tube. AFB smears and TB cultures were negative. Routine cultures were also negative. The clinical symptoms and findings on the chest radiograph resolved with tuberculosis treatment (Fig. 61). This case emphasizes the importance of documentation of the final interpretation of the radiograph, as subtle abnormalities can be missed by inexperienced observers.

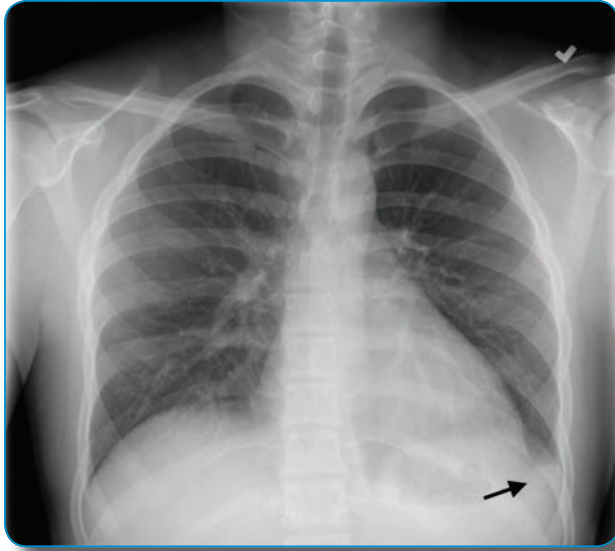


Fig. 59. Case 1.
Chest radiograph shows blunting of the left costophrenic angle by a small pleural effusion.

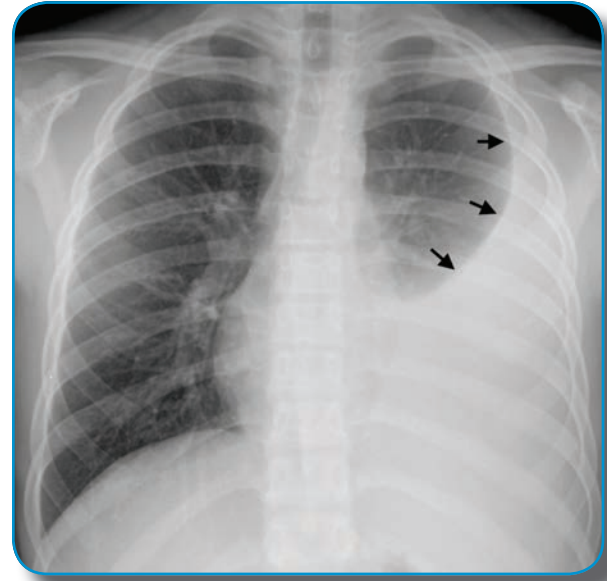
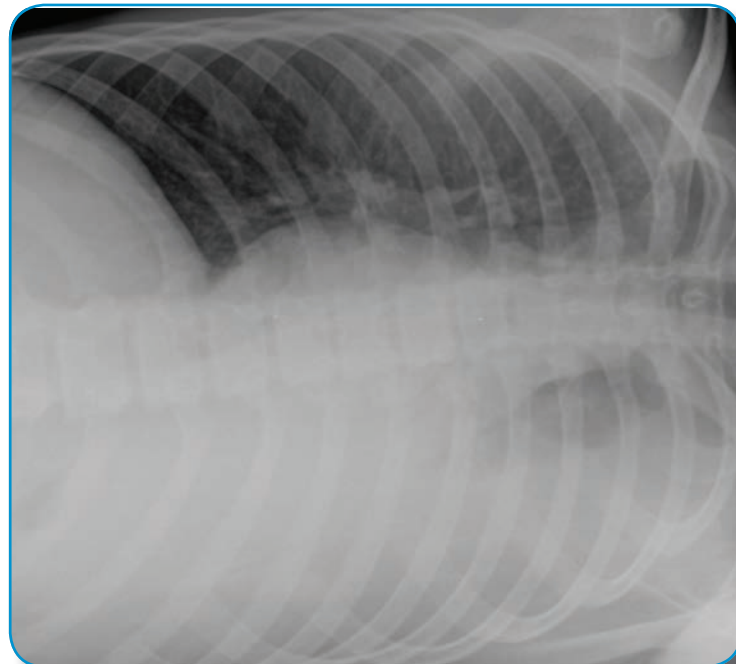


Fig. 60A. Case 1.
Follow-up chest radiograph 6 weeks later shows a large left pleural effusion (arrows).

Fig. 60B.
A left lateral decubitus view on the same date shows that most of the fluid shifts within the pleural space when the patient is in the decubitus position, indicating a predominantly free-flowing effusion.

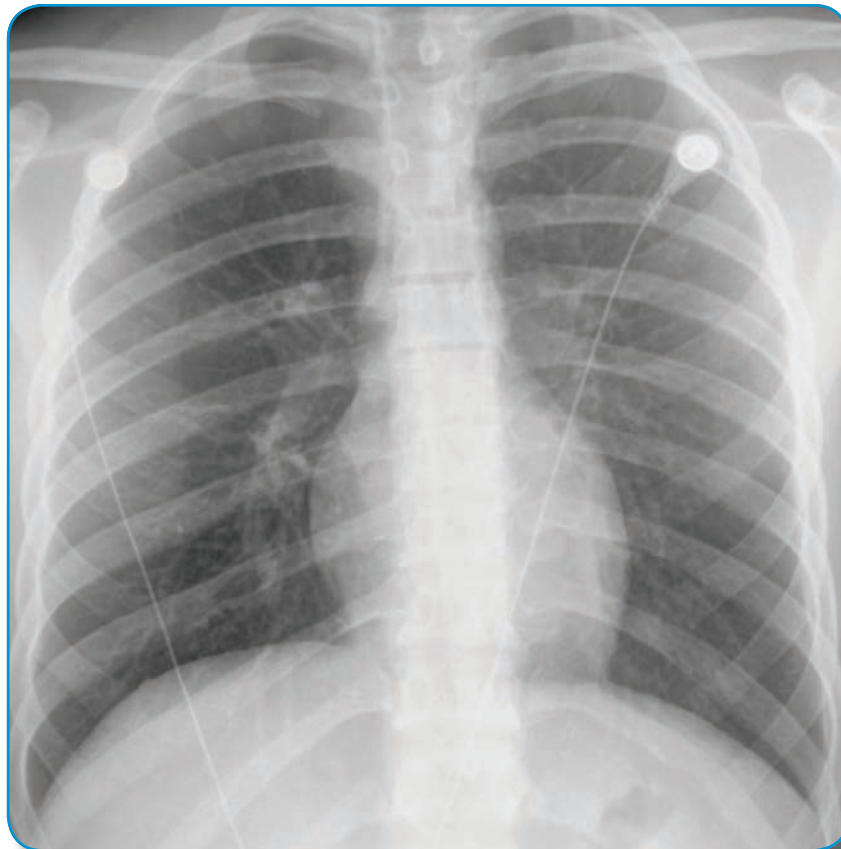


Clinical Cases (cont...)



Fig. 60C. Axial CT image shows a left pleural effusion with no visible pleural enhancement or evidence of loculation. Note lymphadenopathy in the subcarinal region (arrow).

Fig. 61. Case 1. After therapy, the left pleural effusion resolves completely.



CASE 2.

A 4-month-old infant was exposed to an adult with cavitary pulmonary TB, AFB smear and culture positive. The infant's initial TB skin test measured 0 mm. Two weeks later the baby developed symptoms of cough, fever and tachypnea. Chest radiograph at that time is shown (Fig. 62).

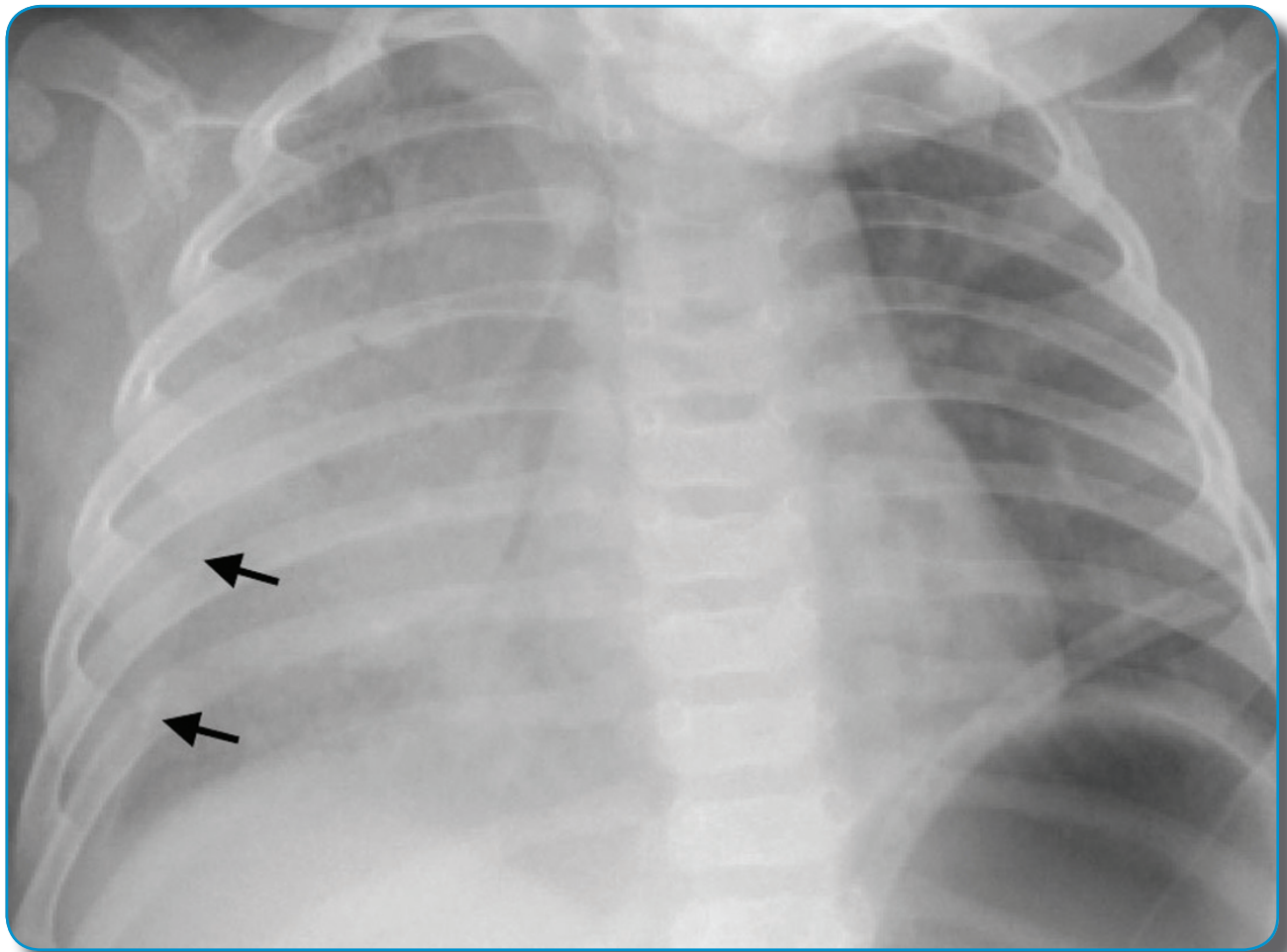


Fig. 62. Case 2.
The initial radiograph shows extensive alveolar opacity in the right lung and a small right pleural effusion (arrows).

Clinical Cases (cont...)

The child was hospitalized with respiratory distress. Repeat TB skin test measured 12 mm induration. Early morning gastric aspirates were AFB smear and culture positive for TB. Cerebral spinal fluid (CSF) showed elevated white blood cells of 26 with lymphocyte predominance and the CSF protein was elevated at 98, consistent with TB meningitis. The brain MRI was normal with no evidence of inflammation or infarcts. One month after initiation of treatment the patient developed respiratory distress and repeat chest radiograph is shown (Fig. 63). The patient was treated for 12 months with standard TB medications and had a full recovery.

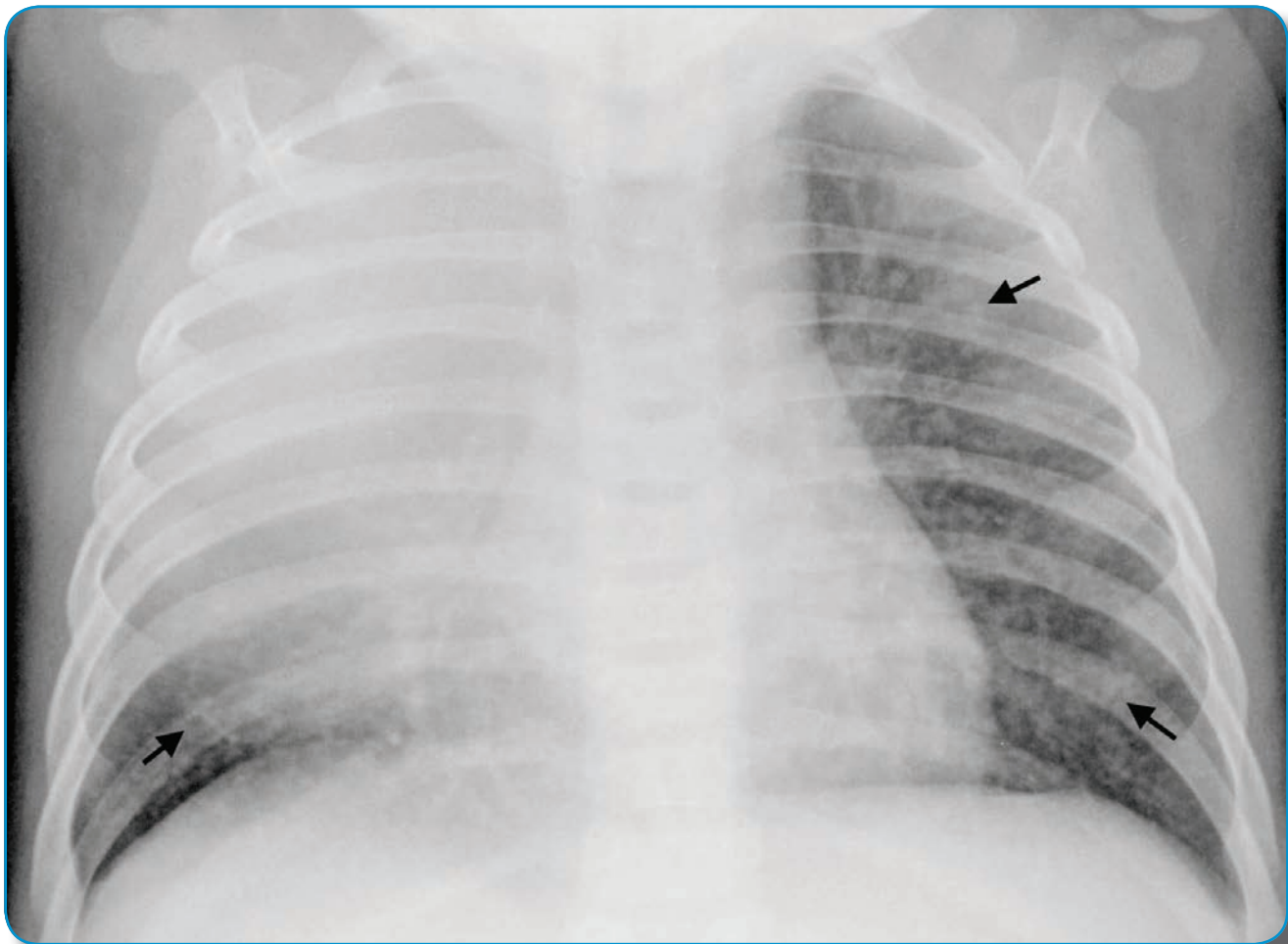


Fig. 63. Case 2.

A radiograph obtained one month later continues to show a large area of consolidation in the right lung. New tiny miliary nodules are seen in both lungs (arrows).

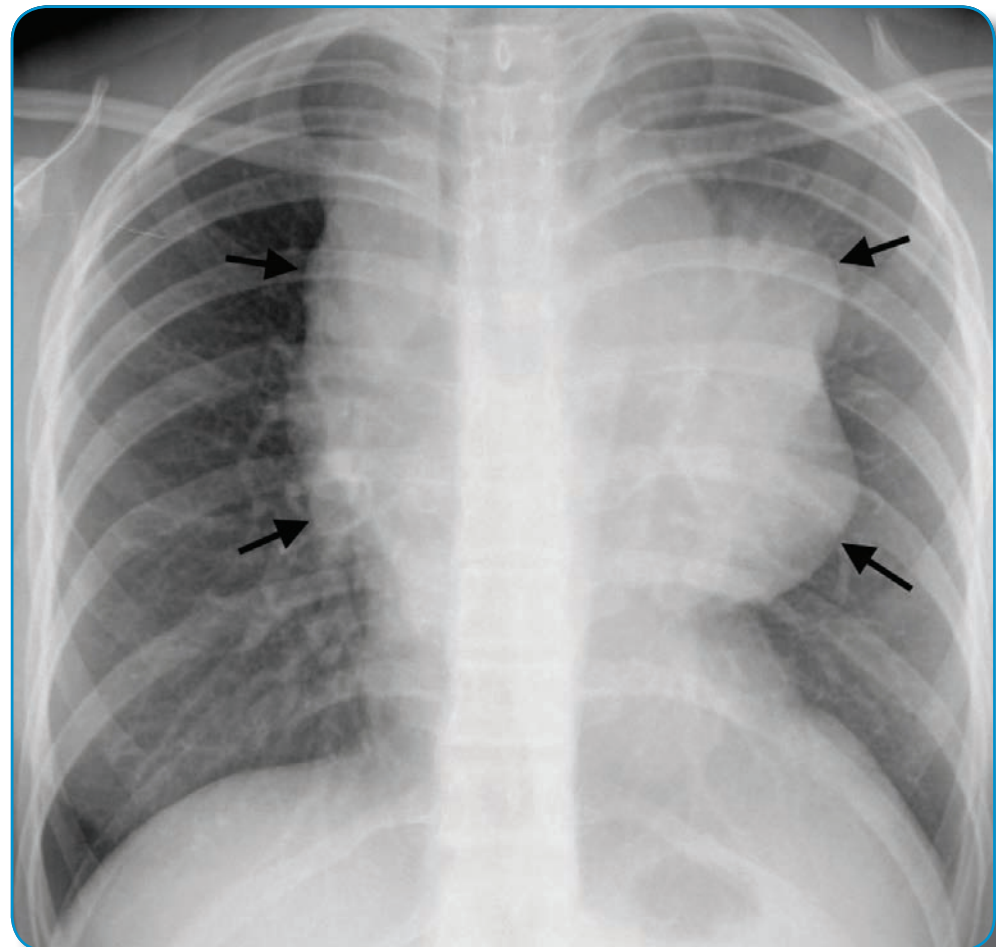
CASE 3.

A 10-year-old Hispanic boy had a 2 month history of nontender cervical lymphadenopathy measuring 5 cm on examination.

The patient was born in Mexico and had BCG vaccination at birth. He was healthy with no significant past medical history. The physical examination was normal except for cervical lymphadenopathy and a 1 cm supraclavicular lymph node. The TB skin test measured 15 mm induration. The chest radiograph is shown (Fig. 64).

Biopsy of the supraclavicular and cervical lymph nodes showed Hodgkin's lymphoma on pathology and no evidence of TB. AFB smear and culture for tuberculosis were negative. The child was successfully treated for Hodgkin's lymphoma. He also completed treatment with isoniazid for latent TB infection.

Fig. 64. Case 3. PA chest radiograph shows a large, lobulated mass in the anterior superior mediastinum (arrows).



CASE 4.

A 6-month-old Hispanic infant came to the emergency room with a 2 week history of upper respiratory symptoms, cough, congestion and fever. The chest radiograph is shown (Fig. 65). On physical examination the infant had left hemiparesis and deviated lateral gaze.

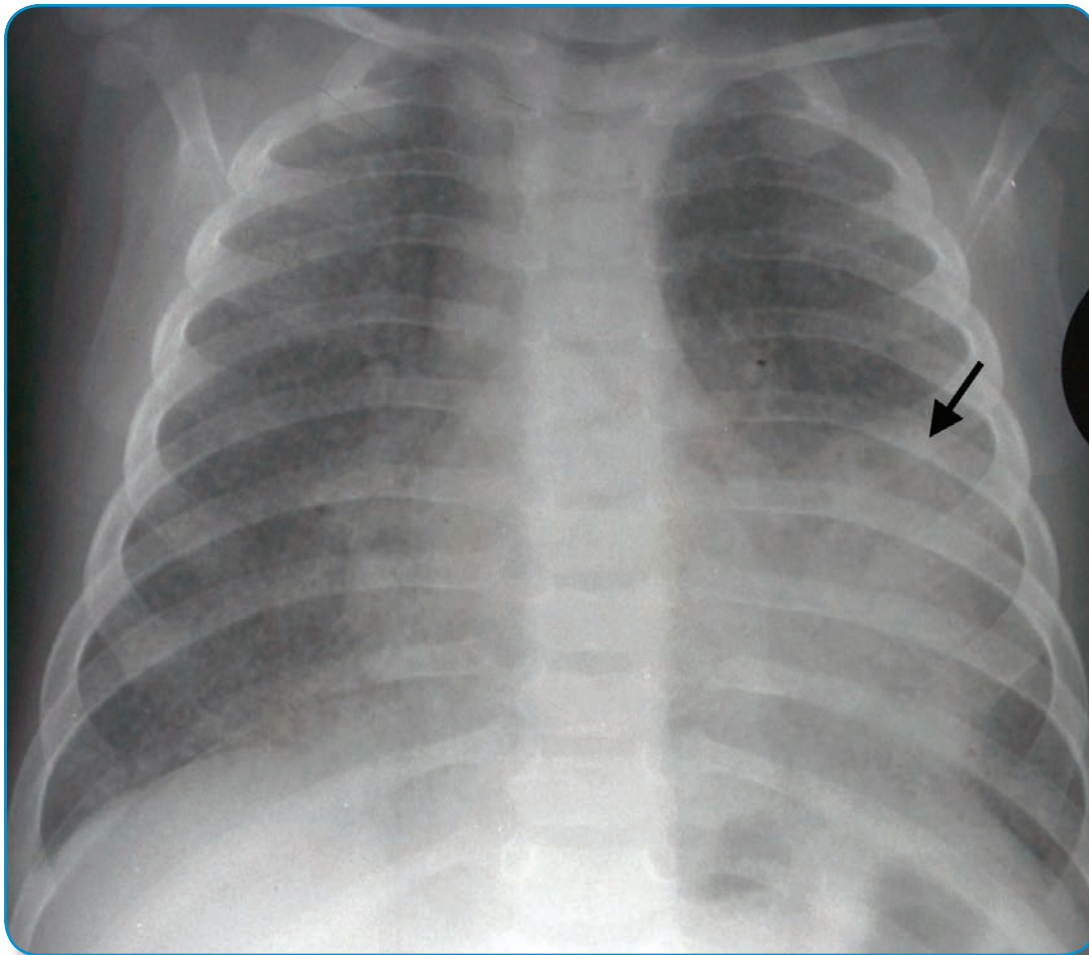


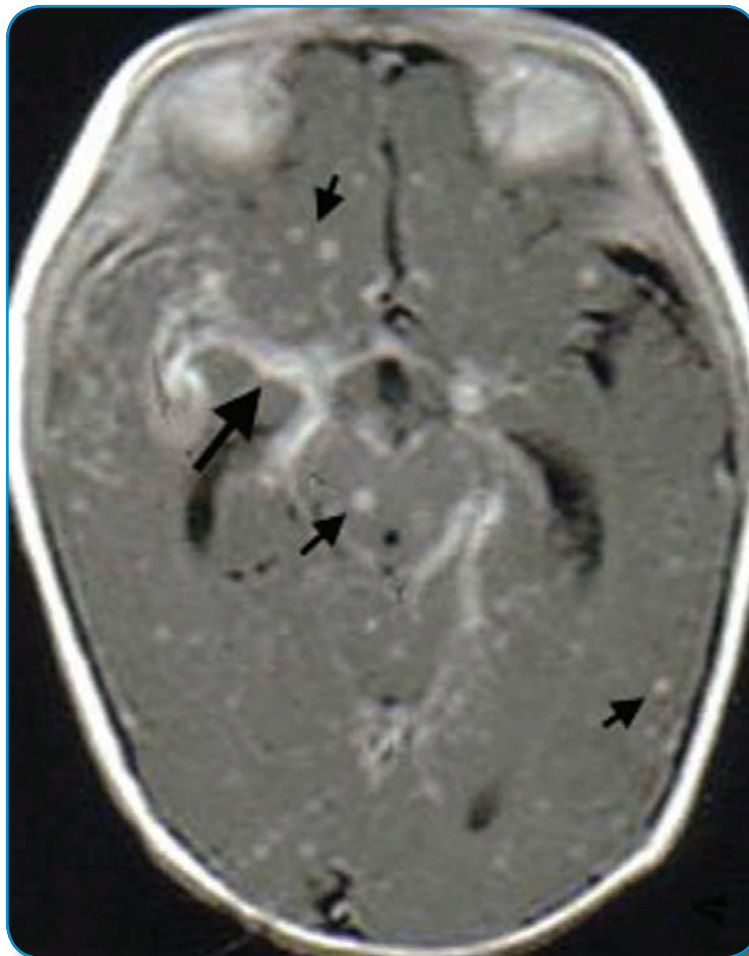
Fig. 65. Case 4. PA chest radiograph shows consolidation in the lingula on the left (arrow), accompanied by diffuse lung haziness and numerous tiny miliary nodules.

Clinical Cases (cont...)

The CSF showed elevated white blood cells of 64 with lymphocytic predominance and elevated CSF protein of 108 consistent with TB meningitis. The brain MRI is shown (Fig. 66). The patient was started on standard 4 drug TB medications and treated for 12 months. Steroids were given during the first month of treatment. The diagnosis of TB meningitis was based on clinical findings including the MRI. Cultures from gastric aspirates and CSF were negative for TB.

Follow up image 3 months after treatment was started is shown (Fig. 67). After completion of treatment, mild gross motor deficits and left sided weakness persisted. But the patient was able to walk, use the hands and arms and had an otherwise normal developmental assessment.

Fig. 66A. Case 4.
Axial contrast-enhanced T1-weighted MRI image reveals leptomeningeal enhancement (large arrow) and numerous small enhancing nodules in the brain and brainstem (small arrows).



Clinical Cases (cont...)



Fig. 66B.
Same MRI sequence at a different level shows gyriform enhancement on the right (large arrow) indicating infarction. Multiple ring enhancing nodules are present (small arrows).

Fig. 67. Case 4.
Follow-up axial MRI image obtained 3 months later shows resolution of the brain nodules but residual abnormal signal in the right cerebral infarct (arrow).



CASE 5.

A 15-year-old boy had a 1 month history of fever, 25 pound weight loss and night sweats. The physical examination was significant for cervical lymphadenopathy, and the TB skin test measured 0 mm induration. The chest radiograph was normal.

Evaluation included a negative HIV test, a normal CBC and peripheral smear. An interferon gamma release assay (IGRA) blood test for TB was positive, indicating TB infection or disease. CT of the abdomen and neck showed lymphadenopathy (Fig 68 A,B). Biopsy of the cervical lymph node was positive on AFB smear and TB culture. Pathology from the lymph node biopsy was consistent with TB lymphadenitis and showed no evidence of cancer. The patient was treated for 9 months for disseminated TB disease with resolution of symptoms and a full recovery.



Fig. 68A. Case 5. Contrast-enhanced CT of the abdomen shows enlarged lymph nodes with ring enhancement (arrows).



Fig. 68B. Contrast CT of the neck in the same patient also shows enlarged lymph nodes with characteristic peripheral enhancement (arrows).

CASE 6.

A 3-year-old boy presented with chronic pain and swelling of the left knee. Plain radiographs and MRI of the leg are shown (Fig. 69).

A biopsy of the lesion for malignancy versus osteomyelitis revealed granulomatous osteomyelitis and cultures grew TB.⁷¹ The tuberculin skin test measured 20 mm induration. There were no known risk factors for TB, but contact investigation identified a source case with pulmonary TB. The patient was treated for 12 months for TB osteomyelitis with standard therapy.

Fig. 69A. Case 6. AP radiograph of the right knee shows well-defined osteolytic defect with sclerotic margins and widening of the adjacent physis. Focal soft tissue swelling is present in the medial soft tissues over the knee.

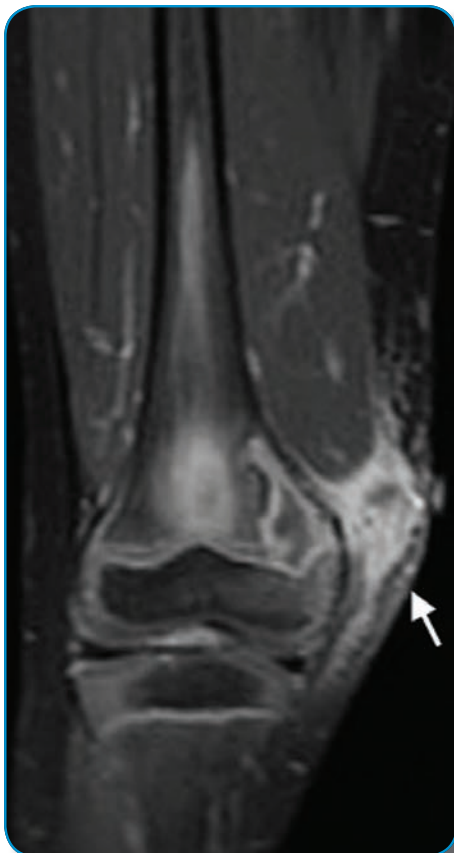


Fig. 69B. Coronal post-Gadolinium image shows peripheral enhancement surrounding the abscesses in the bone and soft tissues (arrow).

CASE 7.

A 15-year-old girl presented with a 3 week history of pleuritic chest pain, tachypnea, shortness of breath, high fever, productive cough, hemoptysis, night sweats and an 18 pound weight loss. She was treated with levaquin followed by azithromycin for pneumonia. The chest radiograph is shown (Fig. 70).

An extensive evaluation including a biopsy of the lung showed necrotizing granulomatous process with rare multi-nucleated giant cells and no evidence of malignancy. AFB stains and cultures were negative. The tuberculin skin test was negative and an IGRA blood assay for TB was negative. There was no known TB exposure or risk factors. A positive antineutrophil cytoplasmatic autoantibody test (C-ANCA) confirmed the diagnosis of Wegener granulomatosis. This systemic vasculitis is rarely encountered in children and may present with pulmonary infiltrates and cavitary lung disease. The most common presentation includes sinusitis, fever epistaxis and hematuria.

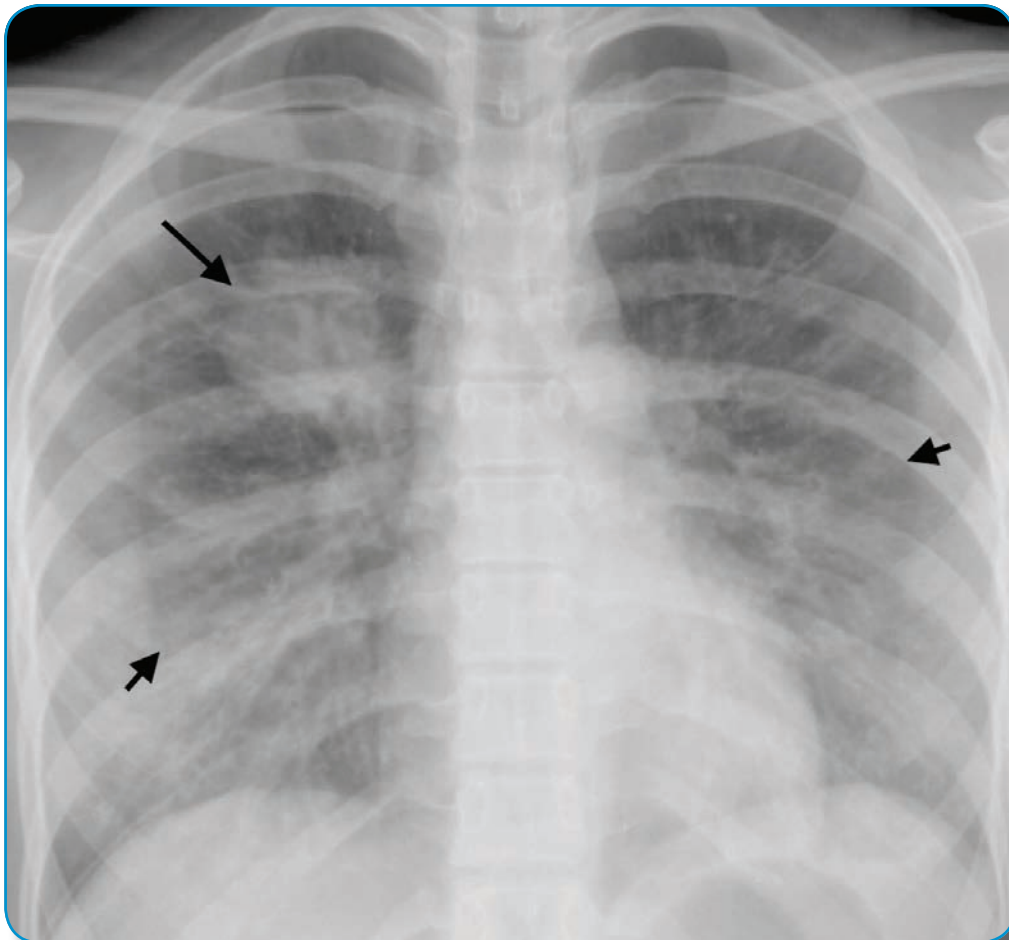


Fig. 70. Case 7. PA chest radiograph shows a large nodular opacity in the right upper lobe (long arrow), with smaller opacities scattered elsewhere in the lungs (short arrows).

CASE 8.

A 4-month-old Hispanic girl was evaluated for a pulmonary mass on chest radiograph (Fig. 71). The initial differential diagnostic considerations included pneumonia, thymus, central obstructive process, or congenital agenesis of left upper lobe. Chest CT is shown (Fig. 72). Tuberculin skin test measured 18 mm induration. Pulmonary TB disease was diagnosed in the child's mother. Gastric aspirates from the infant were AFB smear positive and the culture grew TB. The child was treated with standard therapy and follow up radiographs showed gradual resolution (Fig. 73).

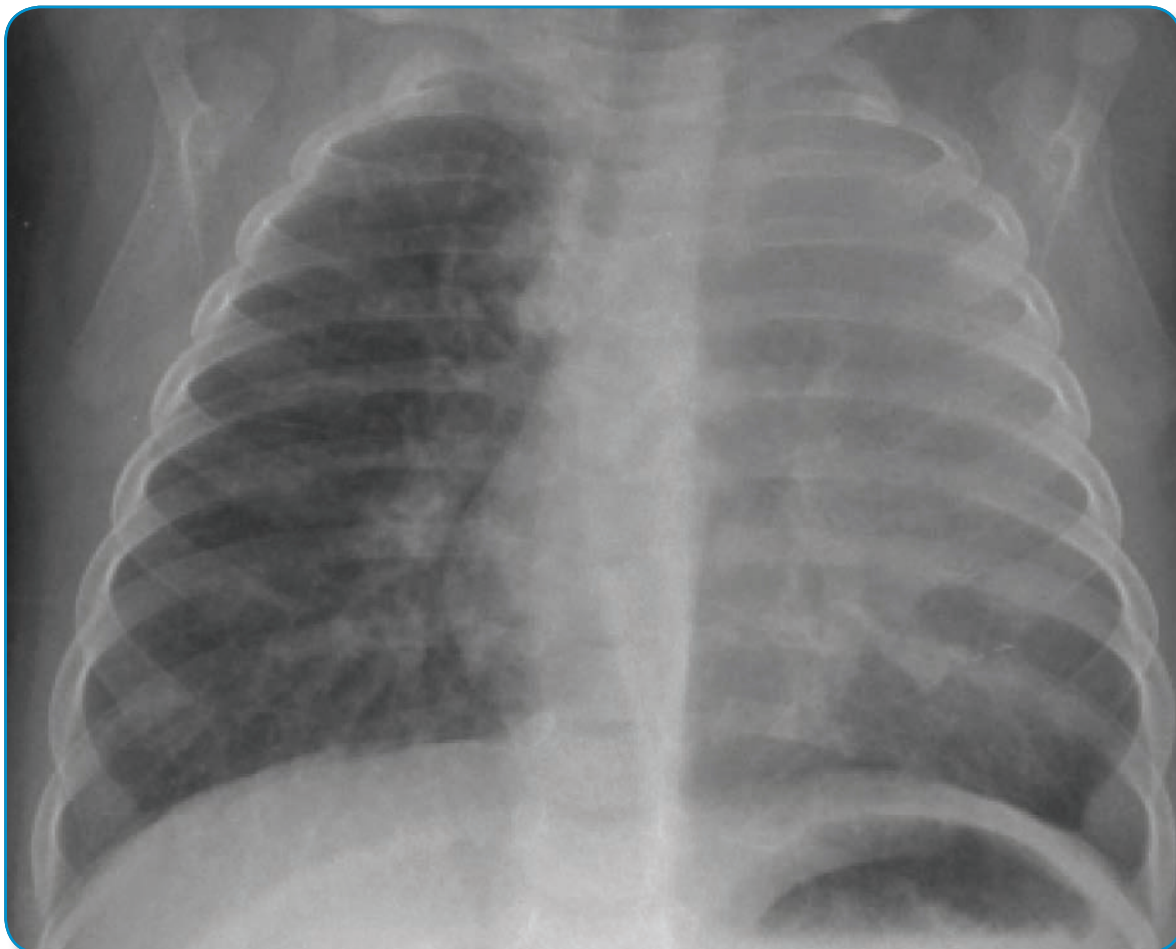


Fig. 71. Case 8.
PA chest radiograph shows a large area of air space consolidation in the left upper lobe without shift of the mediastinum.

Clinical Cases (cont...)

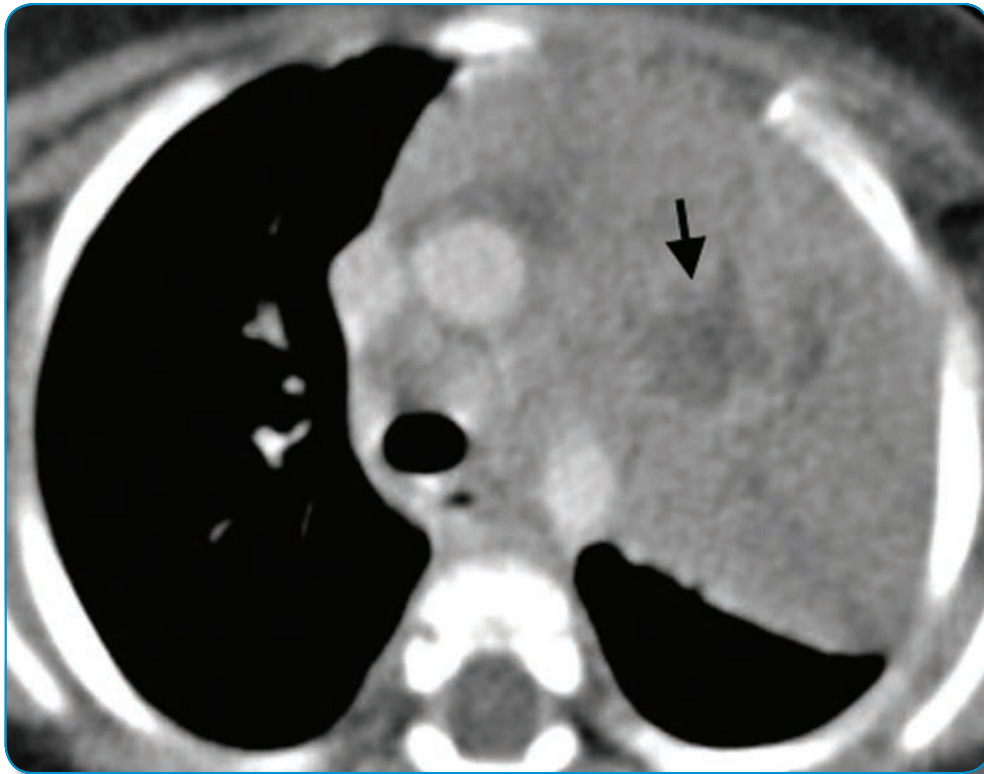


Fig. 72A. Case 8. Contrast enhanced CT image shows the left upper lobe consolidation with an area of lower attenuation and peripheral enhancement near the mediastinum that could represent an area of necrosis or an enhancing lymph node (arrow).

Fig. 72B. Another image from the same CT scan shows peripherally enhancing lymphadenopathy in the subcarinal and left hilar regions (arrows).



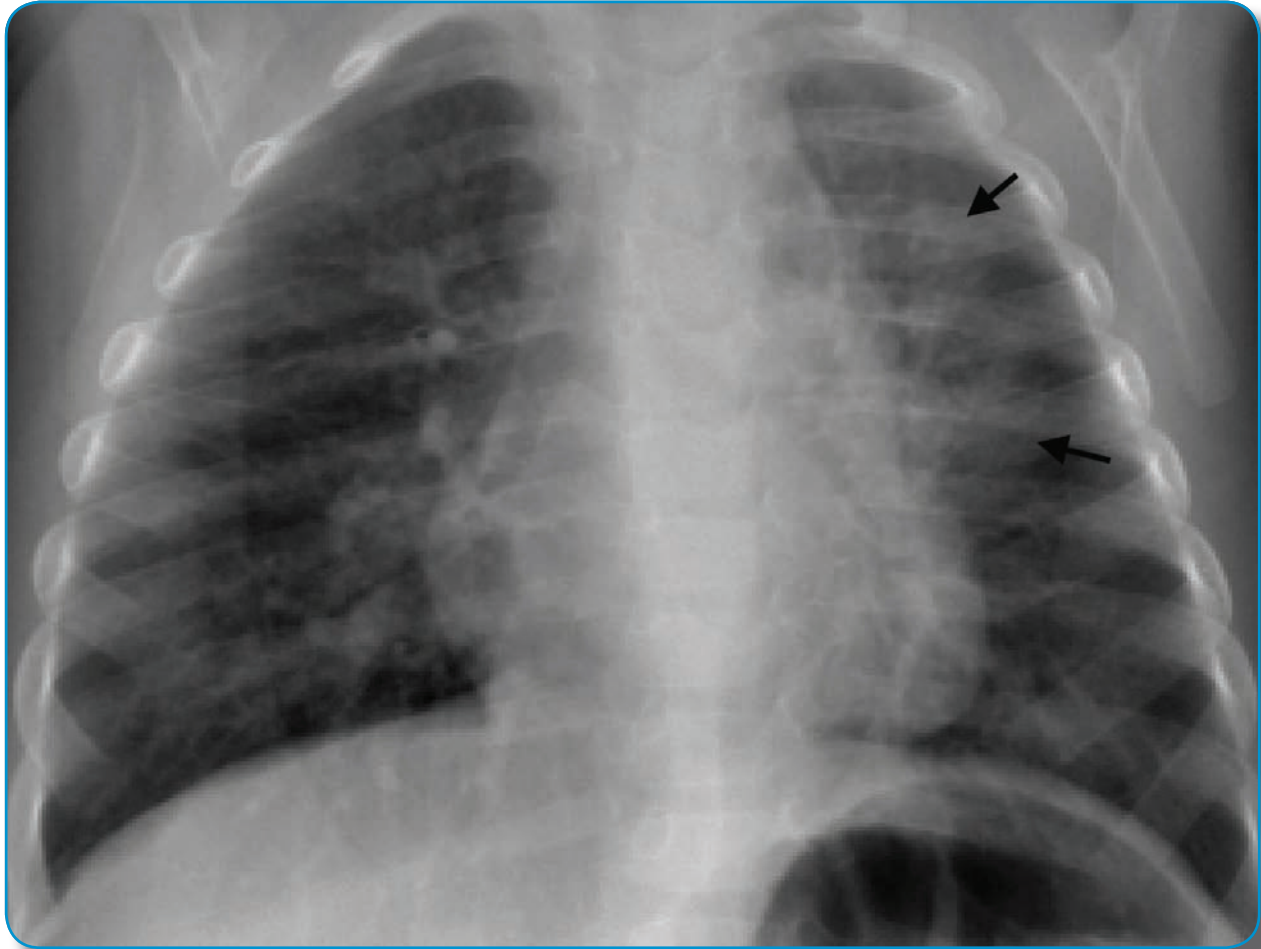


Fig. 73. Case 8.
A follow-up radiograph obtained 6 months later shows improvement in the left upper lobe consolidation, with mild residual opacity (arrows).

CASE 9.

An 8-year-old boy was followed for chronic eosinophilic inflammation of the urinary bladder (eosinophilic cystitis). Prior to starting steroid therapy he had a negative tuberculin skin test that measured 0 mm. There were no risk factors for TB. An initial chest radiograph from the referring clinic was reported as "normal except for aortic calcification." Steroids were started for treatment of the cystitis and a follow up chest radiograph is shown (Fig. 74).

Repeat TB skin test was negative. An IGRA blood assay for TB was positive. Sputum and urine samples were positive for TB. The patient was treated for 12 months with standard therapy and follow up chest radiograph is shown (Fig. 75).

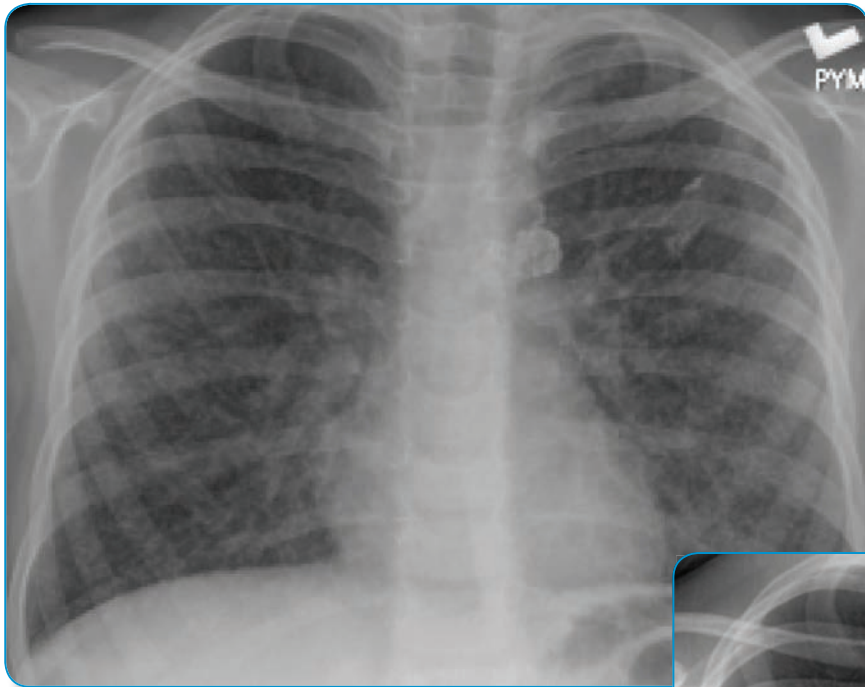


Fig. 74. Case 9. PA chest radiograph shows a fine diffuse miliary nodular pattern in the lungs. Calcified lymph nodes are present in the left mediastinum, which were mistaken for aortic calcifications on the earlier radiograph.

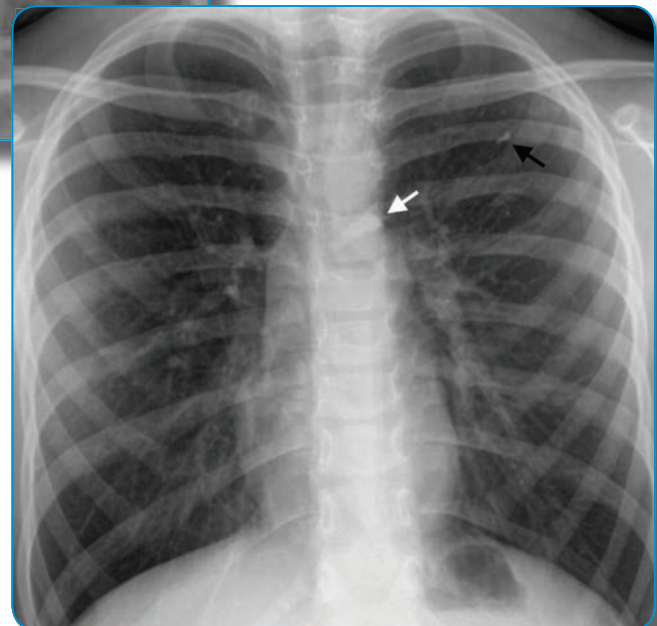


Fig. 75. Case 9. A post-treatment radiograph shows decreased size of the calcified lymphadenopathy (white arrow) with a tiny calcified granuloma in the left upper lobe (black arrow). The miliary nodules have resolved.

CASE 10.

A 15-month-old boy was seen for fever, a 3 week history of draining otitis media and acute mastoiditis. He developed seizures and cerebral spinal fluid showed 360 WBC, 67% lymphocytes, and CSF protein of 210, consistent with meningitis. There were no risk factors for TB and the tuberculin skin test was negative, measuring 0 mm. Chest radiograph was normal. An IGRA blood assay for TB was positive. Brain MRI is shown (Fig. 76). The patient developed hydrocephalus and ischemic infarcts as complications of TB meningitis. Cultures of the cerebral spinal fluid grew TB. The patient was treated with standard therapy for 12 months, including steroids during the first month.

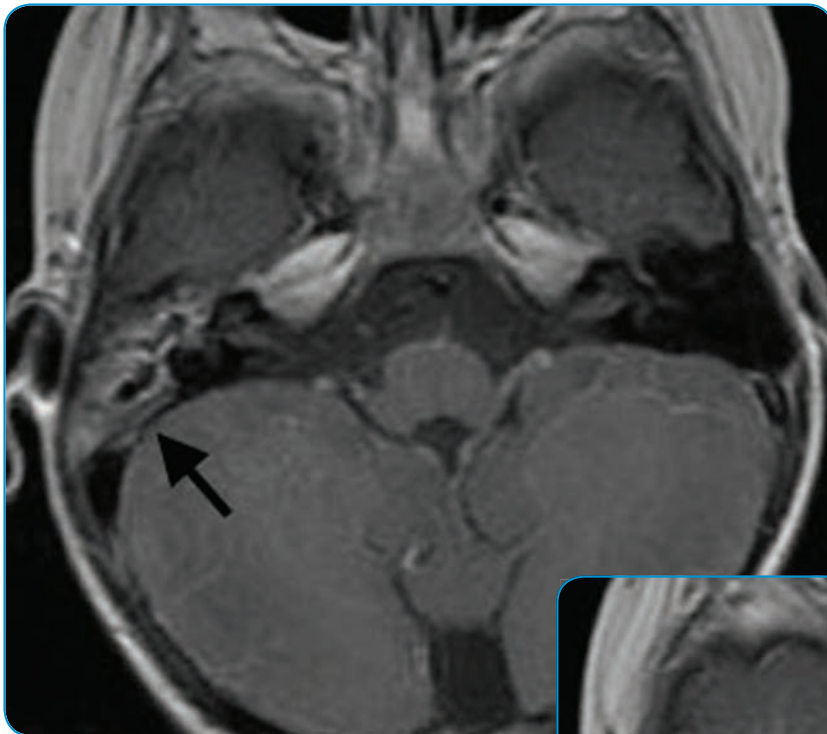


Fig. 76A. Case 10. Contrast enhanced MRI shows abnormal signal in the right mastoid air cells with enhancement (arrow).

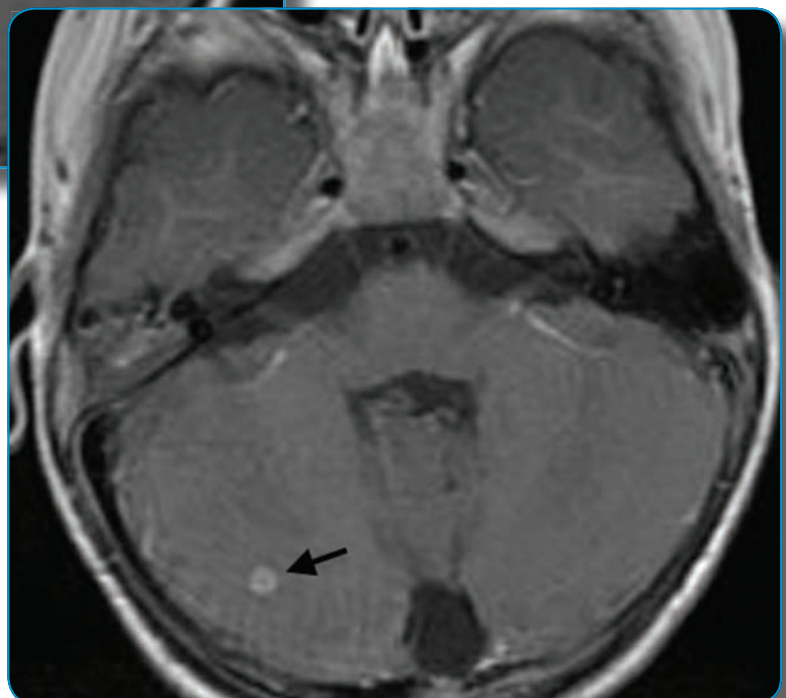


Fig. 76B. The same MRI at a different level reveals a small ring-enhancing nodule in the right occipital lobe (arrow).

Conclusion

Conclusion

Tuberculosis is an important disease worldwide and is sometimes difficult to recognize in children who do not follow the same patterns of disease as adults. In children the lungs, lymph nodes or central nervous system are more commonly involved. In general, radiographic findings may be suggestive but often are not specific for TB. Characteristic patterns in children with TB include unilateral hilar lymphadenopathy with or without consolidation and miliary disease. Cavitory lesions are uncommon except in adolescents who may demonstrate findings similar to adult disease. Contrast CT and/or MRI are the best diagnostic imaging modalities for extrapulmonary disease. Pediatric TB may present with confusing and difficult to interpret clinical information. Radiographic images are among the most important diagnostic tools.



References

- ¹ Marais BJ, Gie RP, Schaaf HS, et al. The natural history of childhood intra-thoracic tuberculosis - a critical review of the literature from the prechemotherapy era. *Int J Tuberc Lung Dis.* 2004;8:392-402.
- ² Gie R. Diagnostic atlas of intrathoracic tuberculosis in children: A guide for low income countries 2003. International Union Against Tuberculosis and Lung Disease, Paris, France, 1-55, 2003.
- ³ Miller FJ, Seal RM, Taylor MD. Tuberculosis in children. J and A Churchill Ltd, London, UK, 1963.
- ⁴ Weber HC, Beyers N, Gie RP, et al. The clinical and radiological features of tuberculosis in adolescents. *Ann Trop Paediatr.* 2000;20, 5-10.
- ⁵ Lincoln EM, Sewell EM. Tuberculosis in children. McGraw-Hill, New York, pp 1-327, 1963.
- ⁶ Bosch-Marcet J, Serres-Creixams X, Borrás-Perez V, et al. Value of sonography for follow-up of mediastinal lymphadenopathy in children with tuberculosis. *Journal of Clinical Ultrasound.* 2007 Mar-Apr;35(3):118-124.
- ⁷ Im J-G, Itoh H, Shim Y-S, et al. Pulmonary tuberculosis: CT findings-early active disease and sequential changes with antituberculous therapy. *Radiology.* 1993;186:653-660.
- ⁸ Bentley FJ, Grzybowski S, Benjamin B. Tuberculosis in childhood and adolescence. The National Association for the Prevention of Tuberculosis. London, England: Waterlow and Sons Ltd, 1954:1-213 and 238-253.
- ⁹ Schaaf HS, Beyers N, Gie RP, et al. Respiratory tuberculosis in childhood: the diagnostic value of clinical features and special investigations. *Pediatr Infect Dis J.* 1995 Mar;14(3):189-94.
- ¹⁰ Milkovic D, Richter D, Zoricic-Letoja I, Raos M, Koneul I. Chest radiography findings in primary pulmonary tuberculosis in children. *Coll Antropol.* 2005 Jun;29(1):271-276.
- ¹¹ Neu N, Saiman I, San Gabriel P, et al. Diagnosis of pediatric tuberculosis in the modern era. *Pediatr Infect Dis J.* 1999 Feb;18(2):122-126.
- ¹² Andronikou S, Joseph E, Lucas S, et al. CT scanning for the detection of tuberculous mediastinal and hilar lymphadenopathy in children. *Pediatr Rad.* 2004 Mar; 34(3):232-6.
- ¹³ Delacourt C, Mani TM Bonnerot V, et al. Computed tomography with normal chest radiograph in tuberculous infection. 1993, *Arch Dis Child.* Oct;69(4):430-432.
- ¹⁴ Andronikou S, Brauer B, Galpin J, et al. Interobserver variability in the detection of mediastinal and hilar lymph nodes on CT in children with suspected pulmonary tuberculosis. *Pediatr Radiol.* 2005 35:425-28.
- ¹⁵ Du Toit G, Swingler G, Iloni K. Observer variation in detecting lymphadenopathy on chest radiograph. *Int J Tuberc Lung Dis.* 2002 6(9):814-817.
- ¹⁶ Donnelly LF, Emery KH, Brody AS, et al. Minimizing radiation dose for pediatric body applications of single-detector helical CT: strategies at a large children's hospital. *AJR AM J Roentgenol.* 2001 Feb;176(2):303-6.
- ¹⁷ Marais BJ, Gie RP, Schaaf HS, et al. A proposed radiological classification of childhood intra-thoracic tuberculosis. *Pediatr Radiol.* 2004 34:886-894.
- ¹⁸ Im JG, Itoh H, Han MC. CT of pulmonary tuberculosis. *Seminars in Ultrasound CT MR.* 1995 Oct;16(5):420-434.
- ¹⁹ Kosaka N, Sakai T, Uematsu H, et al. Specific high-resolution computed tomography findings associated with sputum smear-positive pulmonary tuberculosis. *Journal of Computer Assisted Tomography.* 2005 Nov-Dec;29(6):801-4.
- ²⁰ Jamieson DH, Cremin BJ. High resolution CT of the lungs in acute disseminated tuberculosis and a pediatric radiology perspective of the term "miliary". *Pediatr Radiol.* 1993;23(5):380-3.
- ²¹ Baumann MH, Nolan R, Pitrini M, et al. Pleural tuberculosis in the United States: incidence and drug resistance. *Chest.* 2007; 131:1125-1132.
- ²² Theart AC, Marais BJ, Gie RP, et al. Criteria used for the diagnosis of childhood tuberculosis at primary health care level in a high-burden, urban setting. *International Journal of Tuberculosis and Lung Disease.* 2005 Nov;9(11):1210-1214.
- ²³ Enarson DA, Dorken E, Grzybowski S. Tuberculosis pleurisy. *Can Med Assoc J.* 1982;126:493-5.
- ²⁴ Chiu CY, Wu JH, Wong KS. Clinical spectrum of tuberculous pleural effusion in children. *Pediatr Int.* 2007 Jun;49(3):359-62.
- ²⁵ Andreu J, Caceres J, Pallisa E, Martinez-Rodriguez M. Radiological manifestations of pulmonary tuberculosis. *European Journal of Radiology* 2004;51:139-149.
- ²⁶ Schaaf HS, Marais BJ, Whitelaw A, et al. Culture-confirmed childhood tuberculosis in Cape Town, South Africa: a review of 596 cases. *BMC Infect Dis.* 2007 Nov 29;7:140.

- 27 Shewchuk JR, Reed MH. Pediatric postprimary pulmonary tuberculosis. *Pediatr Radiol*. 2002 Sep;32(9):648-51.
- 28 Griffith-Richards SB, Goussard P, Andronikou S, et al. Cavitating pulmonary tuberculosis in children: correlating radiology with pathogenesis. *Pediatr Radiol*. 2007 Aug;37(8):798-804.
- 29 Kisembo HN, Kawooya MG, Zirembuzi G, Okwera A. Serial chest radiographs in the management of children with a clinical suspicion of pulmonary tuberculosis. *Journal of Tropical Pediatrics*. 2001 Oct;47:276-283.
- 30 Fish RH, Pagel W. The morbid anatomy of epituberculosis. *J Path Bact*. 1938; 47:593-601.
- 31 Kim WS, Moon WK, Kim IO, et al. Pulmonary tuberculosis in children: evaluation with CT. *AJR Am J Roentgenol*.1997;168:1005-1009.
- 32 Morrison JB. Resorption of calcification in primary pulmonary tuberculosis. *Thorax*. 1970;25: 643-648.
- 33 Tsao PC, Lin PY. Clinical spectrum of bronchiectasis in children. *Act Paediatr Taiwan*. 2002 Sep-Oct;43(5):271-5.
- 34 Garg RK. Tuberculous meningitis. *Acta Neurol Scand*. 2010 Aug 1;122(2):75-90.
- 35 Theron S, Andronikou S, Grobbelaar M, et al. Localized basal meningeal enhancement in tuberculous meningitis. *Pediatr Radiol*. 2006 Nov;36(11):1182-5.
- 36 Andronikou S, Smith B, Hatherhill M, Douis H, Wilmsgurst J. Definitive neuroradiological diagnostic features of tuberculous meningitis in children. *Pediatr Radiol*. 2004 Nov;34(11):876-85.
- 37 Bernaerts A, Vanhoenacker FM, Parizel PM, et al. Tuberculosis of the central nervous system: overview of neuroradiologic findings. *Eur Radiol*. 2003 13(8):1876-1890.
- 38 Kumar R, Kohli N, Thavnani H, et al. Value of CT scan in the diagnosis of meningitis. *Indian Pediatr*. 1996;33:465-468.
- 39 Artopoulos J, Chalemis Z, Christopoulos S, et al. Sequential computed tomography in tuberculous meningitis in infants and children. *Comput Radiol*. 1984 8:271-277.
- 40 Bhargava S, Gupta AK, Tandon PN. Tuberculous meningitis – a CT study. *Br J Radiol*. 1982 55:189-196.
- 41 Farinha NJ, Razali KA, Holzel H, et al. Tuberculosis of the central nervous system in children: a 20-year survey. *J Infect*. 2000 41:61-68.
- 42 Kingsley DP, Hnedrickse WA, Kendall BE, et al. Tuberculous meningitis: role of CT in management and prognosis. *J Neurol Neurosurg Psychiatry*. 1987 50:30-36.
- 43 Kumar R, Singh SN, Kohli N. A diagnostic rule for tuberculous meningitis. *Arch Dis Child*. 1999;81:221-224.
- 44 Leiguarda R, Berthier M, Starkstein S, et al. Ischaemic infarction in 25 children with tuberculous meningitis. *Stroke*. 1988 19:200-204.
- 45 Patwari AK, Aneja S, Ravi RN, et al. Convulsions in tuberculous meningitis. *J Trop Pediatr*. 1996 42:91-97.
- 46 Waeker NJ, Connor JD. Central nervous system tuberculosis in children: a review of 30 cases. *Pediatr Infect Dis J*. 1990 9:539-543.
- 47 Altunbasak S, Alhan E, Baytok V, et al. Tuberculous meningitis in children. *Acta Paediatr Jpn*. 1994 36:480-484.
- 48 De JK, Bagchi S, Bhadra UK, et al. Computerised tomographic study of tuberculous meningitis in children. *J Indian Med Assoc*. 2002 42:91-97.
- 49 Kemaloglu S, Ozkan U, Bukte Y, et al. Timing of shunt surgery in childhood tuberculous meningitis with hydrocephalus. *Pediatr Neurosurg*. 2002 37:194-198.
- 50 Ozates M, Kemaloglu S, Gurkan F, et al. CT of the brain in tuberculous meningitis. *Acta Radiol*. 2000 41:13-17.
- 51 Tung Y-R, Lai M-C, Lui C-C, et al. Tuberculous meningitis in infancy. *Pediatr Neurol*. 2002 27:262-266.
- 52 Upadhyaya P, Bhargava S, Sundaram KR, et al. Hydrocephalus caused by tuberculous meningitis: clinical picture, CT findings and results of shunt surgery. *Z Kinderchir*. 1983 38 [Suppl 2]:76-79.
- 53 Scheoman JF, Van Zyl LE, Laubscher JA, et al. Serial CT scanning in childhood tuberculous meningitis: prognostic features in 198 cases. *J Child Neurol*. 1995 10:320-329.
- 54 Przybojewski S, Andronikou S, Wilmshurst J. Objective CT criteria to determine the presence of abnormal basal enhancement in children with suspected tuberculous meningitis. *Pediatr Radiol*. 2006 Jul;36(7):687-96.
- 55 Andronikou S, Wieselthaler N, Smith B, et al. Value of early follow-up CT in paediatric tuberculous meningitis. *Pediatr Radiol*. 2005 Nov;35(11):1092-9.
- 56 Pienaar M, Andronikou S, van Toorn R. MRI to demonstrate diagnostic features and complications of TMB not seen with CT. *Childs Nerv Syst*. 2009 25:941-947.
- 57 du Plessis J, Andronikou S, Wieselthaler N, et al. CT features of tuberculous intracranial abscesses in children. *Pediatr Radiol*. 2007 Feb;37(2):167-72.
- 58 Saczek KB, Schaaf HS, Voss M, Cotton MF, Moore SW. Diagnostic dilemmas in abdominal tuberculosis in children. *Pediatr Surg Int*. 2001;17:111-15.
- 59 Andronikou S, Welman CJ, Kader E. The CT features of abdominal tuberculosis in children. *Pediatr Radiol*. 2002 Feb;32(2):75-81.

- ⁶⁰ Harisinghani MG, McLoud TC, Shepard J-A, et al. Tuberculosis from head to toe. *Radiographics*. 2000;20:449-470.
- ⁶¹ Andronikou S, Jadwat S, Douis H. Patterns of disease on MRI in 53 children with tuberculous spondylitis and the role of gadolinium. *Pediatric Radiol*. 2002 Nov;32(11):798-805.
- ⁶² Teklali Y, El Alami ZF, El Madhi T, Gourinda H, Miri A. Peripheral osteoarticular tuberculosis in children: 106 case-reports. *Joint Bone Spine*. 2003 Aug;70(4):282-6.
- ⁶³ Hsieh S, Kuo Y, Chern M, et al. Mycoplasma pneumonia: clinical and radiographic features in 39 children. *Pediatr Int*. 2007 49:363-367.
- ⁶⁴ Wang RS, Wang SY, Hsieh KS, et al. Necrotizing pneumonitis caused by Mycoplasma pneumoniae in pediatric patients: report of five cases and review of literature. *Pediatr Infect Dis J*. 2004;23:564-7.
- ⁶⁵ Ragosta KG, Clayton JA, Cambareri CB, Domachowske JB. Allergic bronchopulmonary aspergillosis masquerading as pulmonary tuberculosis. *Pediatr Infect Dis J*. 2004 Jun;23(6):582-4.
- ⁶⁶ Ng KK, Cheng YF, Ko SF, et al. CT findings of pediatric thoracic actinomycosis: report of four cases. *J Formos Med Assoc*. 1992 Mar;91(3):346-50.
- ⁶⁷ Graham SM, Coulter JB, Gilks CF. Pulmonary disease in HIV-infected children. *Int J Tuberc Lung Dis*. 2001 5:12-23.
- ⁶⁸ Rennert WP, Kilner D, Hale M. Tuberculosis in children dying with HIV-related lung disease: clinical-pathological correlations. *Int J Tuberc Lung Dis*. 2002 6:806-813.
- ⁶⁹ Fang W, Washington L, Kumar N. Imaging manifestations of blastomycosis: a pulmonary infection with potential dissemination. *Radiographics*. 2007 May-Jun;27(3):641-655.
- ⁷⁰ Singh M, Kothur K. Pulmonary sarcoidosis masquerading as tuberculosis. *Indian Pediatrics*. 2007 44:615-617.
- ⁷¹ Lemme SD, Kevin RA, Cannon CP, et al. Primary tuberculosis of bone mimicking a lytic bone tumor. *J Pediatric Hematology Oncology*. 2007 Mar;29(3):198-202.

